



UNIVERSIDAD DE INVESTIGACIÓN DE TECNOLOGÍA EXPERIMENTAL YACHAY

Escuela de Ciencias Matemáticas y Computacionales

TÍTULO: Mathematical and Computational Modeling for the Design of Smart Cities in Ecuador

Trabajo de integración curricular presentado como
requisito para la obtención
del título de Matemático

Autor:

Yangali Sánchez Roger Joel

Tutor:

Ph.D. Pineda, Israel

Urcuquí, Enero 2022

SECRETARÍA GENERAL
(Vicerrectorado Académico/Cancillería)
ESCUELA DE CIENCIAS MATEMÁTICAS Y COMPUTACIONALES
CARRERA DE MATEMÁTICA
ACTA DE DEFENSA No. UITEY-ITE-2022-00004-AD

A los 21 días del mes de enero de 2022, a las 15:30 horas, de manera virtual mediante videoconferencia, y ante el Tribunal Calificador, integrado por los docentes:

Presidente Tribunal de Defensa Dr. ARMAS ARCINIEGA, JULIO JOAQUIN , Ph.D.

Miembro No Tutor Dr. CUENCA PAUTA, ERICK EDUARDO , Ph.D.

Tutor Dr. PINEDA ARIAS, ISRAEL GUSTAVO , Ph.D.

El(la) señor(ita) estudiante **YANGALI SANCHEZ, ROGER JOEL**, con cédula de identidad No. **0921599072**, de la **ESCUELA DE CIENCIAS MATEMÁTICAS Y COMPUTACIONALES**, de la Carrera de **MATEMÁTICA**, aprobada por el Consejo de Educación Superior (CES), mediante Resolución **RPC-SO-15-No.174-2015**, realiza a través de videoconferencia, la sustentación de su trabajo de titulación denominado: **Mathematical and Computational Modeling for the Design of Smart Cities in Ecuador**, previa a la obtención del título de **MATEMÁTICO/A**.

El citado trabajo de titulación, fue debidamente aprobado por el(los) docente(s):

Tutor Dr. PINEDA ARIAS, ISRAEL GUSTAVO , Ph.D.

Y recibió las observaciones de los otros miembros del Tribunal Calificador, las mismas que han sido incorporadas por el(la) estudiante.

Previamente cumplidos los requisitos legales y reglamentarios, el trabajo de titulación fue sustentado por el(la) estudiante y examinado por los miembros del Tribunal Calificador. Escuchada la sustentación del trabajo de titulación a través de videoconferencia, que integró la exposición de el(la) estudiante sobre el contenido de la misma y las preguntas formuladas por los miembros del Tribunal, se califica la sustentación del trabajo de titulación con las siguientes calificaciones:

Tipo	Docente	Calificación
Miembro Tribunal De Defensa	Dr. CUENCA PAUTA, ERICK EDUARDO , Ph.D.	10,0
Tutor	Dr. PINEDA ARIAS, ISRAEL GUSTAVO , Ph.D.	10,0
Presidente Tribunal De Defensa	Dr. ARMAS ARCINIEGA, JULIO JOAQUIN , Ph.D.	9,0

Lo que da un promedio de: **9.7 (Nueve punto Siete)**, sobre 10 (diez), equivalente a: **APROBADO**

Para constancia de lo actuado, firman los miembros del Tribunal Calificador, el/la estudiante y el/la secretario ad-hoc.

Certifico que *en cumplimiento del Decreto Ejecutivo 1017 de 16 de marzo de 2020, la defensa de trabajo de titulación (o examen de grado modalidad teórico práctica) se realizó vía virtual, por lo que las firmas de los miembros del Tribunal de Defensa de Grado, constan en forma digital.*

YANGALI SANCHEZ, ROGER JOEL
Estudiante

Dr. ARMAS ARCINIEGA, JULIO JOAQUIN , Ph.D.
Presidente Tribunal de Defensa

Dr. PINEDA ARIAS, ISRAEL GUSTAVO , Ph.D.
Tutor

Dr. CUENCA PAUTA, ERICK EDUARDO , Ph.D.
Miembro No Tutor

TORRES MONTALVÁN, TATIANA BEATRIZ
Secretario Ad-hoc

Autoría

Yo, **Roger Joel Yangali Sanchez**, con cédula de identidad **0921599072**, declaro que las ideas, juicios, valoraciones, interpretaciones, consultas bibliográficas, definiciones y conceptualizaciones expuestas en el presente trabajo; así como, los procedimientos y herramientas utilizadas en la investigación, son de absoluta responsabilidad de el autor del trabajo de integración curricular. Así mismo, me acojo a los reglamentos internos de la Universidad de Investigación de Tecnología Experimental Yachay.

Urcuquí, Agosto del 2021.

Roger Joel Yangali Sanchez
CI: 0921599072

Autorización de publicación

Yo, **Roger Joel Yangali Sanchez**, con cédula de identidad **0921599072**, cedo a la Universidad de Tecnología Experimental Yachay, los derechos de publicación de la presente obra, sin que deba haber un reconocimiento económico por este concepto. Declaro además que el texto del presente trabajo de titulación no podrá ser cedido a ninguna empresa editorial para su publicación u otros fines, sin contar previamente con la autorización escrita de la Universidad.

Asimismo, autorizo a la Universidad que realice la digitalización y publicación de este trabajo de integración curricular en el repositorio virtual, de conformidad a lo dispuesto en el Art. 144 de la Ley Orgánica de Educación Superior.

Urcuquí, Agosto del 2021.

Roger Joel Yangali Sanchez
CI: 0921599072

Dedication

“First, I would like to dedicate this work to God! Only you know how much I struggled to get to this point and I appreciate you so much for helping me get here. Alhamdoulilah!

To my parents, Joel Ulises Yangali Aranguena and Emma Coveñas de Yangali who inspired me to be the best version I could be. Thank you for teaching me everything I know. I am the man I am today because of you, and I could not ask for anything else. Thank you for always supporting me, through thin and thick. You are the best parents anyone could ask for.

To my sister and niece, Pilar Yangali Coveñas and Nicole Alexandra Castro Yangali, for always being there when I needed you most, motivating and inspiring me to keep going. Thank you for always believing in me especially when I did not believe in myself. You are both strong, independent women, and I have learned more from you than you can imagine.

To my best friend, Tamara Elshanti, thank you so much Habibi! You have been there since day one, and I could not thank you enough for all that you have inspired me and all that you have done for me. Alhamdoulilah!

I love all of you so much. This work is dedicated to you and to all my family and the wonderful friendships I was so lucky to make. I have been blessed in my life with many friends and family members who have supported and motivated me countless times to keep going. I am truly thankful to you all. I will never forget who was there for me. Alhamdoulilah!”

Acknowledgments

First, and foremost I would like to acknowledge Israel Pineda, Ph.D., for all his advice and guidance since the first day we met. This paper would not be published today if it was not because you were always there to help me and motivate me to keep going. Words cannot fully express my gratitude but thank you. Thanks for giving me ideas to improve my simulations, for helping me with my code errors, for making me be a better researcher, and for reminding me that I chose math because I could apply it to any field to create amazing research like this work.

I would also like to acknowledge Yachay Tech for having given me the tools necessary to achieve my dream but most importantly I want to acknowledge all of my Professors throughout my time at Yachay Tech. Every professor I met, was more than a friend, they gave us advice and treated us like we were part of their families. They gave us extra of their time, to help us when we needed it most. I will always remember what each one of you taught me, and the goods times shared in the classrooms. It is because you taught me so well, that I feel more than ready and capable to do anything I set my mind to, and for that, I thank you very much.

Abstract

During the past decade, billions of dollars have been invested in the planning and implementation of smart cities around the world [1]. Finding intelligent new ways to maintain the infrastructure of a city is crucial. If the infrastructure is not prepared to meet the demands for a rapidly increasing human population growth, the city and all of its citizens might suffer dire consequences. These demands include basic needs such as clean air and water, housing, and food. A city that supervises its natural resources is able to prosper for longer periods. Cities that do not meet the basic needs of their citizens collapse due to overpopulation, air and water pollution, lack of food, and lack of housing space.

Due to improvements in technology, medicines, health, and security, humans tend to live longer, form bigger families, migrate farther and create larger cities. As population and cities expand, so does construction work. To meet growing demand, additional homes, roads, and vehicles are manufactured. This extra construction work utilizes vast resources and emits enormous quantities of pollution into the atmosphere and waterways. Smart cities focus on managing the resources available and finding solutions to help improve the quality of life of their citizens. Smart cities help provide safe areas for families to enjoy, offer better housing options, provide affordable food, technological advances, and design innovative methods to reduce dangerous pollution being released into the atmosphere. High levels of pollution can affect negatively the environment as well as the health and life span of all residents.

Traffic plays a major role in creating pollution and releasing dangerous waste into the environment. The United States Environmental Protection Agency (EPA) [2], calculated that greenhouse gas (GHG) emissions from transportation account for approximately 29% of all U.S GHG emissions. This makes transportation the largest contributor of GHG emissions in the U.S. As of today, Ecuador does not count on an EPA, to help monitor and track the levels of emissions generated from transportation. There is no previously recollected statistical data on GHG emissions so people are not aware they are in danger due to high pollution levels in the environment. On the other hand, countries such as the U.S, Germany, Sweden, Italy, and Japan have been collecting data on GHG for decades. They can compare their yearly emission levels from entire cities. Utilizing this information to improve or create new regulations when GHG emissions levels are too high.

Vehicular emissions generate particles that are not detectable to the human eye. They are smaller than red blood cells, less than 100 nanometers in size, and they can translocate themselves around the human body. This creates a negative long-term effect on all residents, deteriorating their health much faster, raising the costs of medicines and hospital treatments. The five main particles being released by vehicles while in use are carbon monoxide (CO), carbon dioxide (CO₂), hydrocarbons (HC), particulate matter

(PM_x), and nitrogen oxides (NO_x).

CO_2 is known for trapping heat in the atmosphere, causing climate change, increasing the probability of wildfires to occur, and causing respiratory problems from smog and air pollution. CO is similar to CO_2 , it also contributes to climate change, drastically affects the weather, and fails to absorb oxygen in the bloodstream. HC emissions are generated when automobile oil leaks onto the ground. This is the major cause of hydrocarbon contamination in waterways. PM_x is one of the most dangerous emissions and there are two different types of particles. One particle (PM_{10}) is less than 10 micrometers in diameter. The second particle ($\text{PM}_{2.5}$) is less than 2.5 micrometers. $\text{PM}_{2.5}$ can easily travel deep inside the lungs, affecting the organs directly. It causes aggravated asthma, coughing, and premature death in people with heart or lung diseases. Finally, NO_x serves to represent both nitric oxide (NO) and nitrogen dioxide (NO_2). NO is similar to CO , it also fails to absorb oxygen in the bloodstream, and NO_2 is known to increase the probability of acid rain in the environment.

Finding new methods and approaches to reduce GHG emissions will help preserve and improve the quality of life of all citizens. Needless to say, this should be of most importance to government officials and those in charge of passing new environmental regulations. Performing an appropriate, convenient, and relatively affording method to monitor traffic and vehicular emissions is an indispensable subject for a smart city. This allows for better decision-making from public administrators and citizens. Government officials can utilize collected data on traffic and vehicular emissions to regulate vehicular emissions (e.g. restricting vehicle circulation in certain areas or creating new environmental laws for vehicle emissions). With additional statistical results, citizens can make better decisions while driving, allowing them to reach their destination much faster. Roads can be built much better and efficiently while utilizing all available resources to the best capacity. There exists a variety of methods to detect and measure traffic, but creating a widespread deployment through an entire city can result pretty expensive and difficult to implement. For this reason, alternative approaches have been developed that allow us to estimate vehicular emissions in any city based on real-life obtained traffic measurements.

A procedure to simulate the traffic flow in the cities of Guayaquil and Ibarra, Ecuador, has been designed and implemented in this work. This procedure helps obtain useful statistical data on the five GHG emissions previously mentioned for both cities and obtain a comparison. More specifically, we have implemented an approach that combines real-life obtained traffic measurements with the use of the traffic Simulation of Urban Mobility (SUMO) program. Using accurate road maps for each city and the obtained real-life traffic measurements, real-world simulations can be created. SUMO allows us the ability to analyze vehicular emissions obtained throughout the simulation. The final goal for this work is to collect and store this generated statistical data for government officials to use when creating regulations for GHG emissions. Improving air quality and lowering vehicular emissions will help preserve the health of all residents and will be a step closer for Guayaquil and Ibarra to become smart cities.

Keywords: Smart City, SUMO, Python, Simulation, Traffic, Emissions, Statistical Analysis

Resumen

Durante la última década, se han invertido billones de dólares en la planificación e implementación de ciudades inteligentes en todo el mundo [1]. Encontrar nuevas formas inteligentes de mantener la infraestructura de una ciudad es crucial. Si la infraestructura no está preparada para satisfacer las demandas de el crecimiento rápido de la población humana, la ciudad y todos sus ciudadanos podrían sufrir graves consecuencias. Estas demandas incluyen necesidades básicas como aire y agua limpia, vivienda y alimentos. Una ciudad que supervisa sus recursos naturales puede prosperar por períodos más prolongados. Las ciudades que no satisfacen las necesidades básicas de sus ciudadanos colapsan debido a la superpoblación, la contaminación del aire y el agua, la falta de alimentos y de espacio para viviendas.

Debido a las mejoras en la tecnología, los medicamentos, la salud y la seguridad, los humanos tienden a vivir más tiempo, formar familias más grandes, migrar más lejos y crean ciudades más grandes. A medida que la población y las ciudades se expanden, se necesita más trabajo de construcción. Para satisfacer la demanda creciente se fabrican viviendas, carreteras y vehículos adicionales. Este trabajo adicional de construcción utiliza vastos recursos y emite enormes cantidades de contaminación a la atmósfera y las vías fluviales. Las ciudades inteligentes se centran en gestionar los recursos disponibles y encontrar soluciones que ayuden a mejorar la calidad de vida de sus ciudadanos. Las ciudades inteligentes ayudan a proporcionar áreas seguras para que las familias disfruten, ofrecen mejores opciones de vivienda, proporcionan alimentos asequibles, contribuyen con avances tecnológicos y diseñan métodos innovadores para reducir la peligrosa contaminación que se libera a la atmósfera. Los altos niveles de contaminación pueden afectar negativamente al medio ambiente, así como a la salud y la vida de todos los residentes.

El tráfico juega un papel importante en la creación de contaminación y la liberación de desechos peligrosos al medio ambiente. La Agencia de Protección Ambiental (APA) [2] de los Estados Unidos calculó que las emisiones de gases de efecto invernadero (GEI) del transporte representan aproximadamente el 29 % de todas las emisiones de GEI de EE. UU. Esto hace que el transporte sea el mayor contribuyente de emisiones de GEI en los EE.UU. Al día de hoy, Ecuador no cuenta con una APA que ayude a monitorear y rastrear los niveles de emisiones generadas por el transporte. No hay datos estadísticos recopilados previamente sobre las emisiones de GEI. Las personas no son conscientes de que están en peligro debido a los altos niveles de contaminación en el medio ambiente. Por otro lado, países como Estados Unidos, Alemania, Suecia, Italia y Japón han estado recopilando datos sobre GEI durante décadas. Les permite comparar los niveles de emisiones anuales de ciudades enteras. Utilizan esta información para mejorar o crear nuevas regulaciones cuando los niveles de emisiones de GEI son demasiado altos.

Las emisiones vehiculares generan partículas que no son detectables por el ojo humano. Son más pequeños que los glóbulos rojos, con tamaño menor a 100 nanómetros y pueden translocarse por todo el cuerpo humano. Esto crea un efecto negativo a largo plazo a los residentes, deteriorando su salud mucho más rápido, aumentando los costos de medicamentos y los tratamientos hospitalarios. Las cinco partículas principales que emiten los vehículos mientras están en uso son monóxido de carbono (CO), dióxido de carbono (CO₂), hidrocarburos (HC), material particulado (PM_x) y óxidos de nitrógeno (NO_x).

El CO₂ es conocido por atrapar el calor adentro de la atmósfera, contribuir a cambios climáticos, aumentar la probabilidad de incendios forestales y crear problemas respiratorios por smog y la contaminación en el aire. El CO es similar al CO₂, también contribuye al cambio climático, afecta drásticamente a el clima y no permite absorber el oxígeno en el torrente sanguíneo. Las emisiones de HC se generan cuando el aceite de automóvil se derrama al suelo. Ésta es la causa principal de contaminación por hidrocarburos en las vías fluviales. PM_x es una de las emisiones más peligrosas y existen dos tipos diferentes de partículas. Una partícula es menor a 10 micrómetros de diámetro (PM₁₀). La segunda partícula es más pequeña, menos de 2,5 micrómetros (PM_{2,5}). El PM_{2,5} puede viajar fácilmente al interior de los pulmones y afectar directamente a los órganos. Causa asma agravada, tos y muerte prematura en personas con enfermedades cardíacas o pulmonares. Finalmente, NO_x sirve para representar el óxido nítrico (NO) como el dióxido de nitrógeno (NO₂). El NO es similar al CO, tampoco permite absorber oxígeno en el torrente sanguíneo y se sabe que el NO₂ aumenta la probabilidad de lluvia ácida en el medio ambiente.

Encontrar nuevos métodos y enfoques para reducir las emisiones de GEI ayudará a preservar y mejorar la calidad de vida de todos los ciudadanos. No hace falta decir que esto debería ser de suma importancia para los funcionarios gubernamentales y los encargados en aprobar nuevas regulaciones ambientales. Realizar un método apropiado, conveniente y relativamente económico para monitorear el tráfico y las emisiones vehiculares es un tema indispensable para una ciudad inteligente. Esto permite una mejor toma de decisiones por parte de los administradores públicos y los ciudadanos. Los funcionarios gubernamentales pueden utilizar los datos recopilados sobre el tráfico y las emisiones vehiculares para regular las emisiones vehiculares (por ejemplo, restringiendo la circulación de vehículos en ciertas áreas o creando nuevas leyes ambientales para las emisiones de los vehículos). Con resultados estadísticos adicionales, los ciudadanos pueden tomar mejores decisiones mientras conducen, lo que les permite llegar a su destino mucho más rápido. Las carreteras se pueden construir de mejor manera y más eficiente mientras se utilizan todos los recursos disponibles a la mejor capacidad. Existe una variedad de métodos para detectar y medir el tráfico, pero crear una implementación generalizada en toda una ciudad puede resultar bastante costoso y difícil de implementar. Por esta razón, se han desarrollado enfoques alternativos que nos permiten estimar las emisiones vehiculares en cualquier ciudad con base a mediciones de tráfico obtenidas en la vida real.

En este trabajo se ha diseñado e implementado un procedimiento para simular el flujo de tráfico en las ciudades de Guayaquil e Ibarra, Ecuador. Este procedimiento ayuda a obtener datos estadísticos útiles sobre las cinco emisiones de GEI mencionadas anteriormente para ambas ciudades y obtener una comparación. Más específicamente, hemos implementado un enfoque que combina las mediciones de tráfico obtenidas en la vida real con el uso del programa de Simulación de Tráfico de Movilidad Urbana (SUMO). Utilizando mapas de carreteras precisos para cada ciudad y las mediciones de tráfico obtenidas en la vida real,

se pueden crear simulaciones del mundo real. STMU nos permite la capacidad de analizar las emisiones vehiculares obtenidas a lo largo de la simulación. El objetivo final de este trabajo es recopilar y almacenar los datos estadísticos generados para que los funcionarios gubernamentales los utilicen al crear regulaciones para las emisiones de GEI. Mejorar la calidad del aire y reducir las emisiones vehiculares ayudará a preservar la salud de todos los residentes y será el primer paso para que Ibarra y Guayaquil se conviertan en ciudades inteligentes.

Palabras Clave: Ciudad Inteligente, SUMO, Python, Simulacion, Traffico, Emisiones, Analisis Estadistico

Contents

Dedication	v
Acknowledgments	vii
Abstract	ix
Resumen	xi
Contents	xv
List of Figures	xvii
1 Introduction	1
1.1 Background	2
1.2 Problem Statement	3
1.3 Objectives	3
1.3.1 General Objective	3
1.3.2 Specific Objectives	4
2 Theoretical Framework	5
2.1 Traffic Flow Model	5
2.2 Car-Following Models	8
2.3 Gipps' Car-Following Model	10
2.3.1 Proposed Car-Following Model	11
2.3.2 "Phantom" Vehicle	14
2.4 Krauß Car Following Model	14
2.5 Jam Dynamics in the Krauß model	16
2.6 Simulation of Urban Mobility (SUMO)	17
2.7 Smart Cities	22
2.8 Vehicular Gas Emissions	23
3 State of the Art	25
3.1 Improving Traffic Flow Modeling and SUMO	25
3.2 Smart Cities and SUMO	25

3.3	Smart Cities and Emissions	28
4	Methodology	31
4.1	Phases of Problem Solving	31
4.2	Description of the Problem	32
4.3	Analysis of the Problem	33
4.4	Model Proposal	33
4.5	Algorithm Design	34
4.6	Experimental Setup	37
4.7	Implementation	41
4.8	Testing	41
5	Results and Discussion	45
5.1	Results	45
5.2	Discussion	64
6	Conclusions	67
6.1	Recommendations	68
6.2	Future Works	69
	Bibliography	71

List of Figures

2.1	Greenshields fundamental diagram (1935), showing a linear relation between density and speed. Source: [3]	6
2.2	Proposed shapes for the fundamental diagram in density-flow and density-speed plane. Source: [4]	6
2.3	Fundamental diagram proposed by Edie without a capacity drop. Source: [5]	7
2.4	Fundamental diagram proposed by Edie with a capacity drop. Source: [5]	7
2.5	Densities-Avg.Speeds Observed. Hysteresis Phenomenon. Source: [6]	8
2.6	Pipes Safe-Distance Model. Source: [4]	9
2.7	Gazis-Herman-Rothery Car-Following Model. Source:	9
2.8	Traffic flow as a function of traffic density. Left: Original traffic flow data Right: Simulation results using the Krauß model. Source: [7]	16
2.9	From traffic jam to free flow. Top: Traffic jam developing, Bottom: Free flow traffic. Notice there are 25s between each image, red represents standing vehicles, blue represents vehicle travelling at faster speeds. Source: [7]	17
2.10	Open Street Map (Ibarra). Source: [8]	18
2.11	NetEdit Program (Ibarra)	19
2.12	NetEdit Road Connections (Ibarra)	19
2.13	NetEdit Traffic Lights (Ibarra)	20
2.14	SUMO GUI Simulation (Ibarra)	20
2.15	SUMO GUI with 3 views for the (Ibarra) Simulation	21
2.16	Number of running vehicles in the (Ibarra) Simulation	21
3.1	Satellite images of NO ₂ and SO ₂ levels for Ecuador one week before the COVID-19 quarantine. Source: [9]	30
4.1	Workflow Diagram	32
4.2	Route File “RoutesIbarra.rou.xml”	35
4.3	SUMO File Example “Ibarra.sumocfg”	36
4.4	SUMO File Example “Ibarra.sumocfg” with Output Files	37
4.5	Google Earth View for Guayaquil. Source [10]	38
4.6	Google Earth View: Guayaquil Intersection (C). Source [10]	38
4.7	Google Earth View (Ibarra). Source [10]	39
4.8	Google Earth View (Ibarra) ABC Triangle. Source [10]	40
4.9	Unrealistic Simulation in SUMO GUI for Guayaquil at point (D)	41
4.10	Perfected Simulation in SUMO GUI for Guayaquil at point (D)	42
4.11	Unrealistic Simulation in SUMO GUI for Ibarra at point (A)	42

4.12	Perfected Simulation in SUMO GUI for Ibarra at point (A)	43
4.13	Perfected Simulation in SUMO GUI for Ibarra at point (B)	44
4.14	Perfected Simulation in SUMO GUI for Ibarra at point (C)	44
5.1	SUMO GUI Guayaquil simulation at point (C)	45
5.2	SUMO GUI Guayaquil simulation at point (D)	46
5.3	SUMO GUI with 3 different views for Guayaquil	46
5.4	Number of running vehicles for Guayaquil using SUMO GUI	47
5.5	SUMO GUI Ibarra Simulation at point (A)	47
5.6	SUMO GUI Ibarra Simulation at point (B)	48
5.7	SUMO GUI Ibarra Simulation at point (C)	48
5.8	SUMO GUI with 3 different views for Ibarra	49
5.9	Number of running vehicles for Ibarra using SUMO GUI	49
5.10	Comparison Summary Ibarra & Guayaquil	50
5.11	Location of traffic lights for selected area in Guayaquil	51
5.12	Location of traffic lights for selected area in Ibarra	51
5.13	Lanes Speed Limit: Guayaquil (50km/h = 13.88 , 70km/h = 19.44)	52
5.14	Lanes Speed Limit: Ibarra (50km/h = 13.88 , 70km/h = 19.44)	53
5.15	Total vehicular emissions for Guayaquil	54
5.16	$\log(x + 1)$ Transformation for vehicular emissions for Guayaquil	55
5.17	Total vehicular emissions for Ibarra	56
5.18	$\log(x + 1)$ Transformation for vehicular emissions for Ibarra	57
5.19	Percentage of CO emissions per vehicle for Guayaquil	58
5.20	Percentage of CO ₂ emissions per vehicle for Guayaquil	58
5.21	Percentage of HC emissions per vehicle for Guayaquil	59
5.22	Percentage of PM _x emissions per vehicle for Guayaquil	59
5.23	Percentage of NO _x emissions per vehicle for Guayaquil	60
5.24	Percentage of CO emissions per vehicle for Ibarra	60
5.25	Percentage of CO ₂ emissions per vehicle for Ibarra	61
5.26	Percentage of HC emissions per vehicle for Ibarra	61
5.27	Percentage of PM _x emissions per vehicle for Ibarra	62
5.28	Percentage of NO _x emissions per vehicle for Ibarra	62
5.29	Emissions $\log(x + 1)$ transform bar graph for Guayaquil	63
5.30	Emissions $\log(x + 1)$ transform bar graph for Ibarra	63
5.31	Emissions $\log(x + 1)$ transform bar graph for Guayaquil and Ibarra	64
6.1	Fundamental diagram with infinitely admissible states in the congestion branch (shaded). Source: [11]	77
6.2	Three-Dimensional fundamental diagram, high proportion of trucks leads to lower flows and speeds. Source: [12]	77
6.3	Time vs Acceleration graph for Ibarra simulation using only 1 vehicle	78
6.4	Time vs Acceleration graph for Ibarra simulation using only 2 vehicles	78
6.5	Time vs Acceleration graph for Ibarra simulation using vehicular flow	79
6.6	Traffic Lights 1x Zoom for Guayaquil at location (B)	79
6.7	Traffic Lights 1x Zoom for Guayaquil at location (C)	80
6.8	Traffic Lights 1x Zoom for Ibarra at location (A)	80

6.9	Traffic Lights 1x Zoom for Ibarra at location (B)	81
6.10	Traffic Lights 1x Zoom for Ibarra at location (C)	81
6.11	Lane speed limit Zoom 1x for Guayaquil at location (C). (50km/h = 13.88 , 70km/h = 19.44)	82
6.12	Lane speed limit Zoom 1x for Guayaquil at location (D). (50km/h = 13.88 , 70km/h = 19.44)	82

Chapter 1

Introduction

In the past decade, governments worldwide began researching and investing more of their resources in the implementation of smart cities. New advances in technology, medicine, quality of living, and migration have increased the life expectancy of humans. This has caused an increase in housing, roads, vehicles, food, and natural resources needed. Cities and countries with high population density such as New York, Los Angeles, Madrid, China, and Japan are investing in new and innovative solutions to solve infrastructure problems. This includes clean air and water, safe public areas, and a sufficient food supply for all citizens. Smart cities try to tackle some of these problems to improve the overall well-being of all citizens. One of the main concerns for smart cities is trying to keep under control the number of greenhouse gasses (GHG) that are being emitted into the atmosphere. High levels of GHG in the atmosphere can drastically affect the weather, contaminate the air and waterways, and may cause health problems including premature death [13].

Pollution is responsible for health complications such as aggravated asthma and heart and lungs deterioration. Most pollution emitted into the atmosphere is generated from the industrial burning of fossil fuels, wildfires, and vehicular gas emissions. This work focuses solely on the generation of vehicular gas emissions. More precisely, quantifying emission levels from the five most dangerous GHG, carbon monoxide (CO), carbon dioxide (CO₂), hydrocarbons (HC), particulate matter (PM_x), and nitrogen oxides (NO_x). Vehicular traffic is the major contributor to pollutants released into the air and waterways [14]. Discovering new techniques to measure these emissions is a necessity for smart cities. This data will improve residents living conditions, lower GHG emissions, and decrease global warming.

For this work, we developed a method to quantify vehicular emission levels at specific zones in the cities of Guayaquil and Ibarra using open-source simulation programs. Using statistics with the obtained results, we are able to analyze and compare GHG emission levels in small and large cities. To generate real-life results, this method requires the use of real-life data collected from the specific area that we want to simulate. Using the Simulation of Urban Mobility (SUMO) program and the obtained real-life data, we can create accurate and realistic simulations. These simulations will return accurate and precise values for the levels of vehicular emissions generated by traffic in Guayaquil and Ibarra.

1.1 Background

Traffic flow modeling and management is a key component for smart cities. Being able to monitor the traffic and track the GHG emission levels for 24 hours continuously within a city is crucial but highly expensive when done manually. GHG monitors price range from \$40 - \$400, depending on the brand and specifications [15]. These monitors must be set up in specific areas around the city and checked on daily to prevent loss or damage and to obtain the results generated. This increases the costs to constantly monitor GHG emission levels. Hence, finding new, innovative, and affordable ways to generate GHG emission data is greatly beneficial.

For this reason, we utilize SUMO [16], an open-source, traffic simulation program. It allowed us to create a realistic simulation of specific sections of the cities of Guayaquil and Ibarra. SUMO supports both C++ and Python programming languages. For this work, we focus only on Python as there are additional scripts and useful functions for the generation of vehicular emissions. It is clear to see why SUMO is the preferred tool worldwide for traffic simulations. SUMO also provides the ability to run a micro, macro, mesoscopic (combination of both micro and macro), and even submicroscopic simulations (able to simulate driver actions, e.g. shifting gears). Using the built-in SUMO calibrators allows the user to change each independent variable such as acceleration and the impatience of the driver. This will be explained further in detail in Chapter 4. These functions within SUMO allow the user to run different simulations and obtain all types of results. From calculating the reaction time when a specific driver changes gears to calculating the vehicular emissions from all vehicles in an entire city for hours, days, weeks, or even months.

The main application for traffic flow modeling is providing advantageous information on vehicular emissions, the major contributor to global warming, air pollution, and countless health problems. These GHG emissions are CO, CO₂, HC, PM_x and NO_x. They are considered highly dangerous and are constantly tracked and monitored by the Environmental Protection Agency (EPA), mainly in North America and Europe [14]. As stated, these emissions contribute to global warming, trapping considerable heat inside the atmosphere. This causes ice caps to melt faster, and flooding to occur frequently in certain areas of the world. GHG emissions produce smog, acid rain, natural disasters and contaminate the clean air and water sources creating health complications for all residents in the long run. That is why finding innovative ways to generate this type of information on emissions is crucial for cities. The data obtained can be used by governments to help regulate emissions and improve the quality of life of their citizens.

Cities in Ecuador, especially large cities such as Guayaquil and Quito, are faced with large vehicular traffic congestion during peak hours every day. They generate tons of emissions that are damaging to the populations' health and trap GHG that negatively affect the weather. Smaller cities such as Ibarra are currently seeing an increase in vehicle use given the population growth. Meanwhile, these dangerous emissions are not being quantified nor are they being recorded, thus there is no clear idea of how bad emissions levels are currently in the cities of Ecuador. Using SUMO we can use simulations to obtain and record vehicular emissions from entire cities, but for this work, we only focus on simulating specific zones for the cities of Guayaquil and Ibarra.

The structure of this work is as follows. Chapter 1 describes the problem faced in Ecuador and lists the objectives we would like to achieve by the end of this work. Chapter

2 presents the theoretical framework where we describe in-depth the car-following model utilized by SUMO. We define the relevant formulas as well as any necessary concepts and definitions about smart cities and GHG emissions. Chapter 3 discusses the latest technological innovations developed over the past five years. These include the latest works on the SUMO program, vehicular emissions, and smart cities. Chapter 4 describes the methodology employed in this work as well as a detailed step-by-step guide for the reader to create a SUMO simulation and obtain data on vehicular emissions. Chapter 5 will present the results obtained from SUMO using Python scripts and Analysis of Variance (ANOVA). Lastly, Chapter 6 presents the conclusions, recommendations to take into consideration, and ideas for future works to further improve the simulations presented here.

1.2 Problem Statement

The number of people migrating to large cities is increasing by the day due to a rapidly increasing population growth. Large cities count with limited space available, to the point that small cities such as Ibarra and Riobamba are also seeing an increase in residents. This generates an increase in vehicular use which causes longer traffic congestion and higher levels of GHG emissions. Large cities in Ecuador such as Guayaquil and Quito especially, suffer constantly from large traffic jams at peak hours during the day. Residents who lose time commuting from and to work generate higher GHG emission levels due to running vehicles. Humans tend to forget the dangers of vehicular emission particles. These dangerous particles are inhaled constantly into the bloodstream and organs, deteriorating health and causing premature death [17]. To this day, there is no standardized method for obtaining daily vehicular traffic flows or generating data on GHG emitted by traffic congestion in the cities of Ecuador.

Constantly generating and recording data on emission levels is of utter importance. Collecting information from cities for extended periods provides a clear view of GHG emissions levels in the environment. When pollution levels threaten the living conditions of citizens, new measures and regulations should be taken into consideration to reduce them. Using the SUMO program it is possible to obtain readings from specific sectors of the cities of Guayaquil and Ibarra. Registering the environmental GHG emission levels for CO, CO₂, HC, PM_x, and NO_x in both cities is convenient to government officials. Using statistical analysis, we can compare the results obtained from both cities and arrive at beneficial conclusions and advice for future works.

1.3 Objectives

1.3.1 General Objective

The objective of this work is to create a realistic simulation for Guayaquil and Ibarra, using real-life traffic flows to calibrate its parameters and generate data on vehicular GHG emissions.

1.3.2 Specific Objectives

- Quantify the exact number of vehicles that transit during an hour in specific sectors of Ibarra and Guayaquil.
- Create a one-hour traffic simulation that reflects real-life traffic for both cities using collected data.
- Generate realistic and accurate data on the dangerous GHG emissions, CO, CO₂, HC, PM_x, and NO_x.
- Provide graphs and maps generated using Python scripts and SUMO, regarding GHG emissions from all vehicles running throughout the simulation.
- Analyze all information obtained from SUMO using ANOVA and present the results in graphs and charts.

Chapter 2

Theoretical Framework

This chapter presents all information regarding the history of the car-following model utilized by SUMO. It contains a detailed mathematical explanation of the formulas utilized by the car-following model. Then it presents information regarding the SUMO program and the creation of different types of smart cities. Finally, this work describes the long-term, negative side effects from CO, CO₂, HC, PM_x, and NO_x in the environment. Additionally, we offer ideas to reduce emission levels in cities.

2.1 Traffic Flow Model

Traffic flow models have been implemented for almost a century to describe, simulate and predict traffic. The first traffic flow model was called the fundamental diagram. It was introduced originally by Greenshields [18] in 1934 at the 13th annual meeting of the Highway Research Board. This fundamental diagram related the distance or spacing between two vehicles to their speed. The following year Greenshields [3] presented a new and improved fundamental diagram. This diagram related the number of vehicles on a one-unit length of road (vehicular density), to their speed. This new diagram can be seen in Figure 2.1. It is a simple model that marked the beginning for future works on safe-distance and car-following models. Today, these models are commonly implemented in micro, meso, and macro traffic simulation programs such as SUMO.

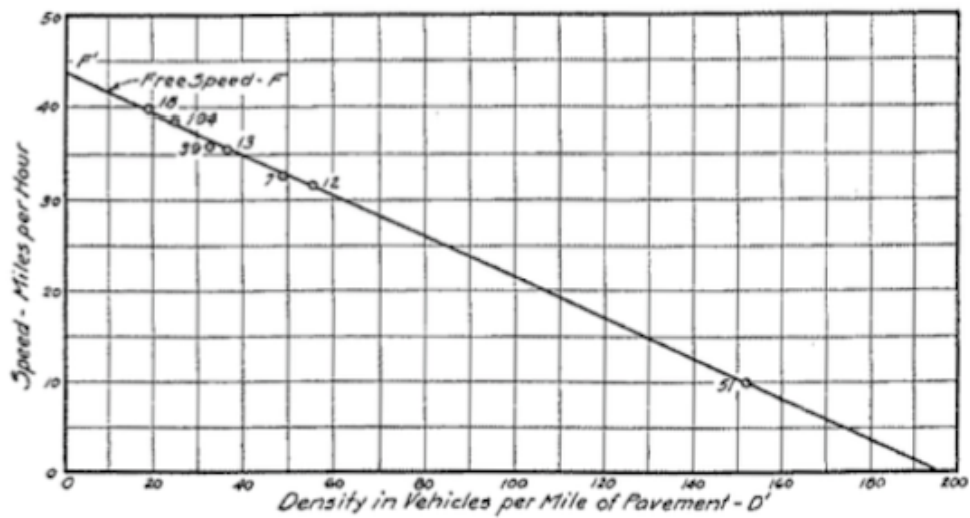


Figure 2.1: Greenshields fundamental diagram (1935), showing a linear relation between density and speed. Source: [3]

After the introduction of the fundamental diagram, there was a debate on its shape. Figure 2.2 shows different shapes proposed throughout time. Beginning with the original parabolic model introduced by Greenshields in 1934, the bell model presented by Drake [19] in 1967, the parabolic-linear model by Smulders [20] in 1990, and lastly, the bi-linear model created by Daganzo [21] in 1994.

Density-flow				
Density-speed				
Shape	Parabolic	Bell	Parabolic-linear	Bilinear
Author	Greenshields	Drake	Smulders	Daganzo
Year	1934	1967	1990	1994

Figure 2.2: Proposed shapes for the fundamental diagram in density-flow and density-speed plane. Source: [4]

The original fundamental diagrams did not represent scatter in observed density-speed plots well enough. Soon after, two fundamental diagrams were introduced by Edie [5] in 1961.

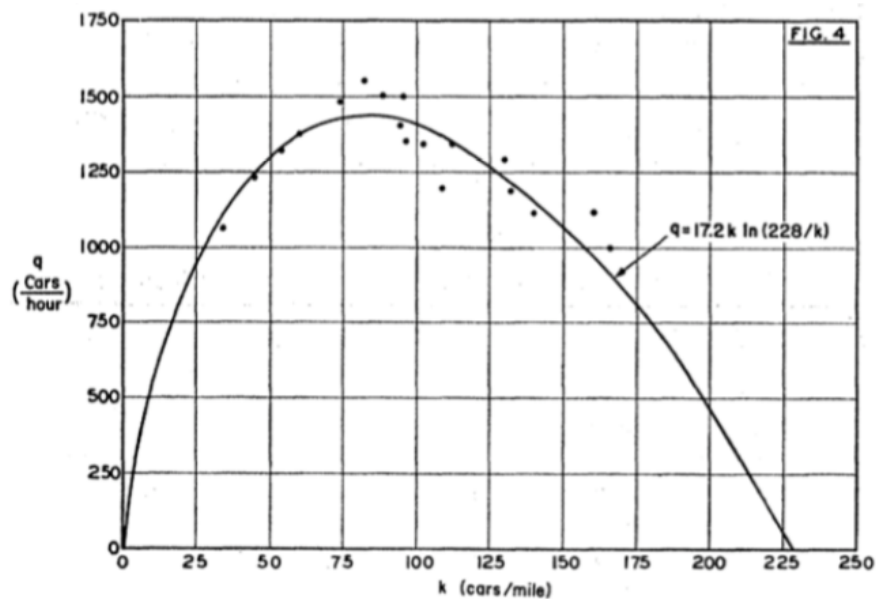


Figure 2.3: Fundamental diagram proposed by Edie without a capacity drop. Source: [5]

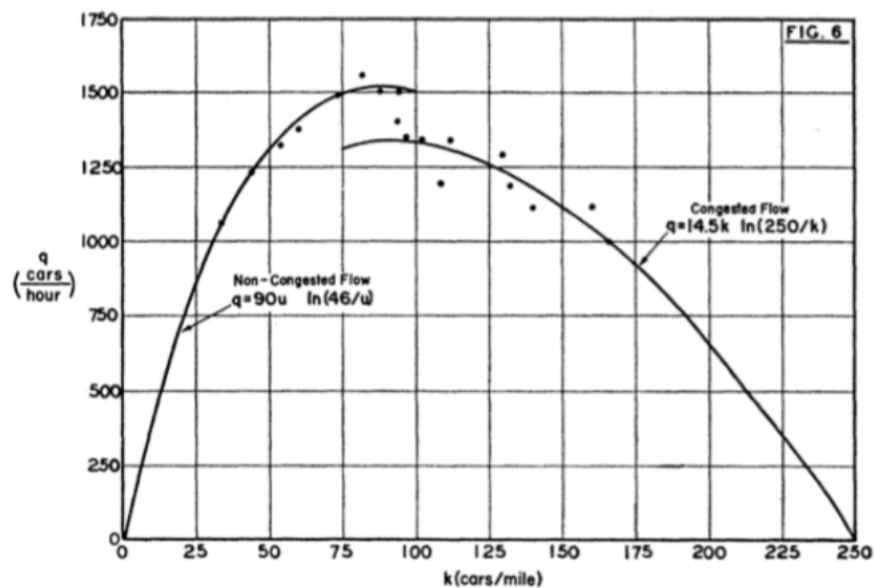


Figure 2.4: Fundamental diagram proposed by Edie with a capacity drop. Source: [5]

Figure 2.3 shows a fundamental diagram with no capacity drop, and Figure 2.4 shows with a capacity drop. This capacity drop indicates that the outflow of vehicles leaving traffic is lower than the flow of vehicles before a traffic jam occurs. Utilizing both graphs, Edie proved that a diagram with capacity drop represented scattered data better than the original fundamental diagram.

A couple of years after Edie proposed his fundamental diagram, Newell [22] introduced the concept of hysteresis in 1965. Newell stated that vehicles during traffic congestion have different density-speed relations when accelerating and decelerating.

Approximately a decade later, Myers and Treiterer [6] demonstrated that the concept of hysteresis presented by Newell could explain much of the observed scattered plot obtained in Figure 2.5.

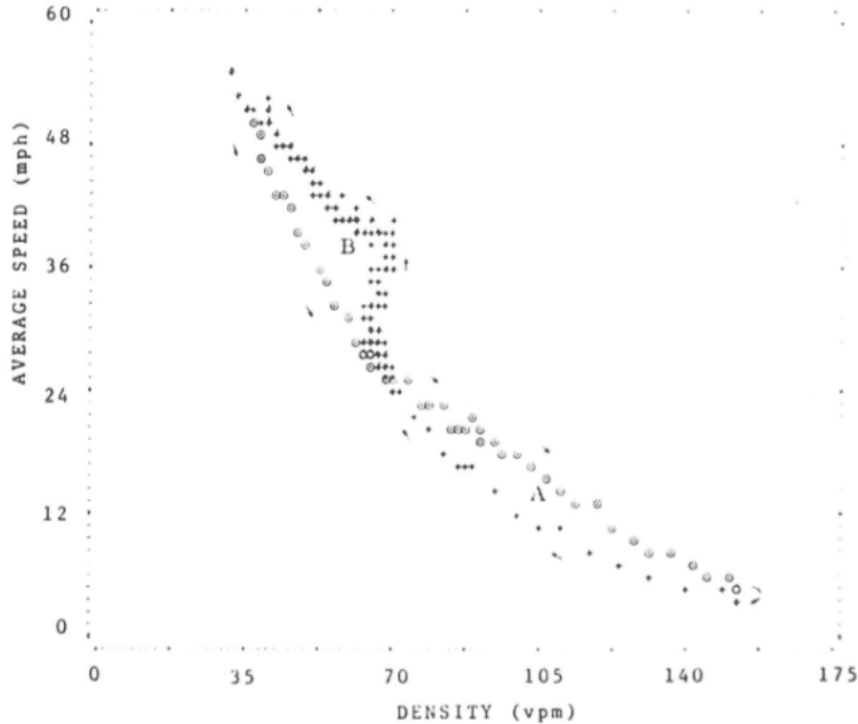


Figure 2.5: Densities-Avg.Speeds Observed. Hysteresis Phenomenon. Source: [6]

Notice that at relatively low vehicular density, vehicles tend to have relatively higher speeds when accelerating (diamonds) than when decelerating (circles). This is inversely proportional thus for higher vehicular density when traffic begins to form, they have relatively lower speeds when accelerating than when decelerating.

A fundamental diagram with infinitely many admissible states, as well as a three-dimensional diagram can be found in Appendix 1.

We have mentioned briefly, the history of the fundamental diagram and the models that originated from it. Now, we will discuss the history and development of car-following models.

2.2 Car-Following Models

This section focuses on the history of car-following models and a detailed explanation of how the Gipps' [23] and Krauß [24] car-following models work. A vehicle is classified as following another when it is restricted by a preceding vehicle and driving at the preferred speed will eventually lead to a collision. When a vehicle is not restrained by another vehicle it is considered free. A vehicle that is free travels at its desired speed.

The first car-following model is the safe-distance model introduced by Pipes [25] in 1953. In this new model, vehicles adjust their speed following a safe distance generated by

a leading vehicle. The rule of safe distance from Pipe states that following another vehicle at a safe distance is to allow at least the length of the car between you and the vehicle ahead for every ten miles of speed at which you are traveling. This car-following model can be seen in Figure 2.6.

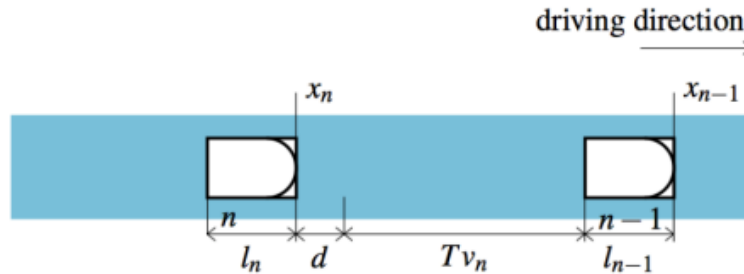


Figure 2.6: Pipes Safe-Distance Model. Source: [4]

Figure 2.6 shows that the position x_n , of the n th vehicle, is determined by the position of the leading vehicle, x_{n-1} and the safe distance between them. This safe distance is constant and is given by the distance when the vehicle is at complete stop d , the vehicle length l_{n-1} and a safe stopping distance Tv_n . The time increase is represented by T and v_n represents the speed.

Next, we discuss a new car-following model. The Gazis-Herman-Rothery (GHR) [23] family of models, presented in 1958. The GHR model is known as the “general car-following model”. Figure 2.7 shows this model and its notation.

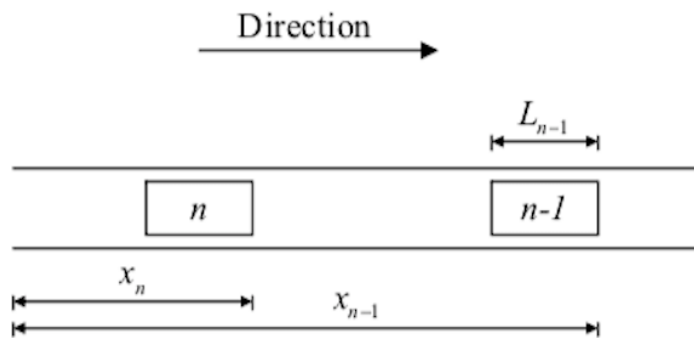


Figure 2.7: Gazis-Herman-Rothery Car-Following Model. Source:

Notice figures 2.6 and 2.7, utilize similar car-following notations. The graphical representation of the vehicle’s safe distance model is the same. It should be noted that every car-following model utilizes its personalized notation, but they all behave similarly. To prevent confusion, the variables used in the GHR model are defined as follows.

- a_n Acceleration, vehicle n , [m/s²]
- x_n Position, vehicle n , [m]
- v_n Speed, vehicle n , [m/s]

Δx	$x_{n-1} - x_n$, space headway, [m]
Δv	$v_n - v_{n-1}$, difference in speed, [m/s]
$v_n^{desired}$	Desired speed, vehicle n , [m/s]
L_{n-1}	Length, vehicle $n - 1$, [m]
s_{n-1}	Effective length ($L_{n-1} + \text{min gap between stationary vehicles}$), for vehicle $n - 1$, [m]
T	Reaction time, [s]

The relationship between the leading and following vehicle in the GHR model is that of a stimulus-response function. This model states that the acceleration of the following vehicle is proportional to the speed of the follower, the speed difference between follower and leader, and the space headway. The acceleration at time t of the vehicle following is calculated by

$$a_n(t) = \alpha \cdot v_n^\beta(t) \cdot \frac{(v_{n-1}(t-T) - v_n(t-T))}{(x_{n-1}(t-T) - x_n(t-T))^\gamma}, \quad (2.1)$$

where $\alpha > 0$, β and γ are model parameters which control the proportionality. The GHR model can be both symmetrical, meaning it uses the same parameter values for acceleration and deceleration, or unsymmetrical, meaning it uses different parameter values for acceleration and deceleration.

A year after the GHR model was introduced, Kometani and Sasaki [26] proposed another model in 1959. In this model, the distance is calculated as the distance necessary to avoid an accident in the case that the leading vehicle decelerates rapidly. This was the first model of its type presented and with time, improved versions of this model were later introduced. Soon after, a new approach to car-following modeling was introduced by Michaels [27] in 1963. The car-following models that apply this new approach are labeled as action-point or psycho-physical models. They are named this way because these models use thresholds or action points where the driver may change his or her behavior. This allows drivers to react to perturbations in the relative velocity or to the spacing between vehicles when they reach such threshold.

2.3 Gipps' Car-Following Model

Gipps' [28] presented his paper on "A Behavioral Car-Following Model For Computer Simulation" in 1980 where he describes several mathematical formulas utilized in the GHR model as well as the formulas used in his model. The formulas proposed by Gipps' eventually become the basis for the Krauß model. Countless models utilized until now are all variations of the GHR formula previously presented such as the following formula.

$$a_n(t + \tau) = l_n \frac{[v_{n-1}(t) - v_n(t)]^k}{[x_{n-1}(t) - x_n(t)]^m} \quad (2.2)$$

Where $n - 1$ represents the leading vehicle, n represents the previous vehicle, τ is the reaction time of the driver, $x_n(t)$ represents the location of the vehicle n at time t , $v_n(t)$

is the speed of vehicle n at time t , $a_n(t + \tau)$ is the acceleration of the vehicle n at time t plus the reaction time of the driver τ , l_n , k , and m are estimated parameters.

There are some problems with Equation 2.2. In 1972, Seddon [29] indicated that it was desirable for the interval between successive recalculations of acceleration, speed, and location to be only a fraction of the reaction time. The problem with Formula 2.2 is that it requires vast quantities of historical data if the model is used in a simulation program.

For this reason, Gipps' proposed new mathematical formulas and a car-following model with the following properties:

1. The model should mimic the behavior of real traffic.
2. The parameters in the model should correspond to obvious characteristics of drivers and vehicles so that most can be assigned values without resorting to elaborate calibration procedures, and
3. the model should be well behaved when the interval between successive recalculations of speed and position is the same as the reaction time.

Property two can be obtained by creating the model on an explanatory basis instead of a descriptive basis. Properties one and three can only be verified after using the model in the simulation.

2.3.1 Proposed Car-Following Model

Gipps' new model is obtained by setting limits on the performance of the driver and vehicle, which allows calculating a safe speed concerning the preceding (leading) vehicle. Vehicles and drivers must select a speed that will ensure they will be able to completely stop the vehicle without creating an accident if the vehicle ahead came to a sudden stop. The following notation is used for the Gipps' model:

a_n	Maximum acceleration which the driver of vehicle n wishes to undertake
b_n	Most severe braking that the driver of vehicle n wishes to undertake ($b_n < 0$)
s_n	Effective size of vehicle n , that is, the physical length plus a margin into which the following vehicle is not willing to intrude, even when at rest
V_n	Speed at which the driver of vehicle n wishes to travel
$x_n(t)$	Location of the front of vehicle n at time t
$v_n(t)$	Speed of vehicle n at time t
τ	Apparent reaction time, a constant for all vehicles

There will be two constraints applied to the vehicle n . First, it will not exceed the desired speed of the driver and second, its free acceleration should first increase with speed. This represents the engine torque which increases then decreases to zero as the

vehicle approaches its desired speed. From these two constraints we obtain the following inequality:

$$v_n(t + \tau) \leq v_n(t) + 2.5a_n\tau (1 - v_n(t)/V_n) (0.025 + v_n(t)/V_n)^{1/2} \quad (2.3)$$

Inequality 2.3 is purely descriptive. This is the result of plotting instantaneous speeds and accelerations obtained from a monitored car. The vehicle is traveling down an arterial road in moderate traffic and demonstrates that traffic flows freely. Using a descriptive expression yields the simplest calculations, and is considered acceptable since it does not impinge or limit the car-following behavior. The car-following behavior becomes dominant if there is a large distance between vehicles or when traveling too fast to have any effect.

Now, let us consider the braking limitation for the model. If the leading vehicle $n - 1$ begins to brake as severely as desirable at time t , it will come to rest at a point x_{n-1}^* , given by

$$x_{n-1}^* = x_{n-1}(t) - v_{n-1}(t)^2/2b_{n-1} \quad (2.4)$$

where b_{n-1} is negative.

From Equation 2.4, vehicle n following directly behind, will not react until time $t + \tau$. Meaning it will not come to a complete stop before reaching x_n^* , given by

$$x_n^* = x_n(t) + [v_n(t) + v_n(t + \tau)] \tau/2 - v_n(t + \tau)^2/2b_n \quad (2.5)$$

To avoid accidents when braking, vehicle n must ensure $x_{n-1}^* - s_{n-1}$ exceeds x_n^* . This leaves little room for error. To avoid this, Gipps' introduced a safety margin by supposing the driver has an additional delay θ when traveling at $v_n(t + \tau)$ before reacting to the vehicle in front $n - 1$. This gives a true reaction time τ and a safety reaction time $\tau + \theta$ which will appear in the following equations. The limitation on braking requires the following

$$x_{n-1}(t) - v_{n-1}(t)^2/2b_{n-1} - s_{n-1} \geq x_n(t) + [v_n(t) + v_n(t + \tau)] \tau/2 + v_n(t + \tau)\theta - v_n(t + \tau)^2/2b_n \quad (2.6)$$

Without the parameter θ , a single-vehicle approaching a stoplight would travel at the desired speed until having to use its maximum braking capacity. The use of θ causes the vehicle to brake ahead of time and then continue to gradually decelerate as to crawl up to the stoplight. Notice that for vehicle n , following right behind the leader $n - 1$, it is possible to estimate all values in Equation 2.6 except for b_{n-1} , the most severe braking that the leading driver will have. For this reason, let $b_{n-1} = \hat{b}$, then Equation 2.6 becomes

$$-v_n(t + \tau)^2/2b_n + v_n(t + \tau)(\tau/2 + \theta) - [x_{n-1}(t) - s_{n-1} - x_n(t)] + v_n(t)\tau/2 + v_{n-1}(t)^2/2\hat{b} \leq 0 \quad (2.7)$$

If the willingness of the leading vehicle driver to brake hard has not been underestimated and if $\theta = \tau/2$. A vehicle traveling at a safe speed and distance to the vehicle in front will be able to maintain this safety state throughout the entire simulation. Thus, Equation 2.7 becomes

$$\begin{aligned}
& -v_n(t + \tau)^2/2b_n + v_n(t + \tau)\tau - [x_{n-1}(t) - s_{n-1} - x_n(t)] \\
& + v_n(t)\tau/2 + v_{n-1}(t)^2/2\hat{b} \leq 0
\end{aligned} \tag{2.8}$$

Equation 2.8 implies that the safe speed for vehicle n is found between the roots. Given that one of the roots is negative, this root is disregarded, as we are only looking for positive speeds. The positive root gives the following speed,

$$v_n(t + \tau) \leq b_n\tau + \sqrt{\left(b_n^2\tau^2 - b_n \left(2 [x_{n-1}(t) - s_{n-1} - x_n(t)] - v_n(t)\tau - v_{n-1}(t)^2/\hat{b}\right)\right)} \tag{2.9}$$

thus, under severe braking we have

$$v_n(t + \tau) < b_n\tau + v_n(t). \tag{2.10}$$

if it is assumed that vehicle n is capable of braking more than the desired braking rate. For this to occur, the driver of vehicle n chooses a speed with respect to a desired (most severe) braking rate but has the possibility to brake harder if needed.

Equations 2.3 and 2.9 represent two limitations on the speed of vehicle n at time $t + \tau$. When Equation 2.3 is the limiting condition for a considerable amount of vehicles, the traffic flows freely. When Equation 2.9 is the limiting condition for all vehicles, a congested flow forms as rapidly as the volume of vehicles allows it. Thus, if we assume that the driver of vehicle n travels as fast as safely and at the speed limit, the new speed can be calculated by

$$\begin{aligned}
v_n(t + \tau) = \min \left\{ v_n(t) + 2.5a_n\tau(1 - v_n(t)/V_n)(0.025 + v_n(t)/V_n)^{1/2}, \right. \\
\left. b_n\tau + \sqrt{\left(b_n^2\tau^2 - b_n \left[2 [x_{n-1}(t) - s_{n-1} - x_n(t)] - v_n(t)\tau - v_{n-1}(t)^2/\hat{b}\right]\right)} \right\}
\end{aligned} \tag{2.11}$$

The transition of $v_n(t + \tau)$ between both terms in Equation 2.11 occurs smoothly. The limitations imposed by the second (safety) term in Equation 2.11 have an effect that works before it is required to decelerate severely. The only times this model does not transition smoothly is when the leading vehicle $n - 1$ leaves the simulation or brakes harder than the following vehicle n has anticipated. It also occurs when a different vehicle is inserted in the gap between the leading and following vehicles. These, however, are the circumstances where real traffic exhibits a rapid transition between acceleration and deceleration (braking) to avoid collisions.

The Gipps' car-following model can imitate real-life traffic behavior using parameters corresponding to characteristics from everyday drivers and vehicles. These parameters can alter the behavior of the simulated flow in a consistent way. One item to note is that only one or two vehicles in the front can accelerate as they like. The other vehicles are constrained by the vehicle in front of them, the same happens when decelerating. In the proposed model, traffic is mainly controlled by the following three factors,

1. V_n , the distribution of desired speeds

2. τ , the reaction time for drivers, and
3. \bar{b}/\hat{b} , the ratio of mean braking rate to driver's estimates of the mean braking rate

where the distributions of acceleration a_n , braking or deceleration b_n , and the effective size s_n , govern the individual behavior of the vehicles in the simulation.

Lastly, this new model has an advantage when it comes to its calculation speed. Given that Equation 2.9 has square roots and squares but no variables with general powers, it is quick to compute. Gipps' compared his proposed Equation 2.9 with Equation 2.2 and showed that his new car-following model was 15% faster per evaluation. This is significant when considering that Equation 2.2 has to be evaluated several times per reaction time. This makes Gipps' car-following model vastly faster and better.

2.3.2 “Phantom” Vehicle

The “phantom” vehicle [30] is an important concept to understand involving simulations using Gipps' car-following model. This is the method that helps vehicles come to a stop at traffic lights. A vehicle, according to the Gipps' model will adjust its speed depending on its position and the speed of the vehicle in front. Since there are no parameters designed to make a vehicle stop at traffic lights, the term “phantom” vehicle was introduced. The way it works is that when the traffic light turns red, this notional “phantom” vehicle will be placed in front of the leading vehicle such that the leading vehicle will follow behind it, and come to a stop at the stop sign.

Some characteristics of the “phantom” vehicle are that it must be stationary, thus it has a speed of zero. The space occupied by this notional vehicle is also zero. Lastly, the location of the “phantom” vehicle is right at the stop-line. It is a simple concept that greatly improves Gipps' car-following model. We have explained Gipps' car-following model as well as several of its mathematical formulas. Next, we will discuss a Gipps'-derived model known as the Krauß car-following model, currently implemented by SUMO.

2.4 Krauß Car Following Model

The latest model implemented by SUMO was created by Krauß [24] in 1998 and is known as the Krauß car-following model. This model is a variation of Gipps' model. It is a space-continuous, microscopic model based on safe speed. Krauß model follows the rule that the following vehicle driver must try to keep a distance from the leading vehicle driver and a safe speed that allows him to adapt to the deceleration of the leader. This is currently utilized in microscopic simulations within the SUMO program. We will discuss SUMO more in-depth in Section 2.6. Traffic simulations can be divided into four different categories:

- **Microscopic simulations:** Every vehicle and its dynamics are modeled individually.
- **Advantage:** No need to solve differential equations, thus simulations are computationally faster.
- **Disadvantage:** Very time-consuming having to simulate each vehicle individually.

- **Macroscopic simulations:** Average vehicle traffic flows and dynamics simulated.
Advantage: Faster when modeling large simulations compared to Microscopic.
Disadvantage: The model uses ordinary differential equations. Depending on the size of the simulation, it might require more computational time to run.
- **Mesoscopic simulations:** Mixture of both macroscopic and microscopic simulations.
- **Submicroscopic simulations:** Each vehicle and the actions performed inside the vehicle are simulated (ex. changing gears).
Advantage: Offers precise information especially when simulating individual routes or vehicle emissions.
Disadvantage: Consumes more time than microscopic simulations. There are additional variables to modify for each vehicle individually.

For this work, any car-following model derived from the following mathematical formula is known as part of the Gipps' family [24].

$$d(v_f) + v_f\tau \leq d(v_l) + g \quad (2.12)$$

Equation 2.12 states that the braking distance of the vehicle, the velocity of the follower $d(v_f)$ plus his velocity times his reaction time $v_f\tau$, is less than the braking distance of the vehicle given the velocity of the leading vehicle $d(v_l)$ plus the gap between the leading and following vehicle g . Recall that the following vehicle always travels at a safe speed to avoid any collision with the leading vehicle. If Equation 2.12 occurs, the situation is considered safe.

In the Krauß model, the interaction between models is described using the maximum safe velocity v_{safe} defined as follows

$$v_{safe} = v_l(t) + \frac{g(t) - v_l(t)\tau}{\frac{\bar{v}}{b(\bar{v})} + \tau} \quad (2.13)$$

where v_l is the velocity of the leading vehicle, $g(t)$ is the gap between the leading and following vehicle at time t , τ is the drivers reaction time, and $\frac{\bar{v}}{b(\bar{v})}$ is equal to the time scale constant τ_b . This represents the typical deceleration b that a driver is willing to use. The model uses the following parameters:

- a Maximum acceleration of vehicle (in m^2)
- b Maximum deceleration of vehicle (in m^2)
- v_{max} Maximum velocity of vehicle (in m/s)
- l Length of vehicle (in m)
- ϵ Driver imperfection in holding the wished speed (between $[0, 1]$)
- τ Driver reaction time (1s)

From Equation 2.13, the safe velocity v_{safe} can be greater than the max speed allowed on the road or greater than the max speed allowed by the vehicle due to its acceleration capability. Thus, we select the smallest (minimum) of these values and the obtained speed will be denoted as the desired speed. The formula is as follows

$$v_{des}(t) = \min\{v_{safe}(t), v(t-1) + a, v_{max}\}. \quad (2.14)$$

Assuming the driver is not able to adapt to the desired velocity from Equation 2.14, there is a new formula that simulates the driver imperfection value ϵ times the car acceleration that is subtracted from the desired velocity and a random number obtained by

$$v(t) = \max\{0, \text{rand}[v_{des}(t) - \epsilon a, v_{des}(t)]\} \quad (2.15)$$

From Equation 2.15, the velocity is multiplied by the simulation step equal to one second added to the current position of the vehicle. Obtaining the position for the following time step. This model is a collision-free model. It is computationally faster to simulate given that there are only a small number of equations to analyze. Finally, the Krauß model can also replicate the flow function of the traffic density. This can be seen in Figure 2.8

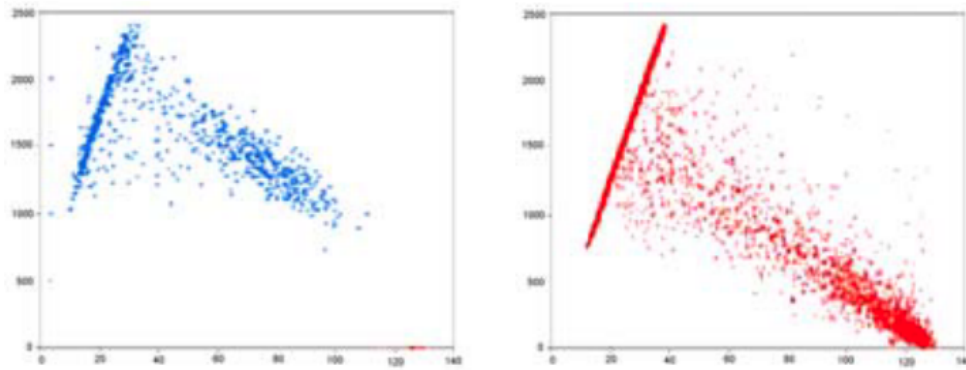


Figure 2.8: Traffic flow as a function of traffic density. Left: Original traffic flow data Right: Simulation results using the Krauß model. Source: [7]

2.5 Jam Dynamics in the Krauß model

Jams in the microscopic simulation tend to grow as long as the amount of vehicles entering the simulation stays relatively high and they wander towards the same location. Imagine there is a high vehicular density in the simulation with a traffic light running at low frequency at the end of the road lane. This traffic light will start causing temporary jams once it turns red, causing vehicles to accumulate behind the leading vehicle once it reaches the stoplight. When the traffic light turns back to green, you can see the model goes back to a free flow.

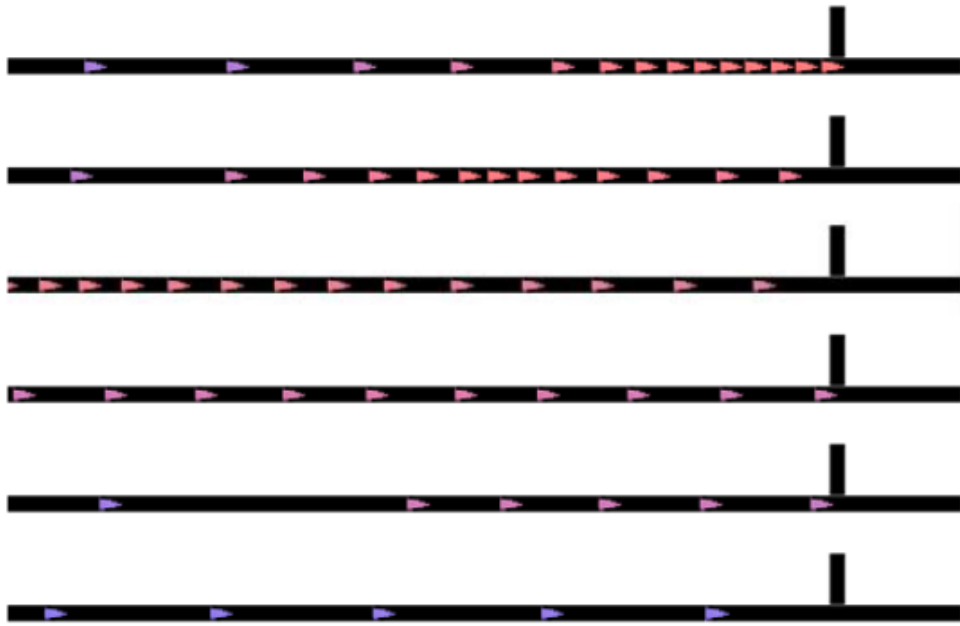


Figure 2.9: From traffic jam to free flow. Top: Traffic jam developing, Bottom: Free flow traffic. Notice there are 25s between each image, red represents standing vehicles, blue represents vehicle travelling at faster speeds. Source: [7]

The formulas in this section are the most important in the car-following model. There are many equations utilized in microscopic simulations, each one used for a different scenario. For instance, a vehicle utilizes different acceleration formulas when in a traffic jam in comparison to when it is in free flow. The same reasoning works with all variables utilized by SUMO. For example the reaction time of the driver τ and the maximum braking b . Since the study of these formulas is not the main focus of this work, we will leave it to the reader. To study the car-following model we encourage the reader to take a look at the publications available on the SUMO website. Next, we shall discuss more in-depth SUMO.

2.6 Simulation of Urban Mobility (SUMO)

SUMO [16] is an open-source, highly portable, microscopic, and continuous traffic simulation package designed to handle large networks. SUMO was created by employees at the Institute of Transportation Systems (ITS) at the German Aerospace Center. SUMO is a great tool to implement vehicular traffic flows. It is used to test the management of traffic and the environmental impact of vehicular congestion.

As stated, SUMO is a free open-source traffic simulation package. Published under the Eclipse Licence, it has approximately 35,000 downloads per year. SUMO has a version that works with both Eclipse and C++, but the version that has the least problems and works perfectly is the Python version. It allows the user to obtain useful output files such as statistical data, charts, and graphs on vehicular emissions. For this work, we focused on the Python version of SUMO.

Next, we present the elements necessary to create a generic SUMO simulation using the city of Ibarra as an example. The same procedure in Section 2.6 was utilized for the city of Guayaquil. To create a traffic simulation, the following variables are to be considered beforehand.

1. Network data (OpenStreetMap, road maps)
2. Traffic Infrastructure (Traffic-light settings, lanes connections)
3. Vehicle flows (Real-life data)
4. Route and Vehicular Flows (Start and end position for vehicles in simulation)

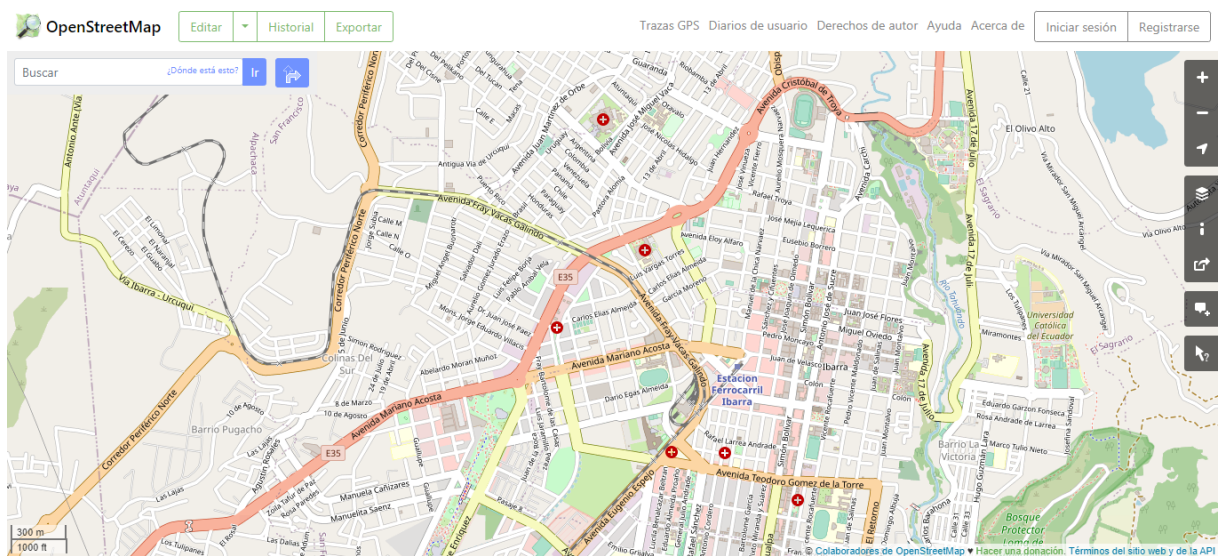


Figure 2.10: Open Street Map (Ibarra). Source: [8]

Figure 2.10 shows the map of Ibarra obtained from the OpenStreetMap (OSM) website[8]. The same was done for the Guayaquil simulation. Using netconvert, we can transform the OSM file into a usable map for our simulation. Once the network data (map) has been converted, it is integrated and modified using NetEdit, seen in Figure 2.11.

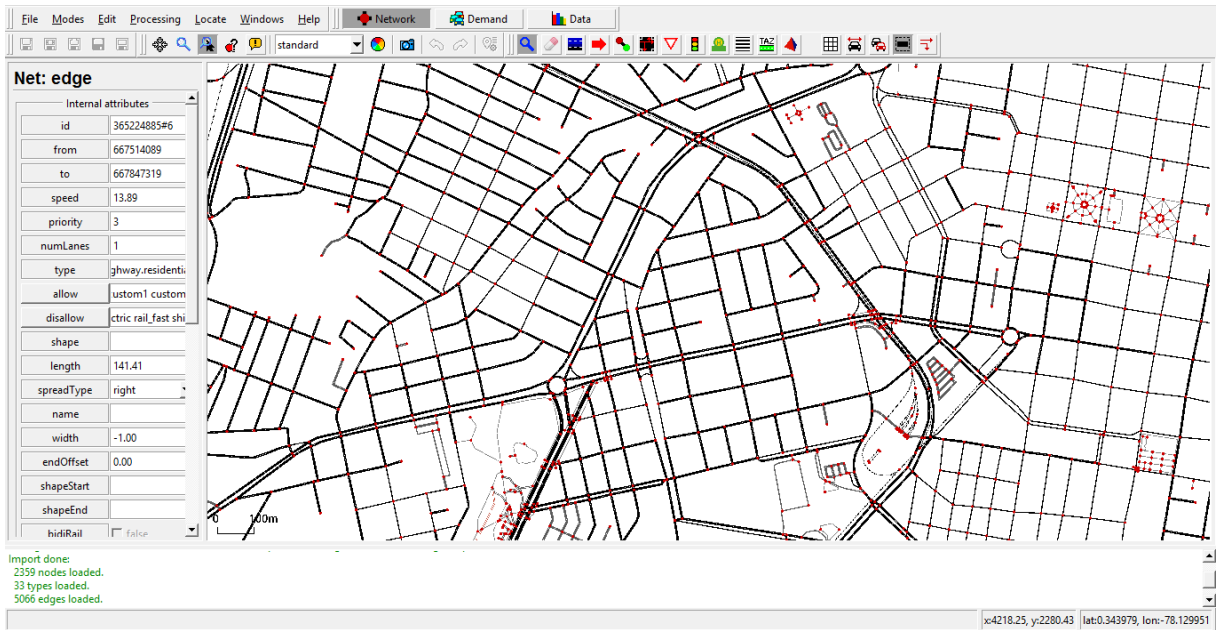


Figure 2.11: NetEdit Program (Ibarra)

Figure 2.11 presents the program NetEdit, a graphical user inter-phase (GUI). NetEdit allows the user to create, delete, and modify road connections and traffic lights for the simulation. This can be seen in figures 2.12 and 2.13.

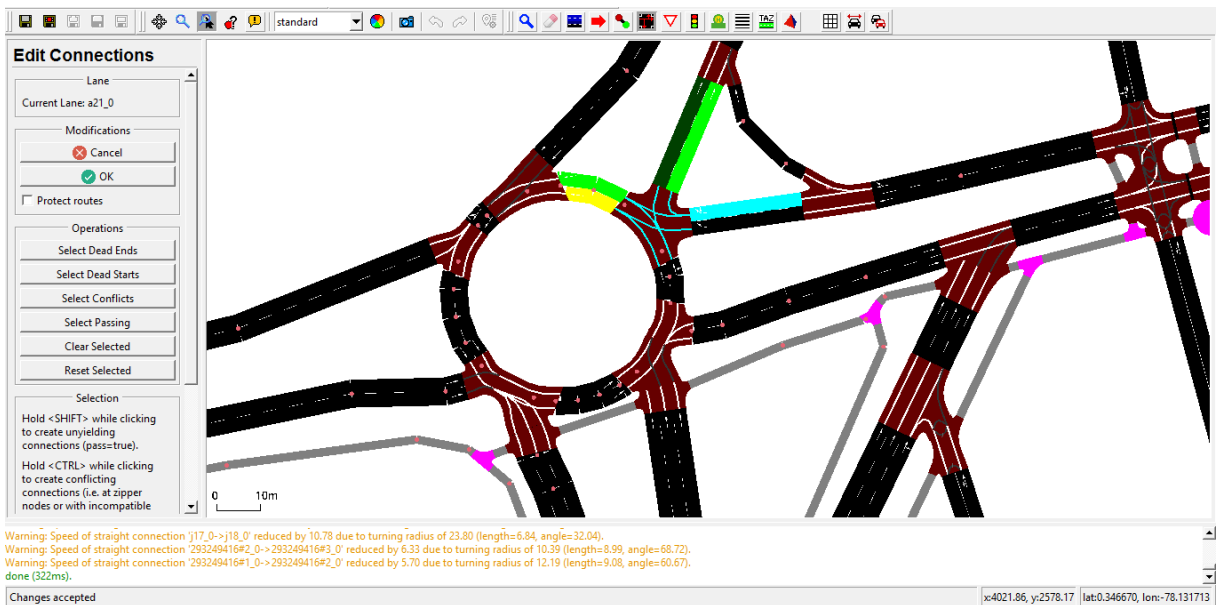


Figure 2.12: NetEdit Road Connections (Ibarra)

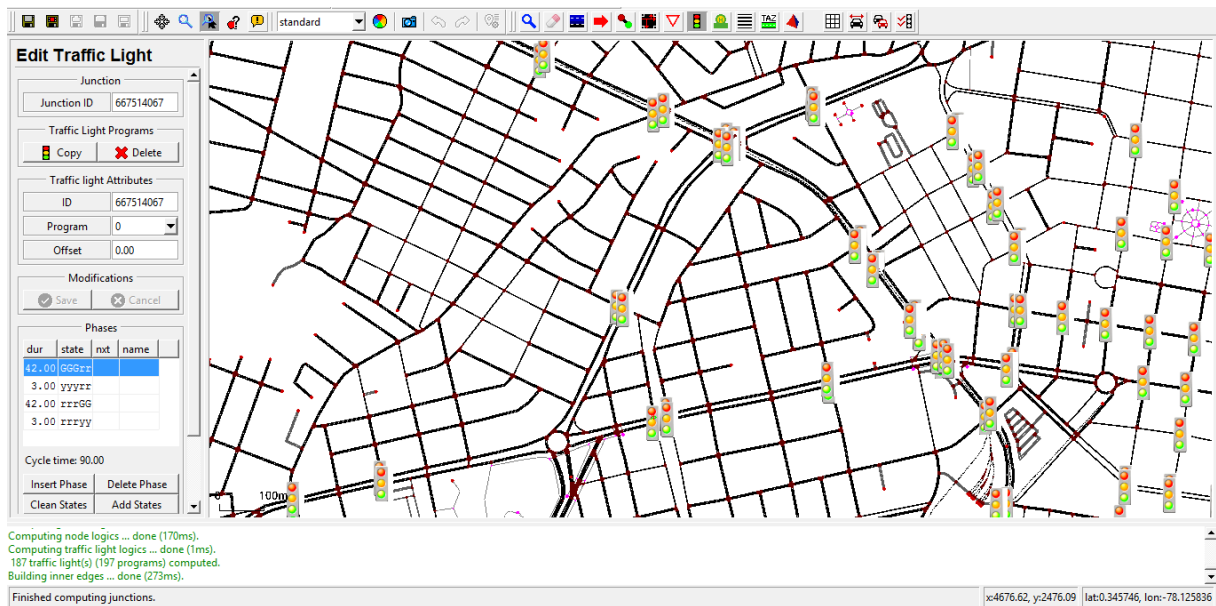


Figure 2.13: NetEdit Traffic Lights (Ibarra)

Once the simulation map has been modified in NetEdit with all the lane connections and traffic light settings, the next step is to define the vehicle routes files and the SUMO configuration file. This will be explained further in detail in Section 4.5.

Once we have the simulation map with all its parameters modified, the routes, and configuration files, we then run the simulation using SUMO GUI. A simulation program that provides useful tools for the analysis of all vehicles throughout the entire simulation.



Figure 2.14: SUMO GUI Simulation (Ibarra)

Figure 2.14 shows the simulation for the city of Ibarra running using SUMO GUI. The same was done for the Guayaquil simulation.

SUMO GUI additionally, allows the user to view the simulation in several windows simultaneously. This provides great utility when simulating large cities or when trying to view the traffic level at specific points.

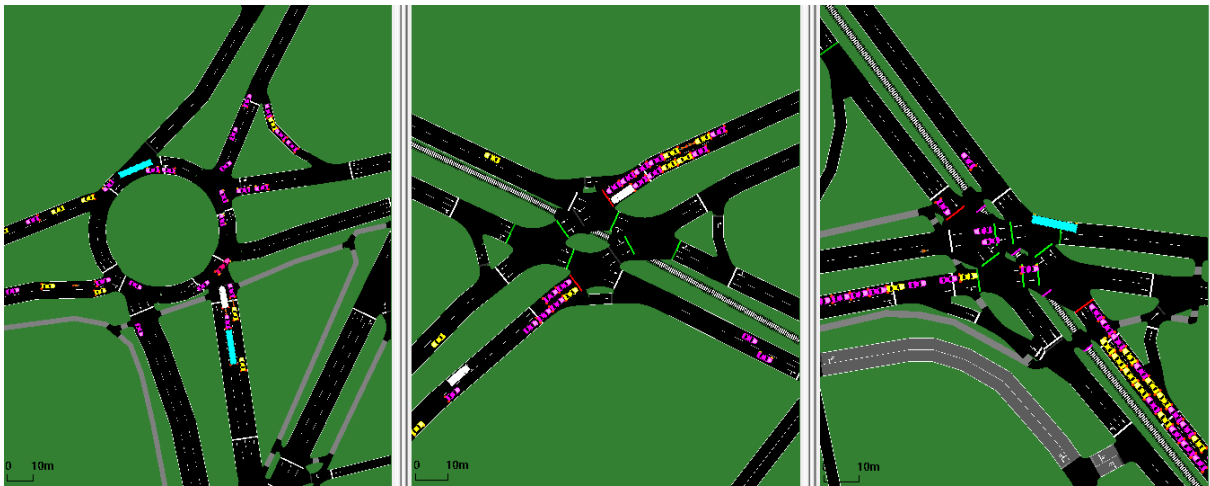


Figure 2.15: SUMO GUI with 3 views for the (Ibarra) Simulation

Figure 2.15 shows the city of Ibarra at points (A), (B), and (C). This is one example of the versatility that SUMO GUI offers the users. Lastly, SUMO GUI can generate graphs on all vehicles while the simulation is running.

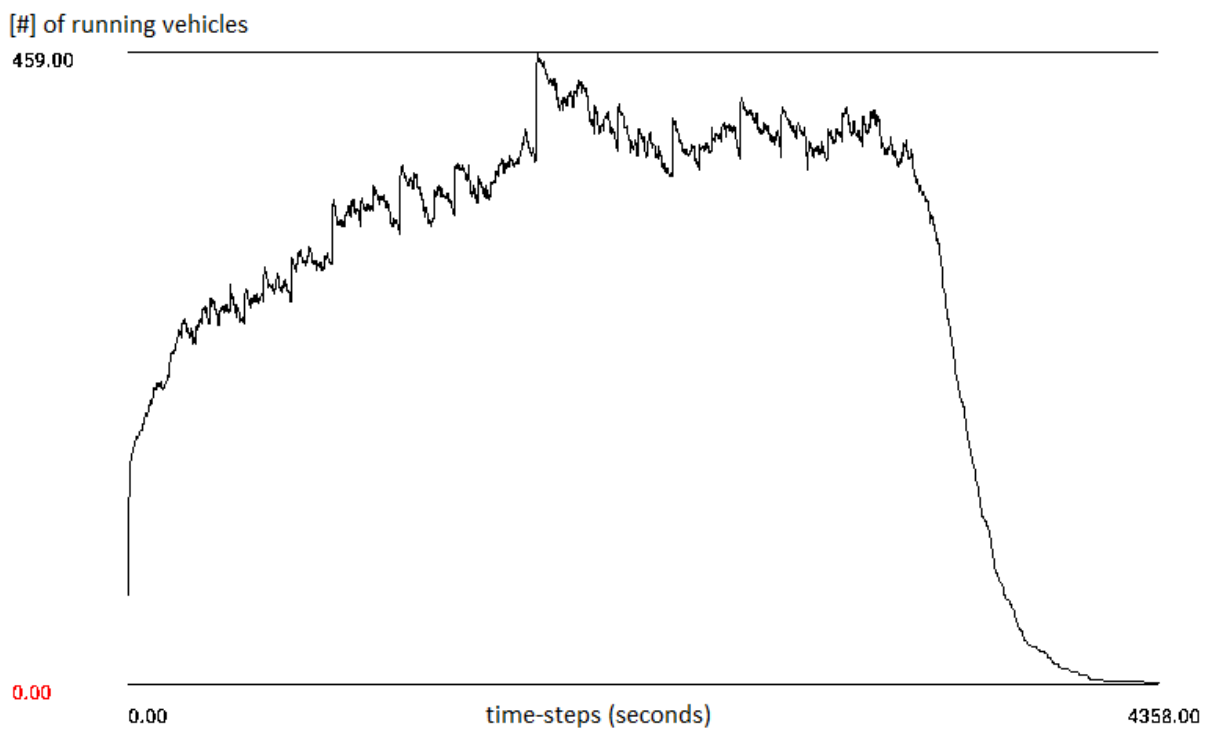


Figure 2.16: Number of running vehicles in the (Ibarra) Simulation

Figure 2.16 was obtained from SUMO GUI and presents the number of vehicles running simultaneously during the Ibarra simulation. The graph begins at “time-step = 0” seconds, and runs until “time-step = 4745” seconds. This is equal to 1 hour and 19 minutes and represents the time for all vehicles to exit the simulation. The peak of 658 vehicles

represents the maximum number of vehicles running simultaneously throughout the city of Ibarra. A further analysis of Figure 2.16 is done in Section 5.1. The same results were obtained for the Guayaquil simulation. These graphs from SUMO GUI are precise and offer an easy method to obtain data on running vehicles during the simulation. The raw data in numbers can also be obtained from output (XML) files. This is explained in detail in Chapter 5.

Using these elements from SUMO and given that traffic simulation models are typically used for stochastic behavior, we can run several simulations. From these simulations, we can draw statistical conclusions on the number of vehicular emissions released into the environment. If the simulation was created using real-world data and it ends behaving as real-life traffic flows, then we can trust the data generated on vehicular emissions to be exact. This is due because SUMO utilizes a measuring system for GHG emissions using the Handbook Emission Factors for Road Transport (HBEFA) [31]. The HBEFA provides emission factors for all current vehicle types such as passenger cars (PC), light-duty vehicles (LDV), heavy goods vehicles (HGV), urban buses, coaches, and motorcycles. Each is divided into different categories for a wide variety of traffic scenarios. Emission factors for all regulated and the most important non-regulated pollutants as well as fuel/energy consumption and CO₂ are included. The HBEFA emissions factors are available online. Everyone can have access to documents on vehicular emissions generated from Germany, Austria, and other European countries. SUMO utilizes this recollected data to automatically calculate all emissions from all vehicles in the simulation. Once the simulation ends it sends back an output file with all vehicular emission values generated during the entire simulation.

Creating a simulation is very time-consuming, especially when using real-life data instead of randomly assigning values. Many variables must be modified for each vehicle independently and certain cities can have vast amounts of vehicles. Approximately 75% of all vehicles in the simulation have to be modified independently. In some cases, all vehicles in the simulation need to be modified independently. To ease this trouble, and mainly for non-real-world macroscopic and mesoscopic simulations, SUMO provides scripts using Python that allows the user to generate random vehicle flows within a city. This script is called the “randomTrips.py” and can save time when running a random scenario.

The methodology and step-by-step guide on how to create a SUMO microscopic simulation will be described more in detail in Chapter 4. Now we will discuss smart cities and the dangers of vehicular emissions.

2.7 Smart Cities

Cities worldwide are currently facing problems such as rapidly increasing population growth, deteriorating infrastructures, global warming, scarcity of resources, air pollution, human health concerns, and traffic congestion. Awareness about the reality each city faces has fueled increased attention in finding solutions to such problems. Billions of dollars are currently being invested in efforts to make cities “smarter” or more intelligent. Especially in aspects such as productivity, sustainability, efficiency, transparency, and effectiveness. A city that fulfills this, is coined the term smart city, intelligent city, digital city, or information city. Notice some of these labels have to do with technology, while others have to

do with physical infrastructures or the development of human capital [32].

Throughout this work, we shall use the term smart city or sustainable city. There are many definitions for smart city, but the definition closest to the focus of this work was defined by Harrison [33]. Smart cities are urban areas that exploit operational data, such as that arising from traffic congestion, power consumption statistics, and public safety events to optimize the operation of city services. This work focuses on exploiting data from traffic congestion in the cities of Guayaquil and Ibarra. The definition from Kahn [34], states that for a city to be “sustainable” it must comply with the following three criteria:

1. Improved quality of life: Access to clean water, clean air, and green areas. These public goods have a direct positive effect on public health and productivity.
2. City Resilience to extreme weather events/natural disasters
3. City greenhouse gas emissions: Developing cities are investing in new infrastructures to reduce emissions. From water treatment, sewage disposal systems, to public transportation and electricity generation. These investments are necessary since short-term decisions have a long-term effect on the carbon footprint affecting cities.

Consider Ecuador, notice that it does meet the first criteria as it has clean water, clean air, and green areas in comparison to other countries. The second criteria are not yet met, as several cities have been affected in the past by earthquakes and volcano eruptions. The third criteria are the least met in Ecuador given that there is not much control on GHG emissions. Industrial factories, mining companies, volcanic ash, and vehicular GHG emissions all contribute to air and waterways pollution in Ecuador. There exists barely any regulations controlling these dangerous contributors to pollution. For this work, we will focus on the third criterion, reducing city GHG emissions. More specifically, analyzing gas emissions from vehicular traffic flows in the cities of Ibarra and Guayaquil.

2.8 Vehicular Gas Emissions

The five most dangerous vehicular GHG emissions monitored by EPA are CO, CO₂, HC, PM_x, and NO_x. Each of these particles can negatively affect the atmosphere, cause respiratory problems, and lower the life expectancy in the country. The most common sources of CO [35] come from incomplete combustion of fuel, wildfires, and industrial burning of fossil fuels. Vehicle exhaust emissions rise the levels of CO in the air. Especially in large cities, it was shown that air pollution from motor vehicle emissions accounts for about 70%. This amount is more than double the air pollution due to heating sources. In some urban areas, the contribution to CO pollution from motor vehicles can exceed 90% [36].

CO molecules can enter the bloodstream through the lungs and create a compound that inhibits the capacity of the blood to carry oxygen throughout the body called carboxy-hemoglobin. This presents complications especially for children and elders suffering from respiratory problems as it is life-threatening to them. With the help of regulations from EPA, vehicles have been modified since approximately the 1970s to lower the amount of CO released into the environment from vehicular combustion. One of these modifications was the implementation of a catalytic converter that was designed to convert CO into CO₂,

reducing CO emissions by up to 80%. Nowadays vehicles are able of reducing more than 90% of CO emissions than back in 1970 [2].

The most common sources of CO₂ [37] come from the burning of fossil fuels such as coal, oil, natural gas, forest fires, land-use changes, and industrial processes. Transports by themselves account for approximately 21% of global CO₂ emissions, with road transport accounting for three-quarters of all transport emissions. Thus, 15% of total CO₂ emissions come from road transport. Cars and busses together contribute to approximately 50% of CO₂ emissions. CO₂ is one of the leading causes of global warming, trapping additional heat in the atmosphere which can lead to ice caps melting and flooding. Health-wise, high levels of CO₂ in the body is harmful given that it can lead to breathing complications or even comma [38].

The most common sources of HC [39] pollution are leaks of toxic organic substances, pesticides, and petroleum which can cause smog and pollute the waterways. The amount of HC in the atmosphere keeps rising each year due to extra pesticides and vehicles being utilized. The increased use of vehicles and automobiles leads to an increase in the use of automobile oil which is the major cause of hydrocarbon contamination in water. This type of contamination occurs when oil from the car drops onto the ground and leaks, where it is then washed off into water streams by runoffs. Once HC particles reach the waterways, carcinogens and neurotoxins are formed. When these particles enter the bloodstream, they can damage the liver, reproductive system, circulatory system, respiratory system, kidneys, and can produce cancer and hormonal problems. In vehicles, HC is released into the environment due to an incomplete combustion process, but some are HC particles are released when decelerating or braking.

PM_x [40] is similar to HC given that some particles are also released from braking, but the majority of emissions are from the burning of fossil fuels. PM represents a mixture of liquid droplets and solid particles found in the air. There are two types of particles. PM₁₀ are particles of size less than 10 micrometers and are usually hard to inhale. PM_{2.5} are fine particles of size less than 2.5 micrometers. Some are so small that they can be only seen using an electron microscope. The most dangerous particles are PM_{2.5} given that they can be easily inhaled and travel deep inside the lungs and bloodstream. While PM_{2.5} is not the only air pollutant that adversely affects health, it is estimated to be responsible for approximately 95% of the global public health impacts from air pollution. Exposure to PM_{2.5} for long periods is linked with higher death rates, cardiovascular diseases such as heart attacks, aggravated asthma, and cancer.

Finally, the last vehicular emission is NO_x [41]. The main sources of NO_x emission are vehicles, electric power plants, and wildfires. Road transports account for a third of all NO_x emissions in heavy traffic urban areas. NO_x is used to represent two different particles in vehicular emissions, nitric oxide (NO) and nitrogen dioxide (NO₂). NO can cause respiratory problems, and is also used in the formation of ozone (O₃). NO₂ is a toxic gas linked to thousands of premature deaths yearly and acid rain. It is estimated that around 7% of the EU urban population is exposed to NO₂ levels above the EU World Health Organization (WHO) limit value. Three-quarters of the urban population is exposed to PM_{2.5} levels exceeding the WHO guideline value. Due to all of the reasons above, it is important to find new ways to help regulate vehicular emissions. This is essential in Ecuador where vehicles utilized are from older years which drastically increases the quantity of pollution in the environment.

Chapter 3

State of the Art

In this chapter, we will discuss the latest technological advances and innovations implemented around the world. We discuss SUMO, car-following models, traffic simulations, smart cities, and vehicular GHG emissions.

3.1 Improving Traffic Flow Modeling and SUMO

There are papers written about SUMO and other simulation programs which verify that the values obtained from the simulation are accurate, feasible, and approximates those seen in real life. These can be used to improve past and new simulations. “Analysis of the traffic behavior of emergency vehicles in a microscopic traffic simulation” written by Bieker-Walz [42] focuses on the behavior of ambulances and other emergency vehicles during a simulation and compares it to the behavior of an emergency vehicle driver in real-life. Results obtained demonstrate emergency vehicles in SUMO tend to cross intersections faster than in real-life situations. This might seem like useless information but greatly contributes to future simulations involving emergency vehicles. The parameters are taken into consideration and modified to improve the final simulation results.

“Design of Traffic Flow Simulation System to Minimize Intersection Waiting Time”, written by Seung-Ju [43], utilized SUMO to simulate a couple of roads starting at Eui University at Busan Metropolitan City and ending at a tunnel nearby. The objective was to create a simulation method that was simple and affordable that could reduce the waiting time of vehicles at intersections. The paper does accomplish a micro-simulation using a small, random sample of vehicles in SUMO. This simulation returns the waiting times for all vehicles at intersections as output. Keep in mind that these results generated will vary drastically once real-life values are utilized in the simulation. Estimate results generated serve as a starting point for future simulations.

3.2 Smart Cities and SUMO

Smart cities have begun looking for new solutions to everyday problems. This includes finding available parking and traffic management. SUMO is an incredible tool for traffic

simulation. It is no surprise it gains fame every day because of its countless applications and uses. One application is the simulation of smart parking systems. In 2018, “Development of a Middleware between SUMO simulation tool and JaCaMO framework”, written by Heijmeijer and Alves [44], was published regarding the implementation of SUMO with the Multi-Agent Parking System (MAPS) which uses the JaCaMo framework. First, a model of an airport parking lot was created using MAPS. Next, utilizing SUMO they were able to run, modify and control all vehicles within the simulation, as well as their parameters.

The simulation was defined with a manager and a driver. Each driver has a trust degree value assigned, which characterizes the commitment of the driver within the parking environment. This parameter was crucial to the simulation as the manager used this trust degree variable to decide if the driver would obtain the requested parking spot. Modifying each parameter independently allowed the simulation to be re-improved and re-optimized until perfected. Once the simulation was perfected they tested SUMO with two different tools. First with CityMobil which simulates an airport-like parking environment, and second with the Jason Programming language. The best results were obtained with MAPS.

Using SUMO and MAPS it was possible to observe the number of vehicles as well as the free and occupied spots in the simulation. The results showed that using both SUMO and MAPS helped achieve a better analysis of the behavior of the driver, easier traffic flow inside the parking lot, and a better understanding of the impact from the trust degree of the driver. The results also showed that the drivers with the highest trust degree received the first parking spot available. This creates more traffic congestion in some lanes than in others. These types of results are useful as they provide insight into new and intelligent parking methods that can be later implemented in real life.

“A SUMO-Based Parking Management Framework for Large-Scale Smart Cities Simulations”, written by Codecá [45], incorporates the mobility simulation framework SUMO with the general-purpose Python Parking Monitoring Library (PyPML). They propose a simple method to simulate, manage, and optimize large-scale cities parking spots. In comparison to the previous paper which uses a micro-simulation, this one uses a macro-simulation which presents a challenge. Large-scale parking management studies are highly complicated to achieve for several reasons. There is a lack of reliable aggregated information, the complexity of city-wide mobility simulation, and the absence of flexible optimization tools to implement and evaluate possible solutions.

Results obtained showed that there is a necessity for large-scale parking management optimization in cities. The paper was able to showcase the capabilities of implementing PyPML with SUMO. Finding a solution to problems such as locating parking spots in large cities is crucial. Keeping cars with engines running while waiting or looking for a parking spot generates tons of unnecessary emissions. This emissions level increases in large cities where parking spots are harder to find like New York, Los Angeles, and Japan. Due to fast migration and the rapidly increasing population growth, finding solutions to these problems will save big cities money and resources. It also contributes to the protection of the environment from dangerous emissions and saves health and valuable time for all citizens.

Another example of SUMO is shown in “Simulating a multi-airport region on different abstraction levels by coupling several simulations”, written by Noyer [46]. This paper created a vehicular, air, and passenger traffic simulation for airport traffic management. This involved the creation of several airports from different regions with high populations

levels. In total, the simulation included three airports of different sizes. All cities were connected by road, railroad, and public ground-level transport where available. Besides these variables, they also modified the individual actions or parameters for all passengers. This includes time spent by each passenger at security checks and during boarding pass checks. This makes the simulation more advanced and requires more computational power. This is time-consuming as the number of parameters to be modified to reach a realistic simulation will be extremely vast.

The author ran several simulation models and recollected the following information when:

- Passenger enters and leaves the main station
- Passenger enters and leaves the airport rail-station
- Passenger enters the airport
- Passenger reaches and passes check-in
- Passenger reaches and passes security
- Passenger reaches and passes immigration
- Passenger reaches his gate
- Passenger leaves the airport and enters aircraft

Once these simulations are implemented using real-world data, they will be able to generate real-life information on traffic congestion and passenger waiting times at airports. This can then be used to find smart solutions to decrease the waiting times at check-in, security, and immigration. This will be greatly beneficial to all passengers as many people tend to lose their flights because they waste too much time at any one of these areas.

Next, we have “Evaluation of Accuracy of Traffic Flow Generation in SUMO”, written by Ma [47]. In this work, there was a human, vehicular, and train simulation created for the Jiangnan zone in Wuhan, China with a population of approximately 683,500 inhabitants. This high population density complicates traveling in the Jiangnan zone. Thus, this paper built a realistic simulation using data from collected public information, websites, and public records to find solutions to this problem. Similar to our work, they used OSM to obtain the map for their simulation. The simulation was created using a macroscopic model from SUMO and ActivityGen. This program works along SUMO to help simulate people going and coming to work or school. They were able to simulate people, vehicles, and trains in the specified area, and obtain statistical data. The data is generated by ActivityGen from its trip files which contain convenient information on inhabitants, car rate, and households.

The eight most representative road sections in the Jiangnan zone were selected. Traffic levels were simulated for 24 hours during an entire week. In addition to simulating the commuting from and to work or home, there are additional actions such as visiting relatives or friends. The results showed that traffic congestion at peak hours such as 8 am or 5 pm during workdays was extremely excessive. The hospitals in the Jiangnan simulation also experienced a high level of traffic jams. This is reflected in real life given that residents

go there accompanied by friends and family members. Results showed that in some areas, traffic congestion was experienced worst at train stations during peak hours and even more on holidays. Normally the number of passengers leaving the Hankou train station is over 70,000 per day. On special or national holidays, this number can be over 140,000. All of these results are beneficial to the Jiangnan zone and residents as they continue to improve the city. Keep in mind that the simulation in this paper was created using information from different sources, most likely outdated. For this reason, results will vary if real-life data was collected and utilized. This generated information provides practical and approximate results.

Lastly, “A SUMO Based Simulation Framework for Intelligent Traffic Management System”, written by Akhter [48] proposes three different algorithms to implement using SUMO to improve the traffic management system. The traffic management system uses Artificial Neural Networks which tend to suffer from clustering strategies. For this reason, the Deep-Neuro-Fuzzy model was implemented. It solved the problem of overlapping weights and removed outliers. A GUI was added which allows the user to control the simulation entirely. Finally, the three different algorithms are tested to trace the optimal route. There were a total of 1,430 vehicles simulated. The model was implemented successfully. The simulation ran well and accurately thanks to the Deep-Neuro-Fuzzy model. The three algorithm results obtained approximated their theoretical values. These new models could lead to improved and precise simulations for vehicular flows.

3.3 Smart Cities and Emissions

Finding ways to reduce emissions in cities is of utter importance for governments worried about the well-being of their citizens. As stated, emissions produce cardiovascular diseases, affect the lungs, cause aggravated asthma, and harm the environment creating floods, smog, acid rain, and trapping higher quantities of heat in the atmosphere. These repercussions cost governments millions in yearly medical and reparation costs. This money can be utilized better by finding intelligent solutions and implementing them as soon as possible.

A proposition for the creation of smart cities, “100 climate-neutral cities by 2030 - by and for the citizens” [49], is a proposition for the creation of climate-neutral and smart cities in Europe from the Mission Board to the European Commission. Cities cover about 3% of the land on Earth, yet they produce about 72% of all global GHG emissions. On top of that, cities are growing at a rapidly fast pace. In Europe, it is estimated that by 2050 almost 85% of Europeans will be living in cities. Therefore, the climate emergency must be tackled by cities and all citizens.

The Mission Board proposes as the goal to support and promote 100 cities in Europe that will commit to transforming and to participate in this smart change. This will greatly benefit the sustainability and improved quality of life in European cities. The Mission Board presents a new model on city governance. It details the role that each citizen must play to help reduce emissions, present new forms of innovations, financing, funding, and everything necessary to ease the transition into becoming a smart city.

Other works like ours, focus on applying traffic flow simulations in cities to reduce vehicular GHG emissions. “Using Smart City Tools to Evaluate the Effectiveness of a Low Emissions Zone in Spain: Madrid Central” by Lebrusán [50], is a paper that utilizes non-

car friendly access zones (pedestrianization measures) called low emissions zones. Green, clean areas where vehicles are not allowed so families can enjoy safely. Madrid Central is the name of one of these low emission zones created in the city of Madrid, Spain. This was designed to verify if it helped decrease emission levels. The study appears to have lasted a total of 30 months, from around 2016 until 2019. It concluded that the creation of low emission zones helped reduce NO_2 , $\text{PM}_{2.5}$, and PM_{10} concentrations levels significantly in the area.

“Traffic Flow Modelling for Pollution Awareness: The TRAFAIR Experience in the City of Zaragoza” by Ilarri [51], is a similar paper that uses SUMO to simulate and estimate traffic flow levels for the city of Zaragoza, Spain. The paper ran different simulations using both mesoscopic and microscopic simulations. It concluded that the mesoscopic model had fewer errors and was better at estimating traffic flows. It is important to notice that both papers implemented new techniques to simulate traffic and obtain data in the country of Spain. Thus, Spain is closer to becoming a smart country if it keeps investing its resources into improving and innovating all of its cities.

“An Incentive-Based Dynamic Ride-Sharing System for Smart Cities”, written by Bakibillah [52], utilizes SUMO and proposes a microscopic traffic simulation model denominated the sharing system. This model reduces fuel consumption, CO and CO_2 emissions, and the average vehicle waiting time while increasing the average speed of the vehicle. The paper presented the formulas utilized as well as the flow chart from the proposed-sharing system. The simulation was implemented in Sunway City, using randomly assigned parameters such as 600 vehicles per hour. Data on average fuel consumption and emission levels were generated from SUMO and then analyzed. The results showed that in certain cases the total fuel consumption and CO and CO_2 emissions did decrease. This is similar to our work but we use real-life data to obtain more accurate results.

“Drastic Improvements in Air Quality in Ecuador during the COVID-19 Outbreak” written by Zalakeviciute [9], utilized nine monitoring stations distributed around Quito and positioned air quality monitoring equipment approved by EPA, to generate data on GHG emissions. They measured the concentration levels of CO, SO_2 , O_3 , NO_2 , $\text{PM}_{2.5}$, as well as meteorological data. The data was collected hourly from January 2020 until April 12, 2020, a month after the quarantine began. Starting March 16, 2020, there was a curfew implemented in Ecuador, and the use of private vehicles was limited to essential tasks such as medicine and food purchases. The number of vehicle use was also reduced in half, as odd and even license plate numbers could only transit every other day. This curfew and regulations implemented throughout all of Ecuador helped reduce air pollution drastically. Zalakeviciute provides information on all the previously mentioned GHG emissions.

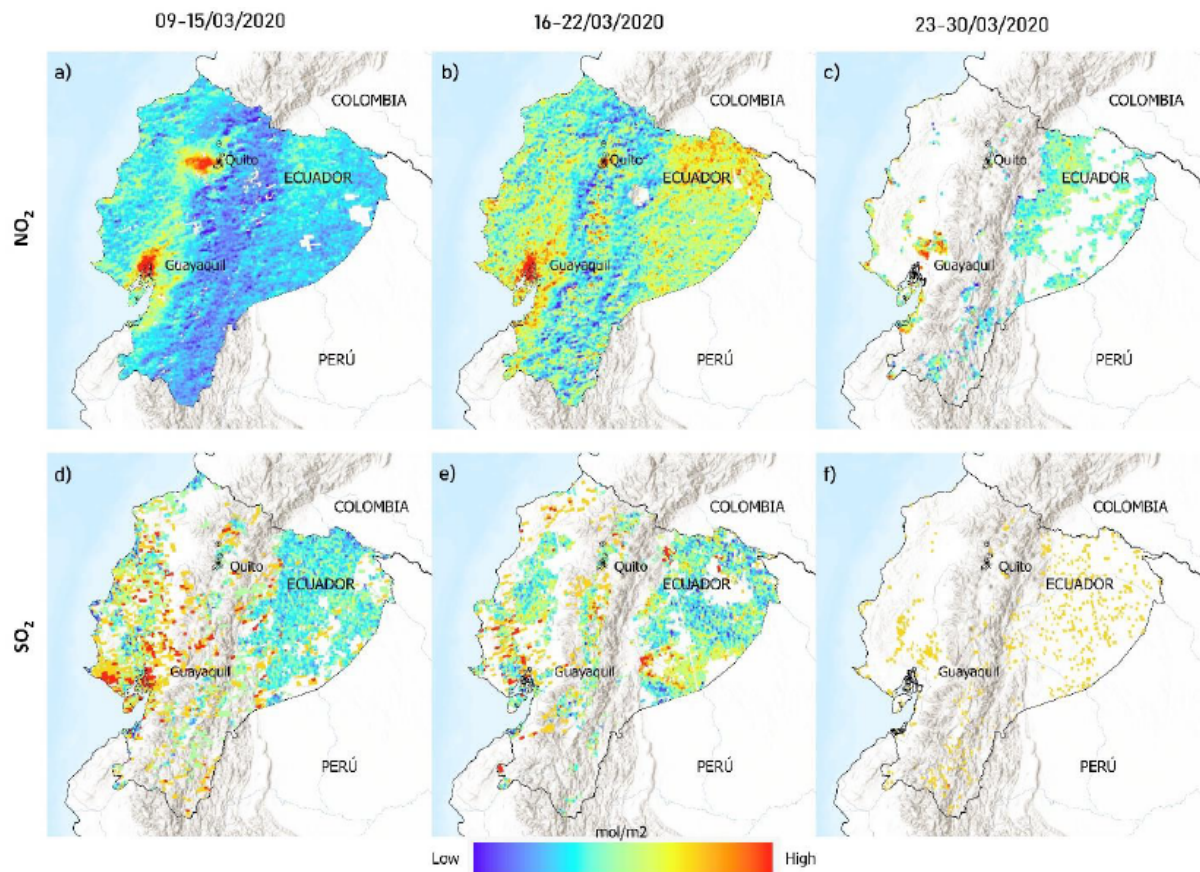


Figure 3.1: Satellite images of NO_2 and SO_2 levels for Ecuador one week before the COVID-19 quarantine. Source: [9]

Figure 3.1 shows the concentration levels for NO_2 and SO_2 before and after the quarantine began. Here, it is clear the impact that vehicle restriction and regulations have on air pollution.

This work is similar to ours since they measure GHG emissions in Ecuador using EPA standards as in the simulations but they require higher costs and longer time to generate similar results. Using real-life simulations with SUMO, it is possible to generate GHG emission data on entire cities or specific points of a city without the need for expensive instruments or having to collect data daily from different locations.

Chapter 4

Methodology

Without a clear and defined method, creating a simulation can be tricky and requires more time than necessary. Small mistakes in the coding such as not defining all vehicles in order of departure time, or missing a symbol can cause the entire simulation to malfunction and give errors. Given the type of simulation, some will require hundreds if not thousands of vehicles defined and modified independently. Looking for errors in extensively large codes utilizes considerable resources and time.

Before running Python scripts to generate statistical data on vehicular emissions, the simulation must be 100% perfect without any flaws. Any additional changes done to the code will generate a completely new simulation and give completely different results. Changing a variable can be both useful and annoying. Depending on the type of simulation implemented, it is useful to modify a variable and generate different emission results. We recommend generating output files once the simulation is perfected. If necessary, variables can be changed later to easily generate new results.

This chapter will present a workflow diagram detailing all steps taken from the identification of the problem to the analysis of obtained results. We then describe and analyze the problem being faced in Ecuador. In the proposed model section, we present an explanation of the real-world data obtained and recorded in the cities of Ibarra and Guayaquil used in the simulations. The next section discusses the algorithm design and all steps necessary for the reader to create a simulation using SUMO. Lastly, we discuss the implementation and testing of both simulations and analyze the generated results.

4.1 Phases of Problem Solving

Figure 4.1 depicts the steps necessary to solve a problem within a city, by creating a real-life simulation and obtaining quick and affordable results. These results can then be used to regulate, reduce or resolve the problem at hand.

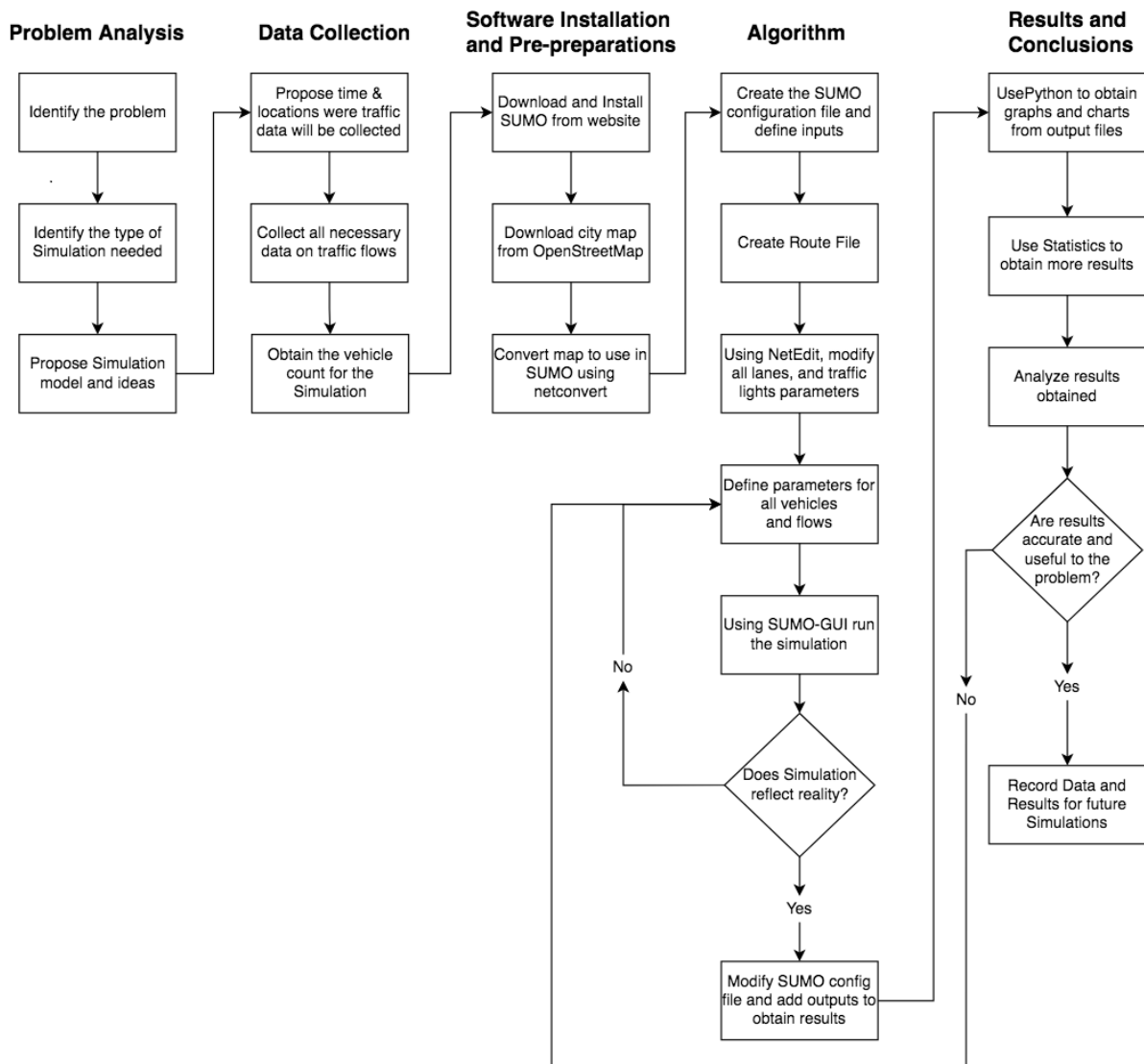


Figure 4.1: Workflow Diagram

4.2 Description of the Problem

One of the main concerns for a smart city is finding ways to control the amount of vehicular pollution being emitted into the environment. This can seriously damage the health of its citizens in the long run as well as being one of the greatest contributors to GHG emissions. The problem in Ecuador is that cities lack resources and information on vehicular emissions. There are no agencies like EPA that are investigating or generating such data. We believe providing a straightforward method to start generating and collecting real-life data on vehicular emissions for cities in Ecuador will be greatly beneficial.

4.3 Analysis of the Problem

Given that cities in Ecuador do not count yet with their own EPA, there is no one funding or tracking the number of vehicular GHG emitted into the environment. There is a lack of important information on the subject. It is the purpose of this work to find a simple and affordable way to create real-life simulations. A real-life traffic simulation was achieved utilizing SUMO and real-life data collected from specific zones in Ibarra and Guayaquil to obtain real concrete values on vehicular GHG emissions. Comparing both city emissions provided information that is beneficial to city officials and those in charge of creating city or vehicle regulations. This marks the starting point for recompilation of data on the five most dangerous emissions, CO, CO₂, HC, PM_x, and NO_x, for the cities of Ibarra and Guayaquil. All additional data compiled on vehicles, traffic flows, and pollution will aid citizens in the future. Especially when implementing the creation of smart cities in Ecuador and new GHG regulations.

4.4 Model Proposal

This work utilized a microscopic model from SUMO to simulate vehicular traffic flows for a small sector in the cities of Ibarra and Guayaquil. We obtained data on vehicular GHG emissions and compared the results from both cities. To implement this model, recollection of vehicular traffic flows was necessary. Data was obtained from strategic locations where all vehicles could be recorded and counted using manual counters. The peak traffic levels in Ecuador are from 7:30 am - 11:30 am and from 5:00 pm - 8:00 pm, depending on the city. The vehicular flow for the simulations of Guayaquil and Ibarra was taken from 10:00 am - 11:00 am.

Guayaquil has more than 380,000 vehicles registered since 2018 [53]. Meanwhile, Ibarra has more than 17,000 vehicles registered since 2007 [54]. Keep in mind that the data obtained was during times of Covid-19 and the pandemic, where people had to stay quarantined for months and vehicles with even and odd license plate numbers could only transit every other day. The number of vehicles transiting in both Guayaquil and Ibarra was half of the normal amount. There would be twice as many vehicles post-pandemic when all license plate numbers are able to transit freely. This is important since it implies that the values of emissions for both cities will be higher than the ones presented in this work if the vehicular data flow is recorded once the pandemic is over.

There was a total of 2918 vehicles transiting for one hour in the small area simulated for Guayaquil. This translates to 0.768% of all vehicles registered in Guayaquil. The total number of vehicles simulated for Ibarra was 3973, which is 23.37% of all vehicles registered. Since Ibarra is a small city, we can simulate and obtain results on a greater percentage of vehicles than in Guayaquil. For this reason, it is advised to begin creating simulations for small cities over large cities as additional information can be generated while using fewer resources.

4.5 Algorithm Design

The following is a step-by-step guide on how to replicate the algorithm for a simpler version than the one presented in this work. We explain the algorithm design using the city of Ibarra as an example. The same procedure in Section 4.5 is utilized for the city of Guayaquil. Building a SUMO traffic simulation in easy steps:

1. First, for Window users, install SUMO and NETEDIT from
<https://www.eclipse.org/sumo/>
SUMO works with Mac but needs HomeBrew installed. For this work, we focused on the Windows version.
2. Next, obtain the map from the area to be simulated from
<https://www.openstreetmap.org>
This website lets us import any city map to be utilized with SUMO.
3. In the OSM website, locate the city you want to simulate and click on “export”. This generates an “.osm” file. Example: Ibarra.osm
4. Open your command (CMD) terminal in Windows and using “dir” and “cd”, locate the folders where you saved the “.osm” file.
5. Once the “.osm” file is located in the CMD terminal, type or copy and paste the following command:

```
netconvert -osm-files Ibarra.osm -o IbarraMap.net.xml
```


The command above takes the file “Ibarra.osm” and converts it to “IbarraMap.net.xml”. The names Ibarra and IbarraMap can be changed as desired.
6. Open NetEdit and open the “IbarraMap.net.xml” file.
Using NetEdit make sure all street turns and traffic lights are set and working correctly.
A tutorial on how to use NetEdit can be found on the SUMO website.
7. Create a new text file and name it “RoutesIbarra.rou.xml”. This is where we create our vehicles and define traffic flows. The name RouteIbarra can be changed as desired. If you need extra help with vehicles types, parameters, and flows, visit
<https://sumo.dlr.de/docs/index.html>
You can also find convenient tutorials to help you.
8. The “RoutesIbarra.rou.xml” file must have the following style

```

<?xml version="1.0" encoding="UTF-8"?>

<routes>
  <vType id="Bus" length="13.0" vClass="bus" maxSpeed="17.67" accel="5.0" decel="7.5" emergencyDecel="10.0"/>
  <vType id="Car" length="5.0" vClass="passenger" maxSpeed="19.5" accel="4.5" decel="6.5" emergencyDecel="9.0"/>
  <vType id="Taxi" length="5.0" vClass="passenger" maxSpeed="19.5" accel="4.5" decel="6.5" emergencyDecel="9.0"/>
  <route id="Col-Panam1" edges="i13 i12 i11 i10 i9 i8 i7 i6 i5 i4 i3 i2 i1 u2 h1 h2 h3 h4 h5 h6 h7 h8 h9 h10"/>
  <route id="Termini-Pan-Obel1" edges="b20 b19 b18 b17 b16 b15 b14 b13 b12 b11 b10 b9 b8 b7 b6 b5 b4 b3 b2 b1 u6"/>
  <route id="Yach-Fray-Redon-Termini1" edges="f13 f14 f15 f16 f17 f18 f19a f19b a11 a12 a13 a14 a15 a16 a17 a18"/>
  <flow id="0b1a" color="205,0,255" begin="0" end="3450" number="104" type="Car" route="Col-B4Redon3"/>
  <flow id="0b1c" color="205,0,255" begin="0" end="3450" number="20" type="Car" route="Col-B4Redon2"/>
  <flow id="8a1" color="0,255,255" begin="0" end="3450" number="4" type="Bus" route="Obel-B4Redon1"/>
  <flow id="8b1a" color="205,0,255" begin="0" end="3450" number="97" type="Car" route="Obel-B4Redon3"/>
  <flow id="57e1b" color="255,255,0" begin="0" end="3450" type="Taxi" number="13" route="Obel-Redon-Yach2"/>
  <flow id="59e1b" color="255,255,0" begin="0" end="3450" number="19" type="Taxi" route="Yach-Mari-B4Redon2"/>
  <flow id="27a1" color="0,255,255" depart="20" end="3600" type="Bus" route="Panam-Mari-Fray-Yach2"/>
  <vehicle id="a33g1" color="255,0,0" depart="25" end="3600" type="Truck" route="Panam-B4Pan2"/>
  <vehicle id="33g1" color="255,0,0" depart="25" end="3600" type="Truck" route="Panam-Co12"/>
  <vehicle id="17g3" color="255,255,255" depart="3048" end="3600" type="Truck" route="Obel-Fray-Co12"/>
  <vehicle id="9d5" color="100,50,0" depart="3066" end="3600" type="Moto" route="Obel-Redon-Panam1"/>
  <vehicle id="17d4" color="100,50,0" depart="3564" end="3600" type="Moto" route="Obel-Fray-Co11"/>
  <vehicle id="34e6" color="255,255,255" depart="3580" end="3600" type="Taxi" route="Panam-Yach3"/>
</routes>

```

Figure 4.2: Route File “RoutesIbarra.rou.xml”

The heading needs to be exactly as seen in Figure 4.2 for the program to work. The “vType id” is the function used to create specific vehicles such as buses, cars, motorcycles, trucks, and trailers. It also allows the user to create personalized vehicles. The “route id” is the name given to the entire lane that we want the vehicle to travel. Notice “r2”, “r3”, . . . are all names of specific roads. All lanes must be connected or else SUMO sends out an error and the simulation will not work.

Finally, the “flow id” is the function that puts together both vehicles and routes created. This is where you can change the variables for several vehicles of the same type but that differ slightly. For example, we have declared only one car in Figure 4.2. Thanks to the “flow” function, we can generate several of the same cars but with different colors and travel different routes.

Recall that this is a simple example. For real-life simulations, the best advice is to create the same vehicle with different parameters to simulate different types of car brands.

9. Extra step for Windows users if you do not see the extension name for your files. You should see the entire name of the file “RoutesIbarra.rou.xml” in your folders. If it only shows “RoutesIbarra” then you must do the following to show the extension name. For Windows 7 or 10, go to the folders tab, go to “View”, then click on “Details”, and finally check the “File Name Extension” box.
10. Finally we must create a text file and name it, “Ibarra.sumocfg”. This file runs the SUMO GUI, which runs the simulations. It is in this file that you can declare input and output files. Figure 4.2 shows an example of this file.

```
<?xml version="1.0" encoding="iso-8859-1"?>

<configuration>
  <input>
    <net-file value="Ibarra.net.xml"/>
    <route-files value="IbarraRoutes.rou.xml"/>
  </input>
  <time>
    <begin value="0"/>
    <end value="2400"/>
  </time>
</configuration>
```

Figure 4.3: SUMO File Example “Ibarra.sumocfg”

Again, the heading must be included exactly as seen. The input is the previously created files. The converted map “IbarraMap.net.xml” and the routes files “IbarraRoutes.rou.xml”. Lastly, we need to include the starting and ending time-step for the simulation. In this example, the simulation begins at “timestep=0” and ends at “timestep=2400”. Notice that each timestep is equivalent to 1 second in real-time.

11. Now open SUMO GUI. Then open the “Ibarra.sumocfg” file, and run the simulation. Notice that SUMO GUI will let you know if there are any mistakes within your files such as missing edges or lanes connections. If presented with any mistakes, fix them in NetEdit and re-run the simulation in SUMO GUI. Repeat this step until no errors appear.
12. Finally, we run some simulation reports and generate output files. The output files are in “.xml” format and give useful data on all vehicles and vehicular GHG emissions. All obtained data will be analyzed statistically in Chapter 5.

It is recommended to add the output line in the “Ibarra.sumocfg” file once the simulation has been perfected. There are several output files available thanks to SUMO. The full lists of these files can be found in the following links

<https://sumo.dlr.de/docs/Simulation/Output.html>

<https://sumo.dlr.de/docs/Simulation/Output/EmissionOutput.html>

13. Now, open and edit the “Ibarra.sumocfg” to include the generation of output files

```
<?xml version="1.0" encoding="iso-8859-1"?>

<configuration>
  <input>
    <net-file value="Ibarra.net.xml"/>
    <route-files value="IbarraRoutes.rou.xml"/>
  </input>
  <output>
    <tripinfo-output value="TripInfoIbarra1.xml" />
    <emission-output value="EmissionsIbarra1.xml" />
  </output>
  <time>
    <begin value="0"/>
    <end value="3200"/>
  </time>
  <report>
    <xml-validation value="never"/>
    <duration-log.disable value="true"/>
    <no-step-log value="true"/>
  </report>
</configuration>
```

Figure 4.4: SUMO File Example “Ibarra.sumocfg” with Output Files

14. Lastly, we can use the output files from the simulations to obtain statistical information regarding vehicular GHG emissions. This was also done for the city of Guayaquil.

4.6 Experimental Setup

We just explained in detail how to replicate a simpler algorithm than the one used in this work. Now, we will show the exact location and area utilized for the simulations of Guayaquil and Ibarra, respectively.

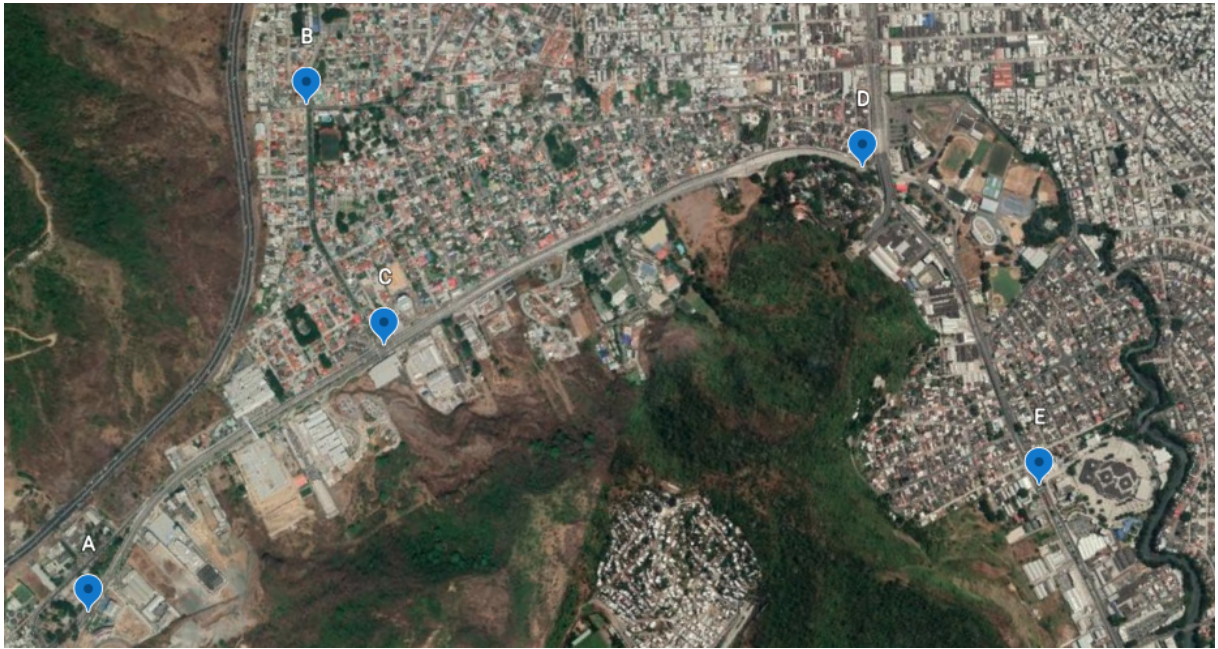


Figure 4.5: Google Earth View for Guayaquil. Source [10]

The area being simulated for the city of Guayaquil is shown in Figure 4.5. This is a one-way traffic flow simulation. All vehicles are inserted into the simulation at two different locations, (A) and (B) and they all travel to the same location (E). The main insertion point (A) is a three-lane road and the second insertion point (B) is a two-lane road. Both roads join at the intersection (C). Then keep traveling until turning to a two-lane road (D). Finally, they leave the simulation after reaching (E). This specific zone was chosen because location (D) is known for creating huge traffic jams during peak hours of the day such as 10 am and at 6 pm. (D) ends up becoming a major bottleneck traffic jam. To recollect data, a camera was set up at a high location where all vehicles at the intersection (C) were visible to record and count.



Figure 4.6: Google Earth View: Guayaquil Intersection (C). Source [10]

From Figure 4.6, a camera was situated on the top floor of the McDonalds restaurant. It recorded the traffic flow from 10:00 am to 11:00 am at the intersection (C) on February 2021. This was the perfect location to obtain the vehicle count as all vehicles from (A) and (B) must pass through the intersection (C) to reach (E). This allowed for a perfect view of all vehicles passing by. Once the vehicle flow was recorded with the camera, using manual counters for each vehicle type, we were able to obtain the total vehicle count. For this work, seven manual counters were used. One for buses, cars, motorcycles, taxis, trucks, trailers, and others (family-size vans). This part was very time-consuming, but also the most crucial to calculate accurate vehicle GHG emissions. For example, simulating only 400 cars per hour when 560 cars are traveling per hour will not give us accurate results on emissions. To be of use, we need to generate irrefutable and precise data.

The results on all vehicular emissions generated from both simulations are presented in Chapter 5.

For the second real-world simulation, an area in the city of Ibarra was chosen. Since Ibarra is a smaller city, we were able to simulate a more compact area and compare emissions obtained with the ones from Guayaquil. This was a two-way traffic flow simulation. This means that additional vehicles flows were created and a greater number of parameters had to be modified independently for the simulation to approximate reality.



Figure 4.7: Google Earth View (Ibarra). Source [10]



Figure 4.8: Google Earth View (Ibarra) ABC Triangle. Source [10]

First, notice the difference in the size of the area simulated from Guayaquil in Figure 4.5 and from Ibarra in Figure 4.8. Points (A), (B), and (C) form a triangle located in the center of Ibarra. This area is where most vehicles transit since these three main roads connect to all routes within the city. For the Ibarra simulation, the vehicular flow was recorded for one hour, from 10:00 am to 11:00 am. The difference is that for locations (A), (B), and (C), the vehicular flow was recorded during different weekdays. To generate more accurate results it is recommended to record traffic on the same day and time, but due to limited resources and personnel, each location was recorded on different days. First, we recorded and simulated the intersection (A) and all points nearby. Then we repeated the same procedure for intersections (B) and (C). Once all three simulations were perfected, by extrapolating the data on all three intersections, we were able to generate a real-life simulation for the city of Ibarra.

For this simulation, there was no specific starting point for vehicles to enter the simulation since it is a two-way traffic flow. To approximate reality, all points, (A) to (I) in Figure 4.7, are used as entry and exit points for all vehicles in the simulation. Due to this, the vehicle count was vastly time-consuming. Several intersections required at most five different vehicle flows, while others required more than twenty different vehicle flows to be created and simulated. All results obtained on GHG emissions for the cities of Guayaquil and Ibarra are found in Chapter 5.

4.7 Implementation

The simulation was conducted in a laptop running Windows 8 Operating System, with an Intel Core i3-3217U CPU @ 1.80GHz 1.80GHz with 8GB memory ram DDR-3 10600. The laptop ran the simulations smoothly and without any lag. Larger and longer simulations can be run with a faster computer and processor.

First, vehicular traffic flows were obtained from specific zones in Guayaquil and Ibarra. This was achieved using a camera to record traffic for one hour, from 10 am - 11 am in both cities. Using manual counters we were able to obtain the vehicular count and flow. The traffic flow was recorded February 24th 2021 for the city of Guayaquil. For Ibarra, the traffic flow was recorded during three different weekdays, on April 24th, 25th and 26th of 2021 due to limited resources and personnel. Given that the data was taken during the Covid-19 pandemic, for safety reasons it was best to record the traffic flow and do the vehicle count later using manual counters. Once the data was generated, we implemented a simulation using SUMO to mimic the traffic recorded. When the simulation behaved like real-life traffic, using Python scripts and ANOVA, we obtained accurate statistical data on vehicular GHG emissions. As stated in Section 2.6, this is possible since SUMO utilizes emission values from the Handbook Emission Factors for Road Transport (HBEFA) for all current vehicle categories [31].

4.8 Testing

For the first simulation created for the city of Guayaquil, this work used random parameters for variables such as the number of vehicles per hour, maximum speed, acceleration, deceleration, and traffic lights timing. The resulting simulation was filled with unrealistic, immense traffic jams that did not assimilate reality as seen in Figure 4.9. It was at this point we realized using real-world data was crucial to achieving a realistic simulation.



Figure 4.9: Unrealistic Simulation in SUMO GUI for Guayaquil at point (D)

Once real traffic data was utilized, numerous trials and errors were run before achieving

the first realistic simulation for Guayaquil. This process was repeated until achieving a perfected, finalized simulation as seen in Figure 4.10. The final version was used to generate data on GHG emissions from all vehicles in the Guayaquil simulation. These results are presented in Section 5.1.



Figure 4.10: Perfected Simulation in SUMO GUI for Guayaquil at point (D)

Next, we present the simulation of Ibarra. Figure 4.11 is one of the trials and errors for the simulation of Ibarra which generated an unrealistic traffic flow simulation.



Figure 4.11: Unrealistic Simulation in SUMO GUI for Ibarra at point (A)

In this specific example for the city of Ibarra, the simulation was implemented using the one-hour vehicle count at location (A) but it does not reflect a realistic traffic flow.

The vehicle flow utilized was for an hour, thus the simulation should last approximately 3600+ time steps or seconds. A real-life scenario simulation lasts approximately 4,500 time-steps (1 hour and 15 minutes). This includes additional time (15-20 minutes) for all vehicles to exit the simulation. It took the simulation in Figure 4.11 over 9000 time-steps (2 hours and 30 minutes) before ending. Numerous modifications to the variables of vehicles and

traffic lights had to be implemented to fix the code. We used the same vehicle count and repeated the process until traffic congestion reflected the real-life traffic flow seen in the city of Ibarra as seen in Figure 4.12.



Figure 4.12: Perfected Simulation in SUMO GUI for Ibarra at point (A)

Figure 4.12 shows the Ibarra simulation once perfected. The simulation is running the same vehicle count as in Figure 4.11. Notice that Figure 4.12 does assimilate real-life traffic for the city of Ibarra at point (A).

As stated previously, creating the traffic flow for all three locations, (A), (B), and (C) at the same time was complex and time-consuming for one person. Thus, we began by doing a simulation only for location (A) such as in 4.12. Next, we created a simulation for location (B) as seen in Figure 4.13.

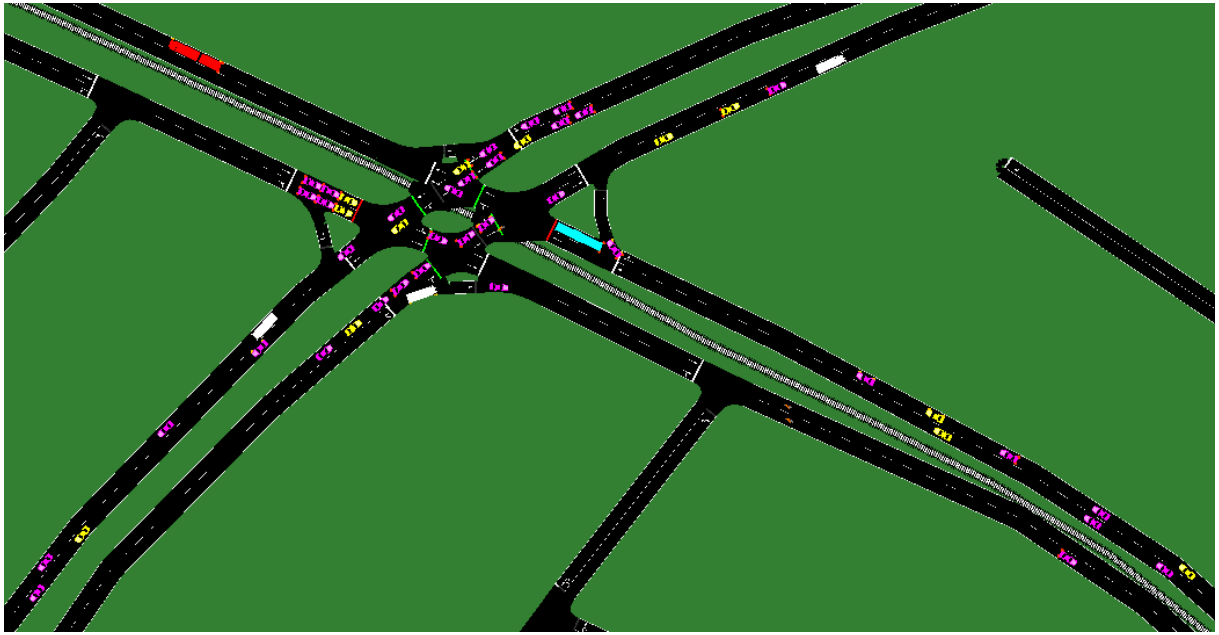


Figure 4.13: Perfected Simulation in SUMO GUI for Ibarra at point (B)

Finally, we repeated the process for location (C) as seen in Figure 4.14. Additional figures can be found in Chapter 5.



Figure 4.14: Perfected Simulation in SUMO GUI for Ibarra at point (C)

Once all three areas were simulated independently, by extrapolating the vehicle flows, we created a simulation integrating all three locations. The final simulation includes a 23.37% of all vehicles registered in Ibarra. This allowed us to generate vehicular GHG emission data from the area seen in Figure 4.8. In the next chapter, we will present and discuss all results obtained from the simulations of Guayaquil and Ibarra, respectively.

Chapter 5

Results and Discussion

This chapter presents the real-life results generated from the simulations for the cities of Guayaquil and Ibarra, respectively. First, we present some graphs generated from SUMO GUI. Followed by graphs generated using the built-in Python scripts. Several scripts can produce graphs such as the number of running vehicles during the simulation, while others create maps illustrating the location of traffic lights in a given area. Lastly, we present the results generated using SUMO and statistical analysis as graphs and tables. In Section 5.2 we discuss our findings in-depth.

5.1 Results

We initiate by presenting the simulation results from the Guayaquil simulation.



Figure 5.1: SUMO GUI Guayaquil simulation at point (C)



Figure 5.2: SUMO GUI Guayaquil simulation at point (D)

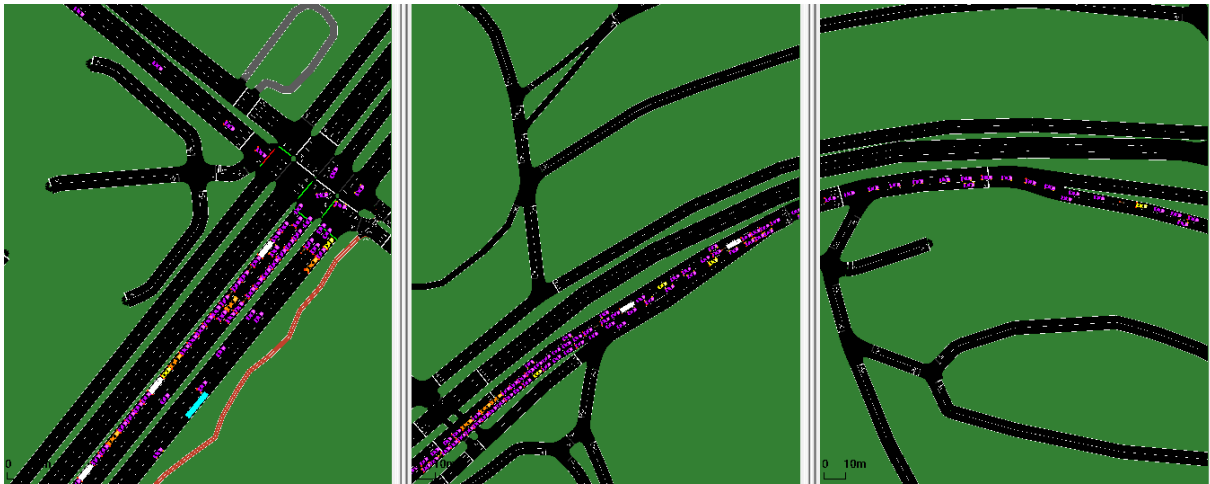


Figure 5.3: SUMO GUI with 3 different views for Guayaquil

Figures 5.1 and 5.2 displays the perfected simulation for Guayaquil at points (C), and (D), respectively. Figure 5.3 shows the simulation of Guayaquil with three different views. The first view is the intersection at point (C) as presented in Figure 4.5. The second view shows the traffic congestion generated between points (C) and (D). The third view shows the bottleneck at point (D).

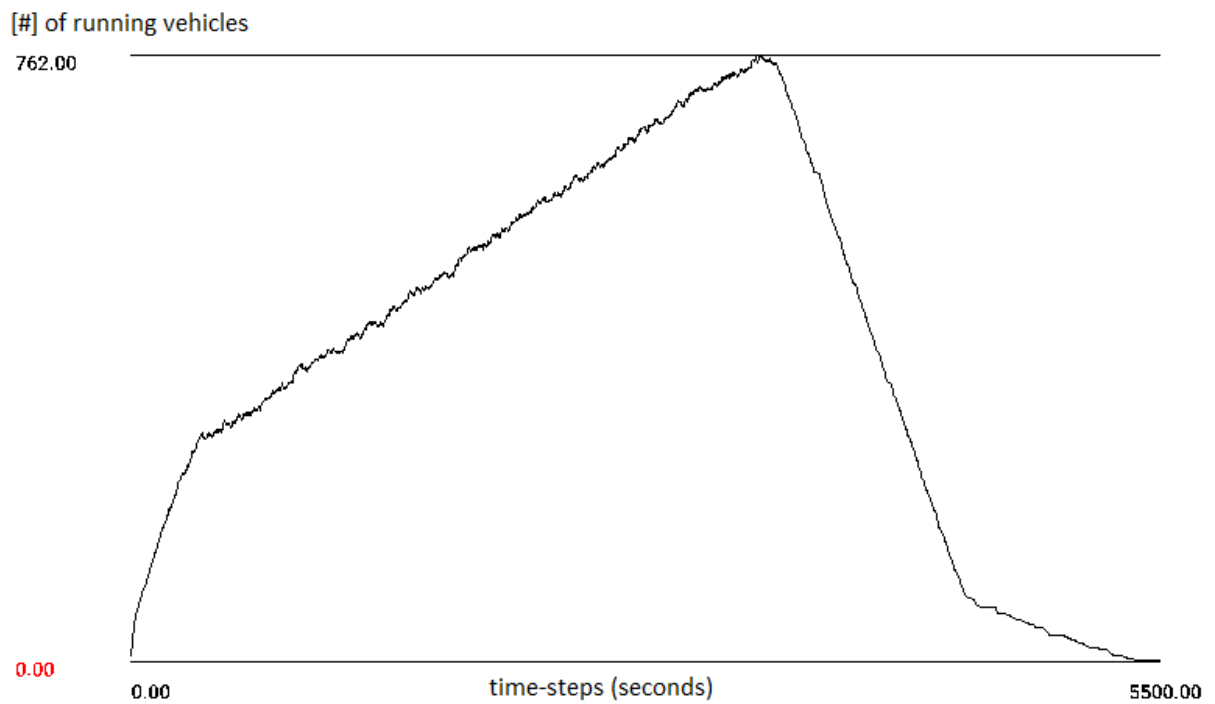


Figure 5.4: Number of running vehicles for Guayaquil using SUMO GUI

Figure 5.4 presents the number of vehicles currently running in the simulation per time-step. This graph was generated by SUMO GUI while the simulation was running simultaneously.

Next, we present the simulation results for Ibarra.

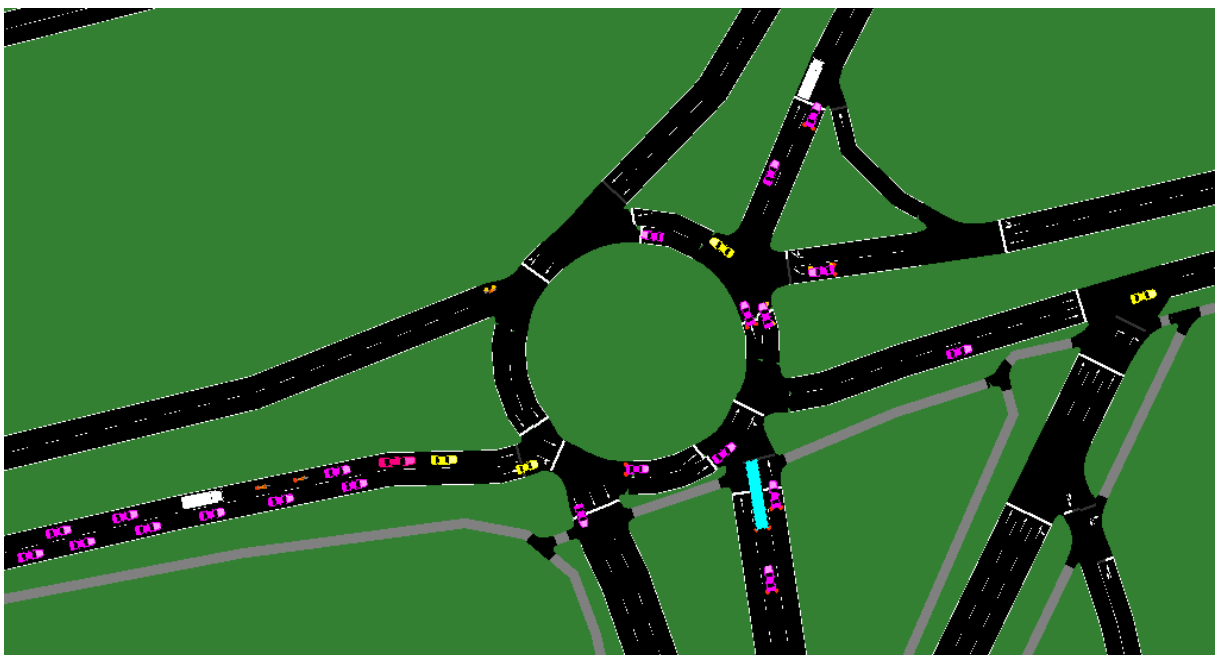


Figure 5.5: SUMO GUI Ibarra Simulation at point (A)



Figure 5.6: SUMO GUI Ibarra Simulation at point (B)



Figure 5.7: SUMO GUI Ibarra Simulation at point (C)

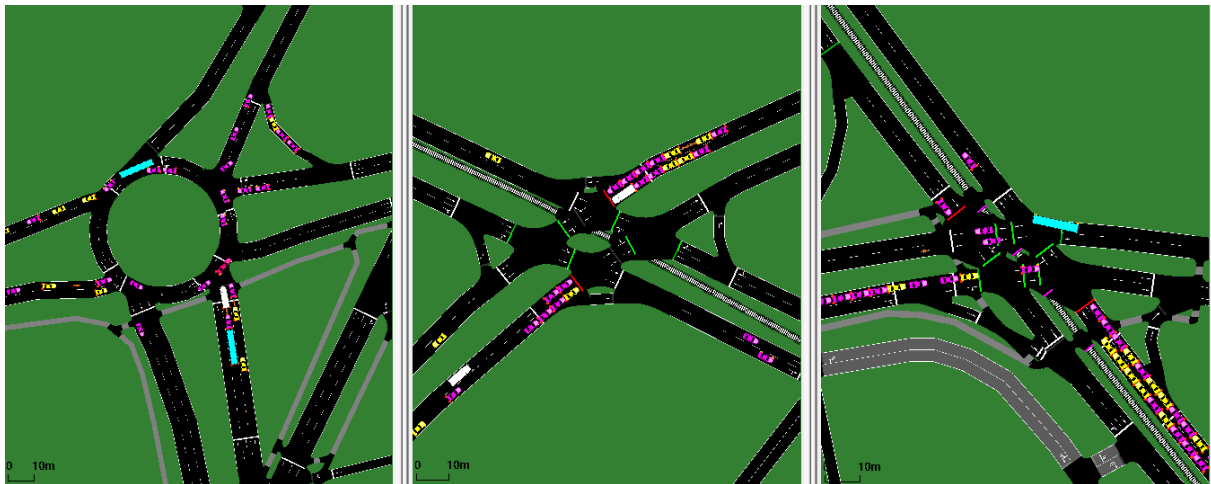


Figure 5.8: SUMO GUI with 3 different views for Ibarra

Figures 5.5, 5.6, and 5.7 displays the perfected simulation for Ibarra at points (A), (B), and (C), respectively. Figure 5.8 shows three different views for the simulation of Ibarra. The first view shows point (A) as seen in 4.8. The second view is of point (B) and the third view of point (C).

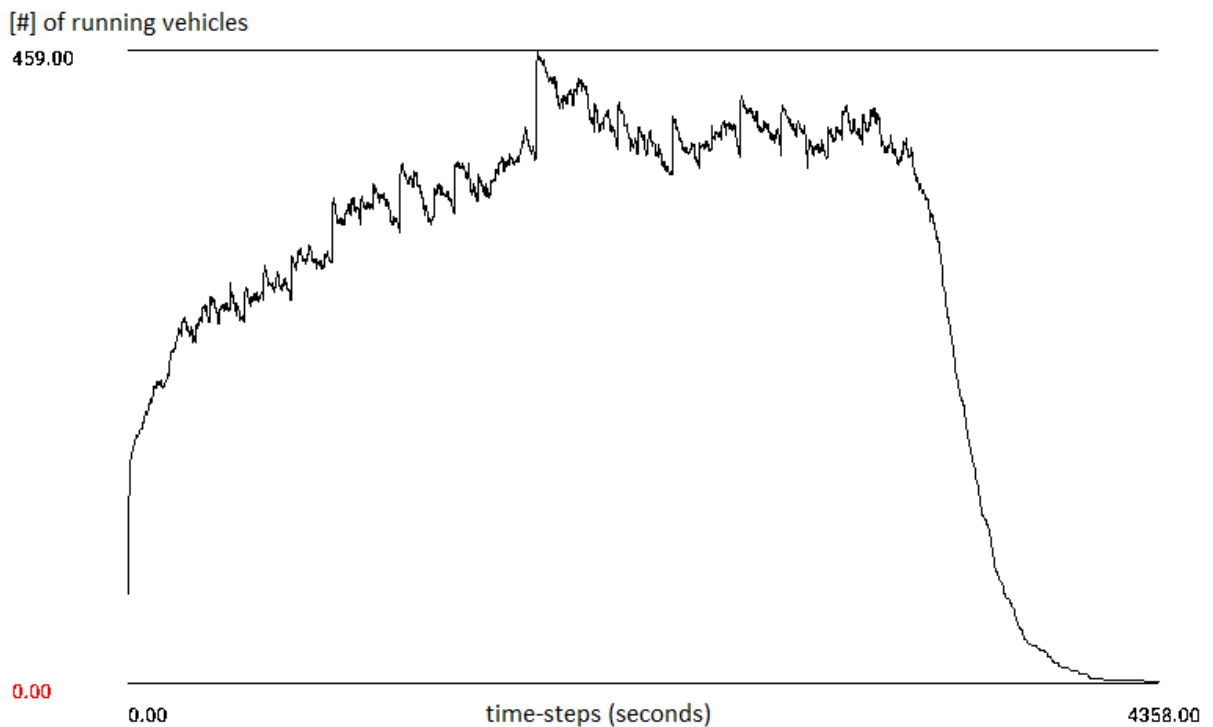


Figure 5.9: Number of running vehicles for Ibarra using SUMO GUI

Figure 5.9 shows the number of vehicles running simultaneously throughout the Ibarra simulation.

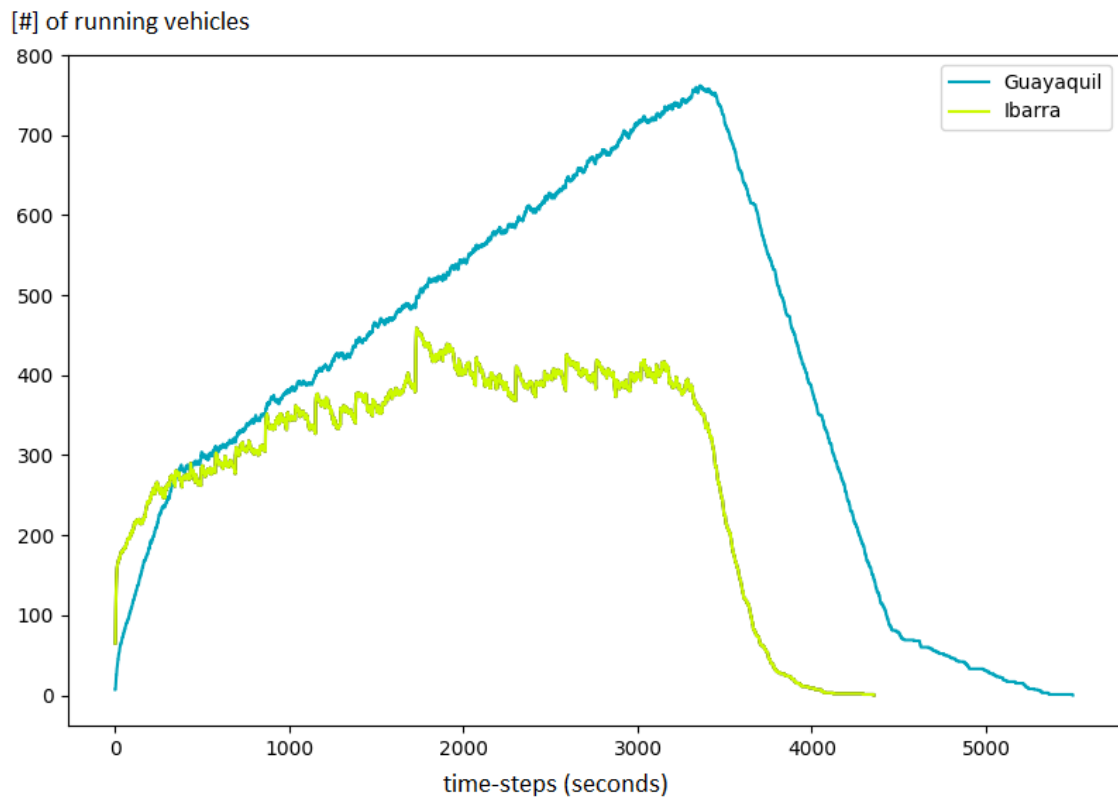


Figure 5.10: Comparison Summary Ibarra & Guayaquil

Figure 5.10 shows a comparison of vehicular GHG emissions between Ibarra and Guayaquil generated using SUMO GUI while running the simulation simultaneously.

Now, we present graphs and maps generated using Python scripts for the city of Guayaquil and Ibarra, respectively.

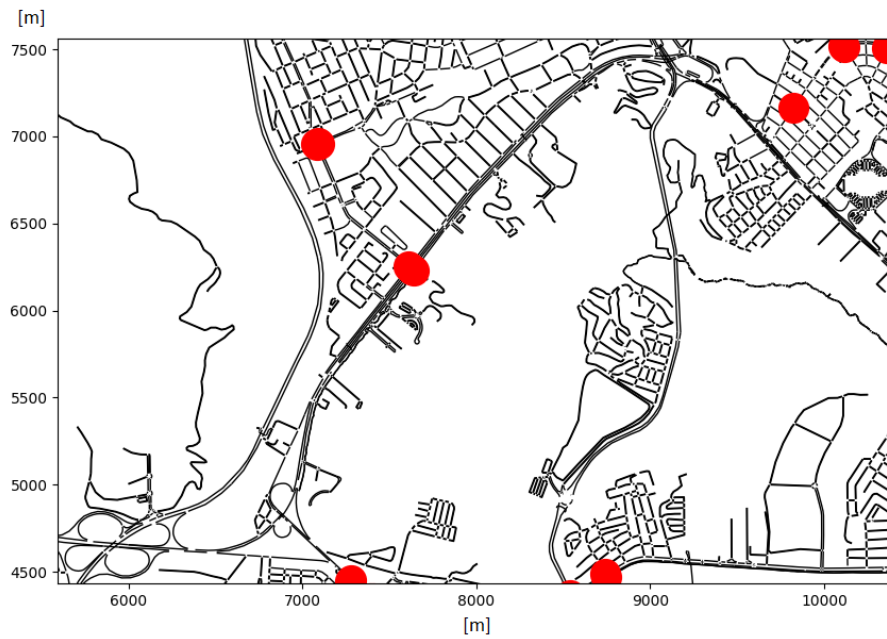


Figure 5.11: Location of traffic lights for selected area in Guayaquil

Figure 5.11 shows the location of all traffic lights in the specified area for Guayaquil.



Figure 5.12: Location of traffic lights for selected area in Ibarra

Figure 5.12 shows the location of all traffic lights in the selected area for Ibarra.

Now, we present some lane speed-limit maps for the city of Guayaquil and Ibarra, respectively.

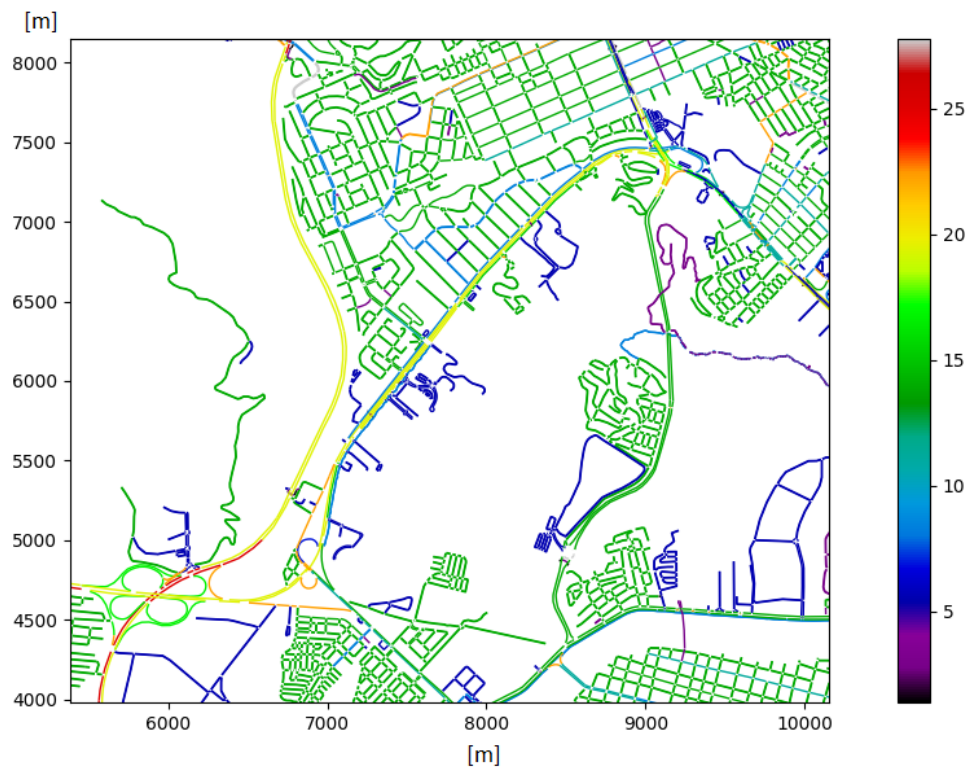


Figure 5.13: Lanes Speed Limit: Guayaquil ($50\text{km/h} = 13.88$, $70\text{km/h} = 19.44$)

Figure 5.13 shows the speed limit for all roads in the selected area for Guayaquil.



Figure 5.14: Lanes Speed Limit: Ibarra ($50\text{km/h} = 13.88$, $70\text{km/h} = 19.44$)

Figure 5.14 shows the speed limits for all roads in the selected area for Ibarra.

Next, we present tables and graphs generated using analysis of variance (ANOVA) and the trip information output files from SUMO. These tables and graphs contain information regarding vehicular GHG emissions for the city of Guayaquil and Ibarra, respectively.

GUAYAQUIL SIMULATION DATA

TOTALS	CO abs (g)	CO ₂ abs (g)	HC abs (g)	PM _x abs (g)	NO _x abs (g)	Fuel abs (Gal)
ALL VEHICLES	165,821.80	5,725,022.04	925.07	294.91	10,432.42	648.79
BUS	380.54	205,115.25	77.08	39.71	1,688.26	23.11
CAR	134,278.24	4,081,900.66	707.74	86.56	1,760.90	463.54
MOTO	14,403.71	257,654.93	58.48	17.82	57.63	29.26
OTHER	7,958.40	197,431.74	40.89	4.38	86.52	22.42
TAXI	7,695.67	246,866.22	40.88	5.22	106.15	28.03
TRAILER	25.36	18,525.75	0.00	3.08	159.10	2.07
TRUCK	1,079.87	717,527.49	0.00	138.14	6,573.85	80.36

AVERAGES	CO avg (g)	CO ₂ avg (g)	HC avg (g)	PM _x avg (g)	NO _x avg (g)	Fuel avg (Gal)
ALL VEHICLES	56.83	1,961.97	0.32	0.10	3.58	0.22
BUS	13.59	7,325.54	2.75	1.42	60.29	0.83
CAR	56.73	1,724.50	0.30	0.04	0.74	0.20
MOTO	72.38	1,294.75	0.29	0.09	0.29	0.15
OTHER	87.45	2,169.58	0.45	0.05	0.95	0.25
TAXI	50.30	1,613.50	0.27	0.03	0.69	0.18
TRAILER	8.45	6,175.25	0.00	1.03	53.03	0.69
TRUCK	14.02	9,318.54	0.00	1.79	85.37	1.04

g/Gal	CO (g)/Gal	CO ₂ (g)/Gal	HC (g)/Gal	PM _x (g)/Gal	NO _x (g)/Gal
ALL VEHICLES					
BUS	16.470	8,877.437	3.336	1.719	73.068
CAR	289.682	8,806.006	1.527	0.187	3.799
MOTO	492.229	8,805.042	1.998	0.609	1.969
OTHER	354.963	8,805.908	1.824	0.195	3.859
TAXI	274.514	8,806.033	1.458	0.186	3.787
TRAILER	12.223	8,928.818	0.000	1.485	76.681
TRUCK	13.438	8,928.867	0.000	1.719	81.805

Figure 5.15: Total vehicular emissions for Guayaquil

Figure 5.15 shows the total values for CO, CO₂, HC, PM_x, and NO_x emissions for the city of Guayaquil. Using a $\log(x + 1)$ transformation, these values are easier to view, we have Figure 5.16.

TRANSFORMATION LOG(x+1)

TOTALS (g)	CO abs (g)	CO2 abs (g)	HC abs (g)	PMx abs (g)	NOx abs (g)	Fuel abs (Gal)
ALL VEHICLES	5.22	6.76	2.97	2.47	4.02	2.81
BUS	2.58	5.31	1.89	1.61	3.23	1.38
CAR	5.13	6.61	2.85	1.94	3.25	2.67
MOTO	4.16	5.41	1.77	1.27	1.77	1.48
OTHER	3.90	5.30	1.62	0.73	1.94	1.37
TAXI	3.89	5.39	1.62	0.79	2.03	1.46
TRAILER	1.42	4.27	0.00	0.61	2.20	0.49
TRUCK	3.03	5.86	0.00	2.14	3.82	1.91

AVERAGES (g)	CO avg (g)	CO2 avg (g)	HC avg (g)	PMx avg (g)	NOx avg (g)
ALL VEHICLES	1.76	3.29	0.12	0.04	0.66
BUS	1.16	3.86	0.57	0.38	1.79
CAR	1.76	3.24	0.11	0.02	0.24
MOTO	1.87	3.11	0.11	0.04	0.11
OTHER	1.95	3.34	0.16	0.02	0.29
TAXI	1.71	3.21	0.10	0.01	0.23
TRAILER	0.98	3.79	0.00	0.31	1.73
TRUCK	1.18	3.97	0.00	0.45	1.94

kg/Gal	CO (kg)/Gal	CO2 (kg)/Gal	HC (kg)/Gal	PMx (kg)/Gal	NOx (kg)/Gal
ALL VEHICLES					
BUS	0.016	8.877	0.003	0.002	0.073
CAR	0.290	8.806	0.002	0.000	0.004
MOTO	0.492	8.805	0.002	0.001	0.002
OTHER	0.355	8.806	0.002	0.000	0.004
TAXI	0.275	8.806	0.001	0.000	0.004
TRAILER	0.012	8.929	0.000	0.001	0.077
TRUCK	0.013	8.929	0.000	0.002	0.082

Figure 5.16: $\text{Log}(x + 1)$ Transformation for vehicular emissions for Guayaquil

IBARRA SIMULATION

TOTALS	CO abs (g)	CO2 abs (g)	HC abs (g)	PMx abs (g)	NOx abs (g)	Fuel abs (Gal)
ALL VEHICLES	158,155.18	5,251,607.48	1,109.92	448.58	16,828.80	594.22
BUS	1,605.95	750,408.39	337.19	165.30	6,536.88	84.52
CAR	93,185.44	2,271,129.60	477.77	50.25	1,000.57	257.91
MOTO	17,606.94	250,918.22	68.55	19.91	57.52	28.50
OTHER	4,044.10	96,659.35	20.69	2.14	42.57	10.98
TAXI	40,132.15	947,663.25	205.06	21.23	418.80	107.62
TRAILER	59.53	38,047.34	0.00	7.78	359.46	4.26
TRUCK	1,394.83	893,178.97	0.00	181.89	8,411.42	100.03

AVERAGES	CO avg (g)	CO2 avg (g)	HC avg (g)	PMx avg (g)	NOx avg (g)	Fuel avg (Gal)
ALL VEHICLES	39.81	1,321.82	0.28	0.11	4.24	0.15
BUS	11.90	5,558.58	2.50	1.22	48.42	0.63
CAR	36.03	878.24	0.18	0.02	0.39	0.10
MOTO	64.49	919.11	0.25	0.07	0.21	0.10
OTHER	60.36	1,442.68	0.31	0.03	0.64	0.16
TAXI	53.65	1,266.93	0.27	0.03	0.56	0.14
TRAILER	9.92	6,341.22	0.00	1.30	59.91	0.71
TRUCK	8.94	5,725.51	0.00	1.17	53.92	0.64

g/Gal	CO (g)/Gal	CO2 (g)/Gal	HC (g)/Gal	PMx (g)/Gal	NOx (g)/Gal
ALL VEHICLES					
BUS	19.001	8,878.621	3.990	1.956	77.343
CAR	361.310	8,805.899	1.852	0.195	3.880
MOTO	617.843	8,804.945	2.406	0.699	2.018
OTHER	368.427	8,805.885	1.885	0.195	3.879
TAXI	372.916	8,805.884	1.905	0.197	3.892
TRAILER	13.970	8,928.866	0.000	1.825	84.357
TRUCK	13.944	8,928.877	0.000	1.818	84.087

Figure 5.17: Total vehicular emissions for Ibarra

Figure 5.17 shows the total values for CO, CO₂, HC, PM_x, and NO_x emissions for the city of Ibarra. Using a $\log(x + 1)$ transformation, these values are easier to view, we have Figure 5.18.

TRANSFORMATION LOG(X+1)

TOTALS (g)	CO abs (g)	CO2 abs (g)	HC abs (g)	PMx abs (g)	NOx abs (g)	Fuel abs (Gal)
ALL VEHICLES	5.20	6.72	3.05	2.65	4.23	2.77
BUS	3.21	5.88	2.53	2.22	3.82	1.93
CAR	4.97	6.36	2.68	1.71	3.00	2.41
MOTO	4.25	5.40	1.84	1.32	1.77	1.47
OTHER	3.61	4.99	1.34	0.50	1.64	1.08
TAXI	4.60	5.98	2.31	1.35	2.62	2.04
TRAILER	1.78	4.58	0.00	0.94	2.56	0.72
TRUCK	3.14	5.95	0.00	2.26	3.92	2.00

AVERAGES (g)	CO avg (g)	CO2 avg (g)	HC avg (g)	PMx avg (g)	NOx avg (g)
ALL VEHICLES	1.61	3.12	0.11	0.05	0.72
BUS	1.11	3.75	0.54	0.35	1.69
CAR	1.57	2.94	0.07	0.01	0.14
MOTO	1.82	2.96	0.10	0.03	0.08
OTHER	1.79	3.16	0.12	0.01	0.21
TAXI	1.74	3.10	0.11	0.01	0.19
TRAILER	1.04	3.80	0.00	0.36	1.78
TRUCK	1.00	3.76	0.00	0.34	1.74

kg/Gal	CO (kg)/Gal	CO2 (kg)/Gal	HC (kg)/Gal	PMx (kg)/Gal	NOx (kg)/Gal
ALL VEHICLES					
BUS	0.019	8.879	0.004	0.002	0.077
CAR	0.361	8.806	0.002	0.000	0.004
MOTO	0.618	8.805	0.002	0.001	0.002
OTHER	0.368	8.806	0.002	0.000	0.004
TAXI	0.373	8.806	0.002	0.000	0.004
TRAILER	0.014	8.929	0.000	0.002	0.084
TRUCK	0.014	8.929	0.000	0.002	0.084

Figure 5.18: $\text{Log}(x + 1)$ Transformation for vehicular emissions for Ibarra

These values are much smaller and simpler to work with especially when graphing skewed values. Next, we present some graphs for the cities of Guayaquil and Ibarra, respectively, that can be generated using ANOVA and the data in figures 5.15 to 5.18.

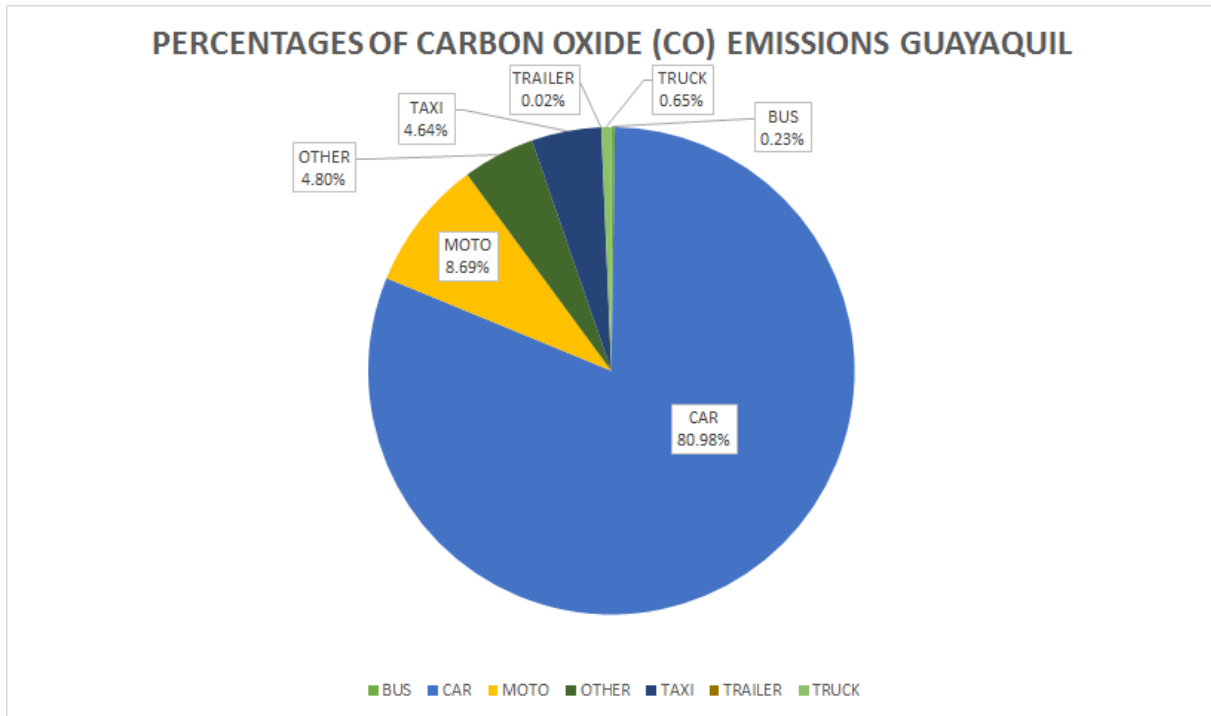


Figure 5.19: Percentage of CO emissions per vehicle for Guayaquil

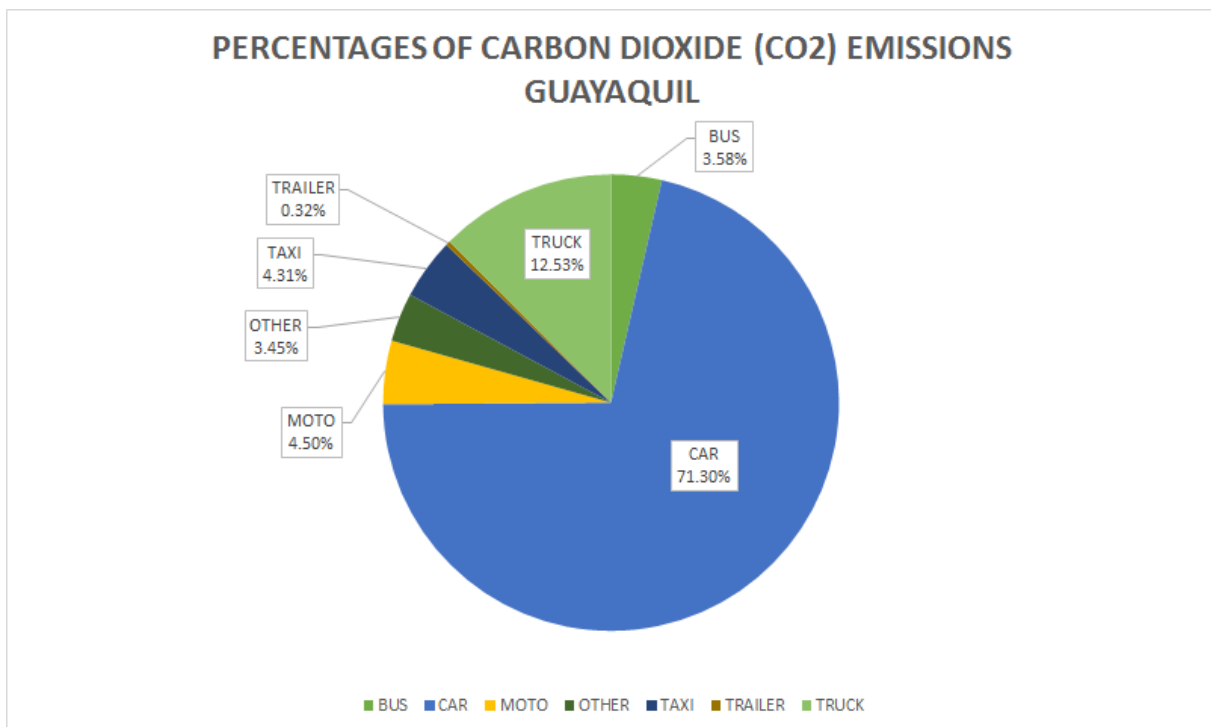


Figure 5.20: Percentage of CO₂ emissions per vehicle for Guayaquil

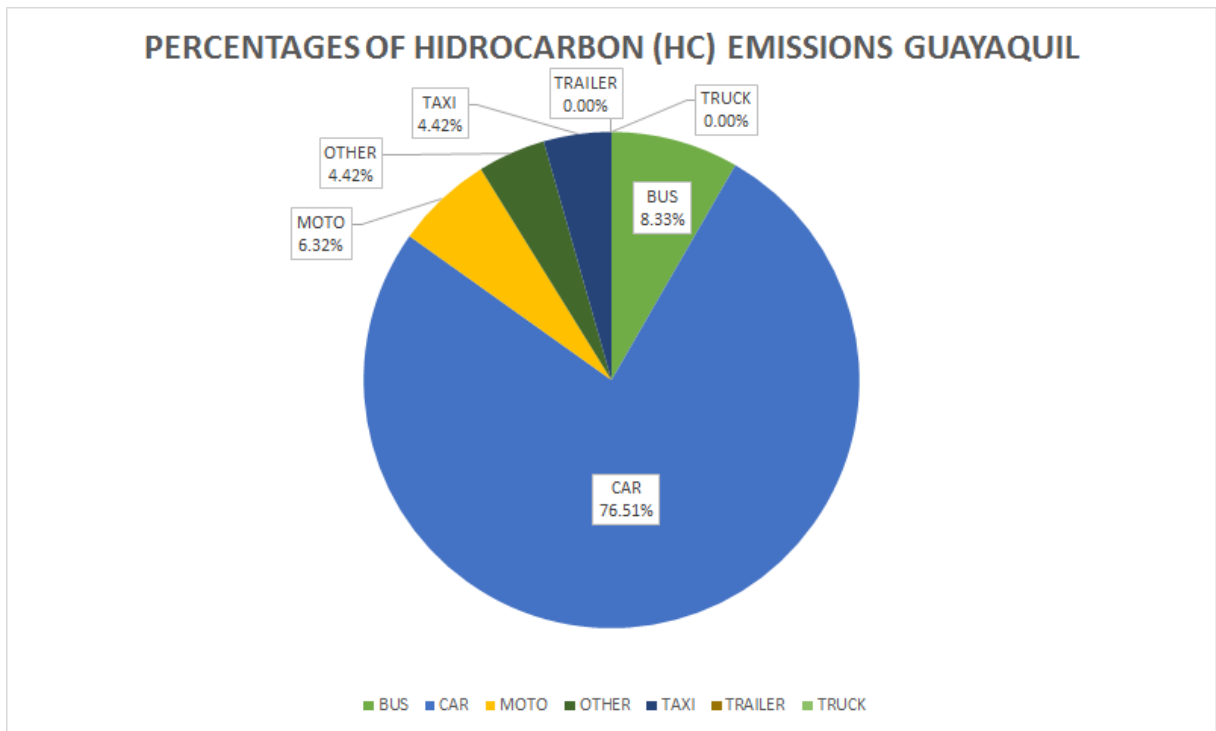


Figure 5.21: Percentage of HC emissions per vehicle for Guayaquil

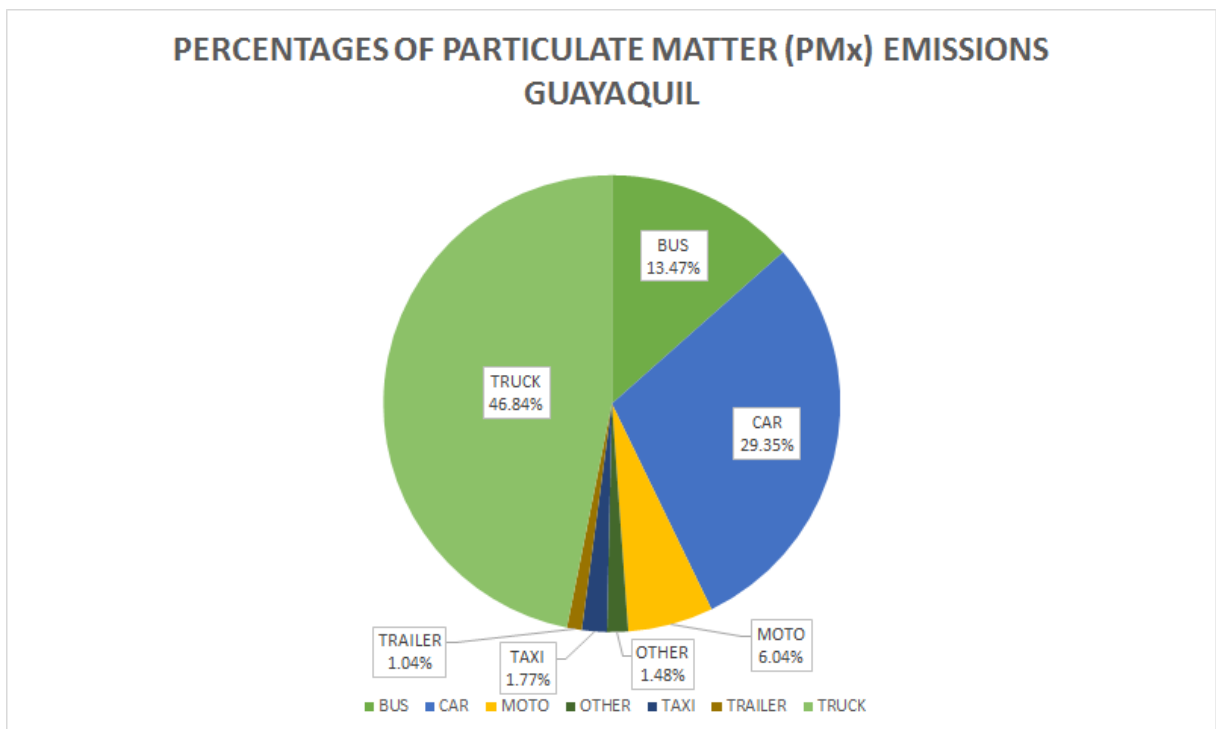


Figure 5.22: Percentage of PM_x emissions per vehicle for Guayaquil

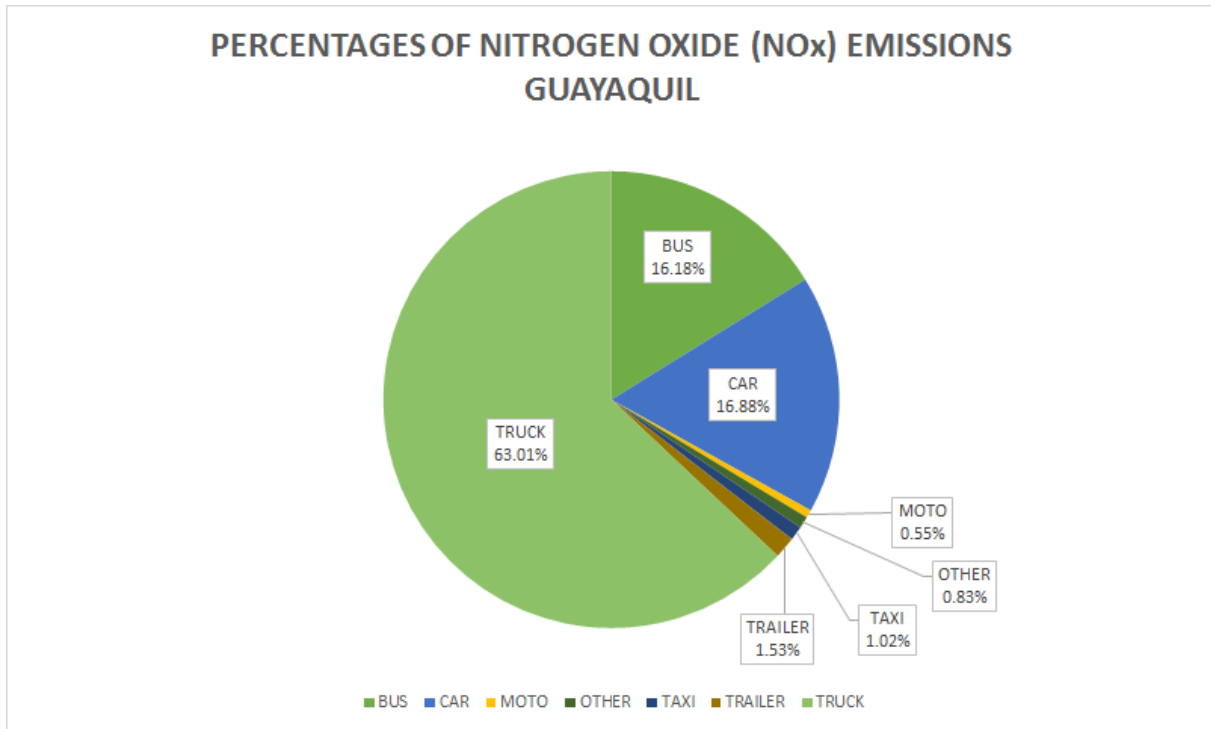


Figure 5.23: Percentage of NO_x emissions per vehicle for Guayaquil

Now, we present the graphs for the city of Ibarra.

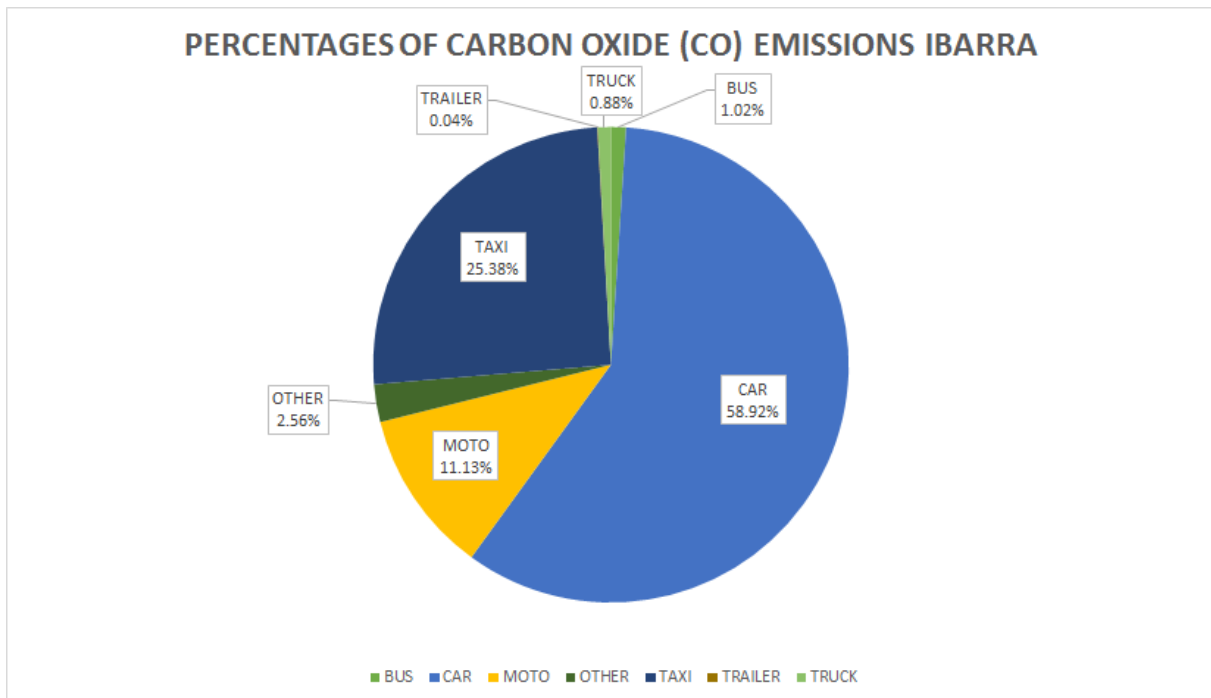


Figure 5.24: Percentage of CO emissions per vehicle for Ibarra

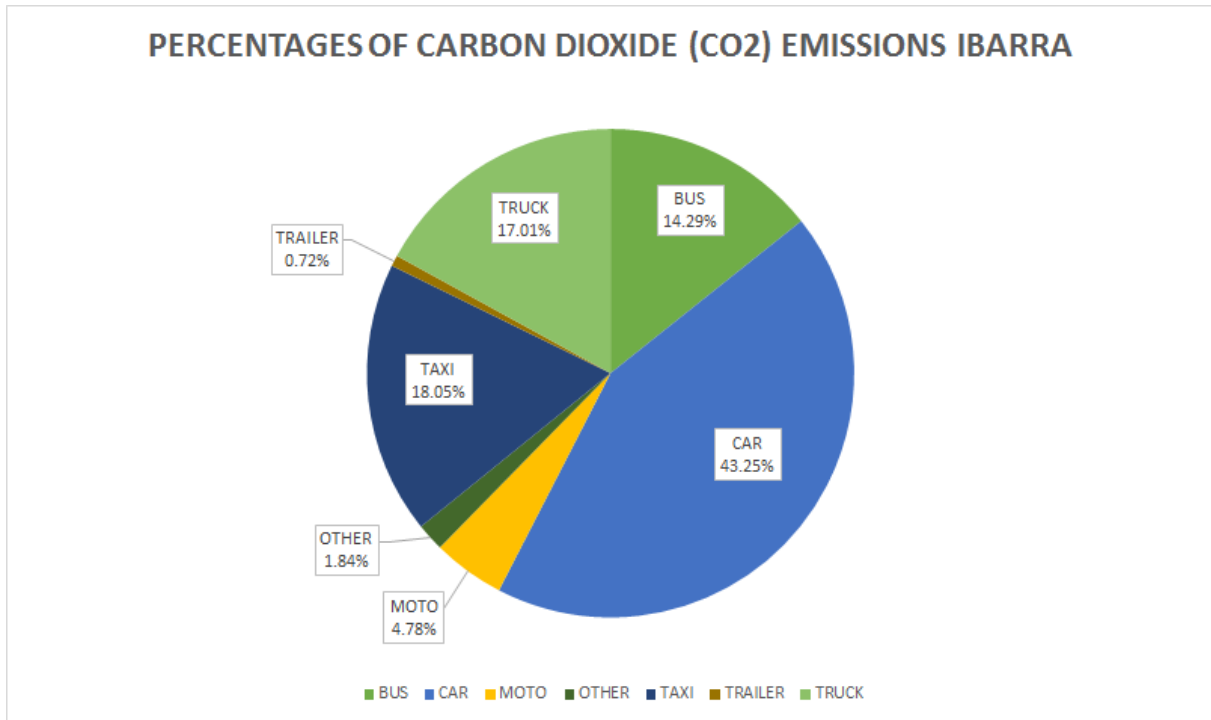


Figure 5.25: Percentage of CO₂ emissions per vehicle for Ibarra

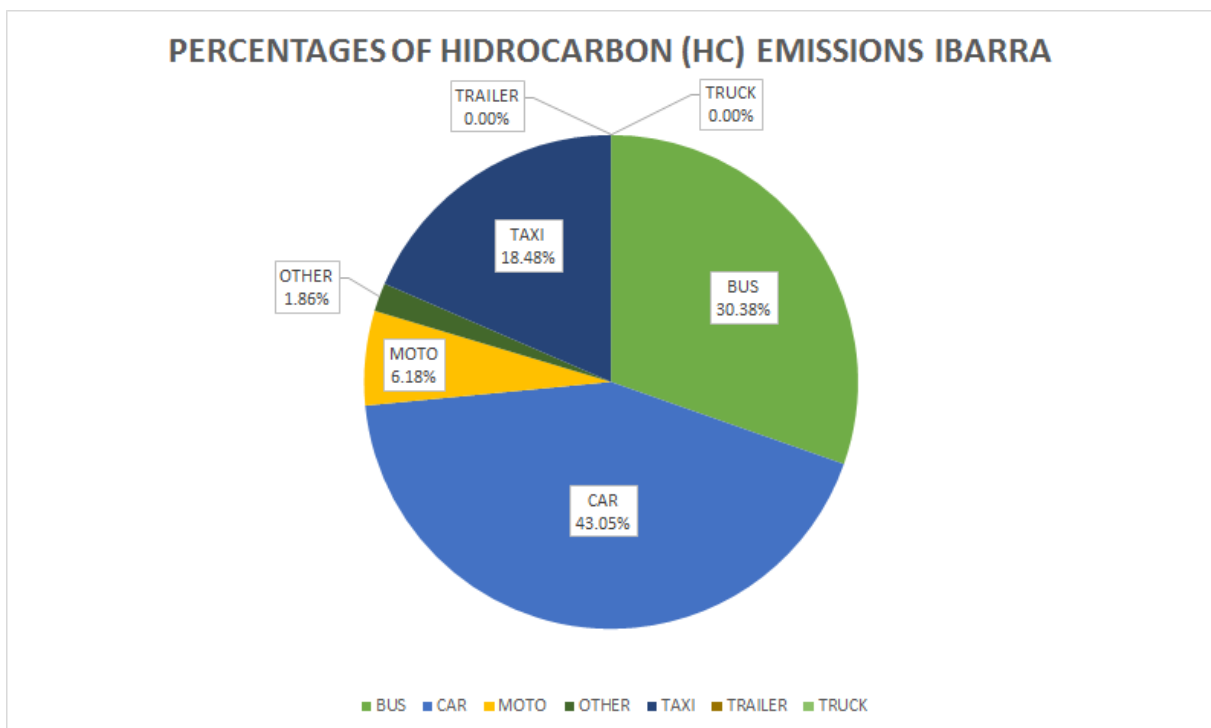


Figure 5.26: Percentage of HC emissions per vehicle for Ibarra

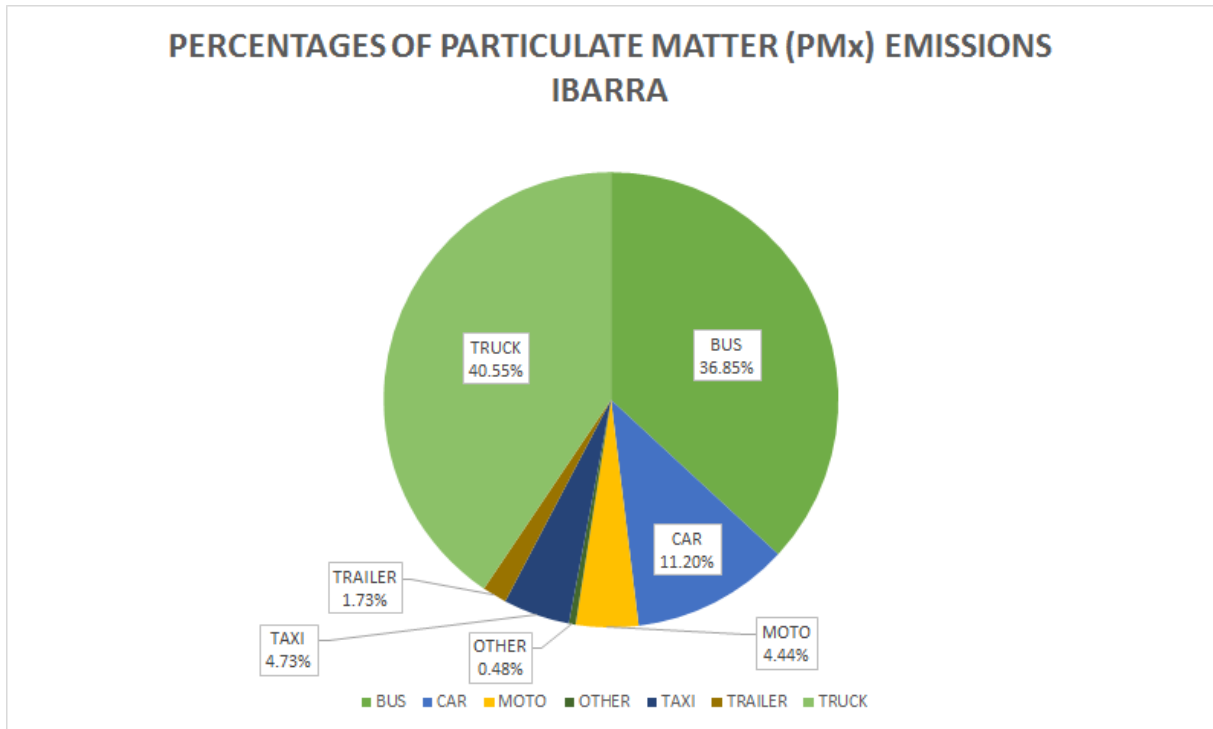


Figure 5.27: Percentage of PM_x emissions per vehicle for Ibarra

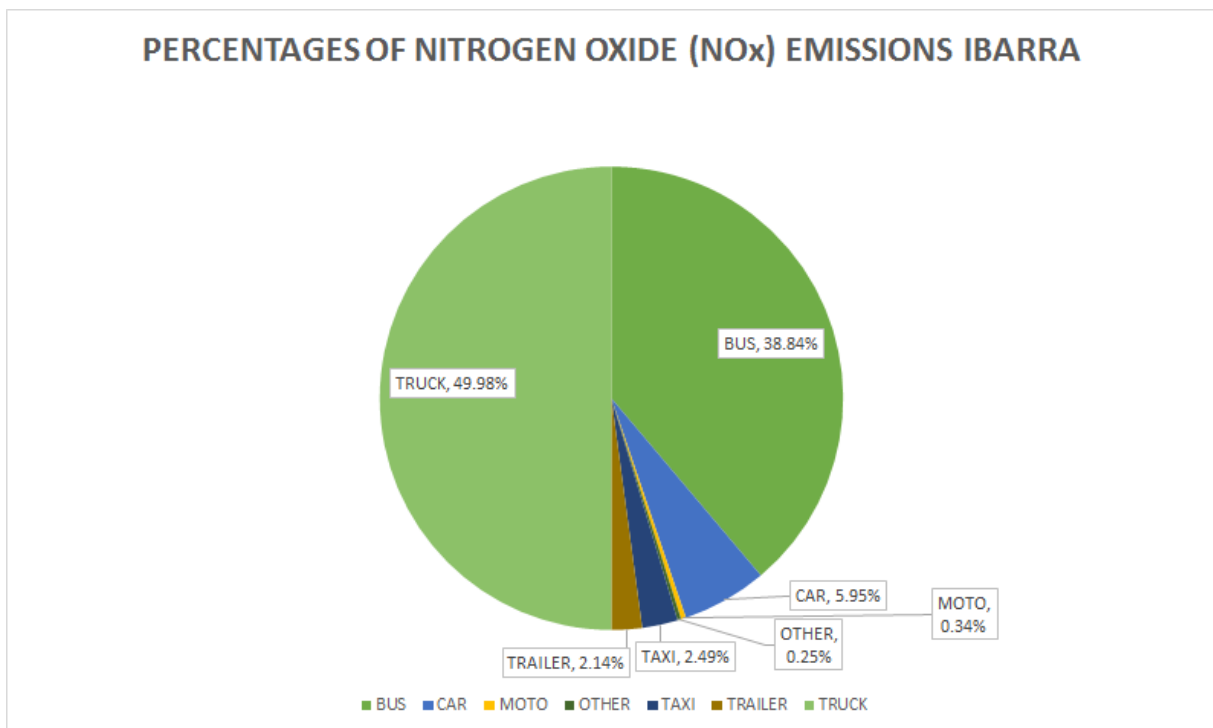


Figure 5.28: Percentage of NO_x emissions per vehicle for Ibarra

Next, we present some bar graphs generated using ANOVA and the data from figures 5.16 and 5.18 for the simulation of Guayaquil and Ibarra, respectively.

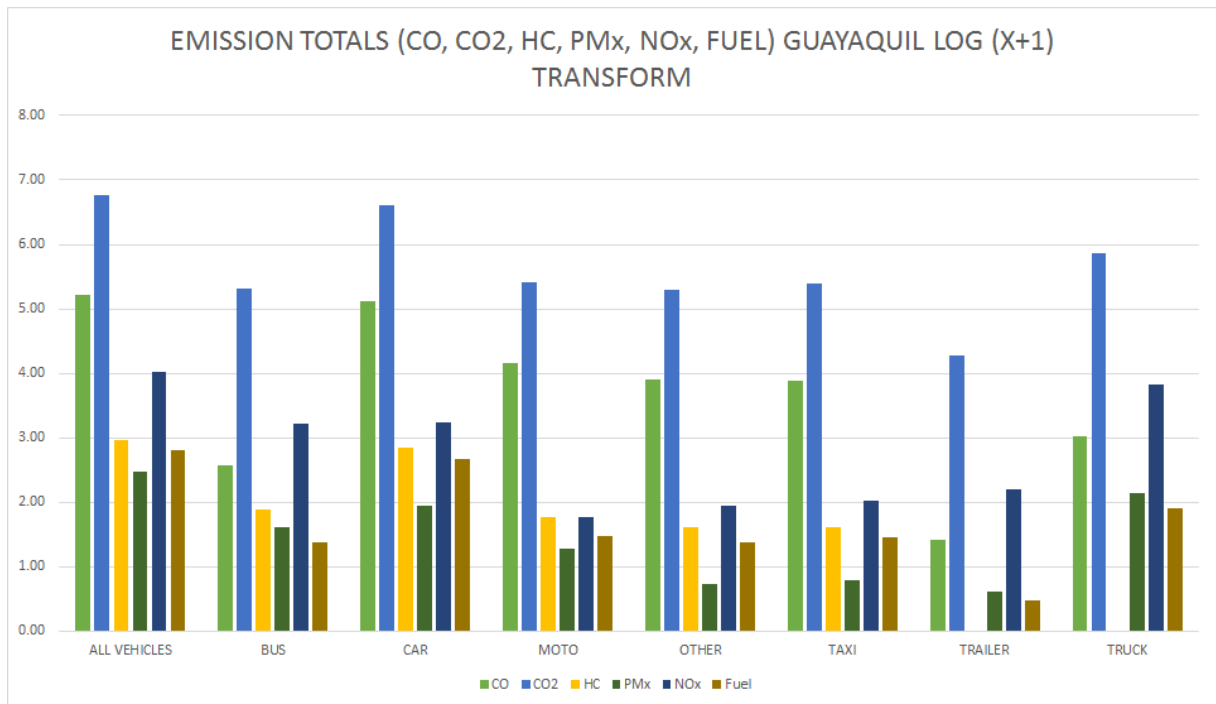


Figure 5.29: Emissions $\log(x + 1)$ transform bar graph for Guayaquil

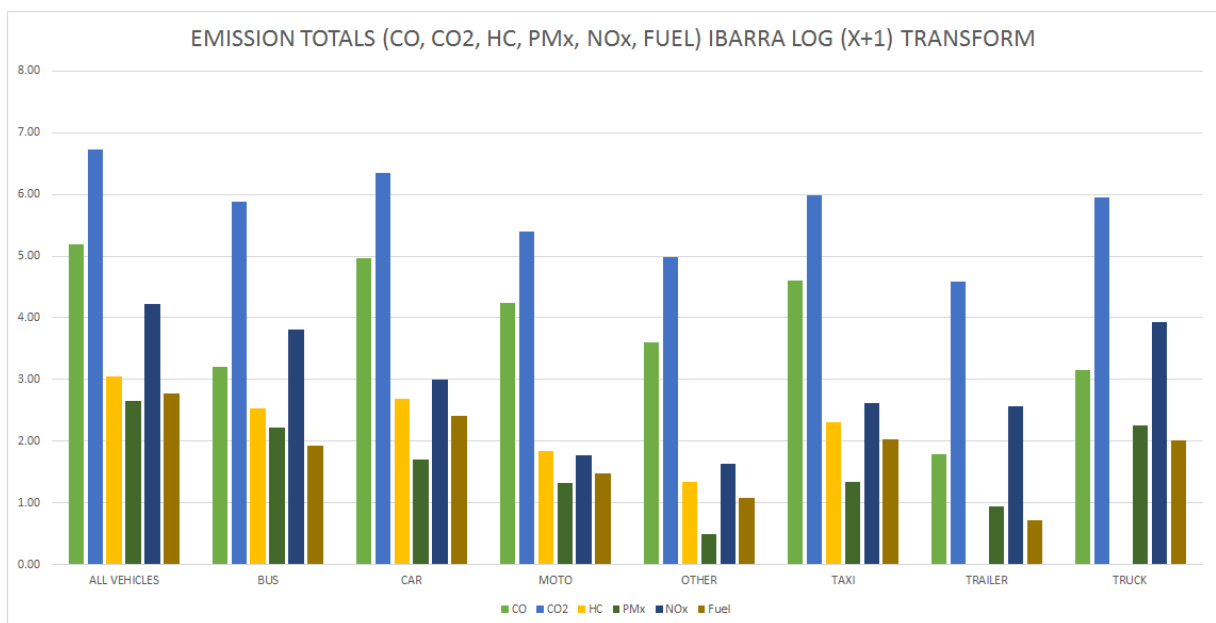


Figure 5.30: Emissions $\log(x + 1)$ transform bar graph for Ibarra

Figures 5.29 and 5.30 illustrates the vehicular GHG emissions using the $\log(x + 1)$ transform for Guayaquil and Ibarra, respectively.

Lastly, we present a bar graph comparing both emissions from Guayaquil and Ibarra.

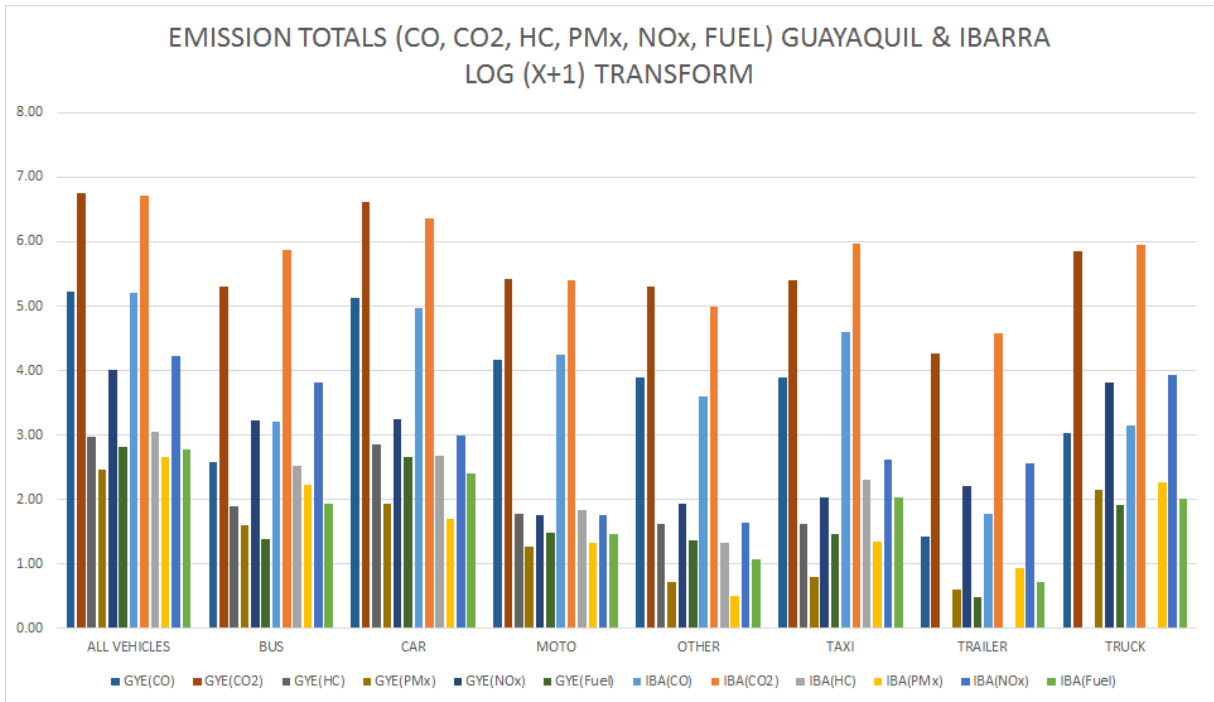


Figure 5.31: Emissions $\log(x + 1)$ transform bar graph for Guayaquil and Ibarra

5.2 Discussion

SUMO resulted to be the ideal tool for simulation and data generation. The amount of information we have generated from both simulations is outstanding.

Figures 5.1 to 5.8 prove our simulations for Guayaquil and Ibarra were successful. We were able to replicate the traffic at specific locations for one hour. We were also able to recollect data on vehicular GHG emissions that will be helpful in the future. Notice that figures 5.4 and 5.9 shows graphs generated from SUMO GUI.

Figure 5.4 shows the maximum number of vehicles running at the same time for the Guayaquil simulation is 762 vehicles. This is the maximum number of vehicles at one specific instance and represents the time when the simulation had the biggest traffic congestion. This graph also shows that the simulation ended at the 5500 time-steps or approximately 1 hour and 32 minutes. Figure 5.9 shows the maximum number of vehicles running simultaneously in Ibarra is 459 vehicles. This graph also shows that the simulation ended at the 4358 time-step or approximately at 1 hour and 12 minutes.

Recall that Guayaquil is a one-way traffic flow simulation in comparison to Ibarra which is a two-way dynamic simulation with vehicles traveling in every direction. The number of vehicles running simultaneously does assimilate reality because Guayaquil is almost twice the size of Ibarra. Guayaquil has a population size of over 2.6 million people with more than 380,000 registered vehicles, meanwhile, Ibarra has a population size of over 220 thousand people with approximately 17,000 registered vehicles. For this reason, a small sector from a large city such as Guayaquil utilizes more vehicles and generates more vehicular GHG emissions than half of a small city such as Ibarra. That is why it is crucial to offer solutions to this type of vehicular congestion, especially in large crowded cities.

Next, we have Figure 5.10, a comparison summary graph for Guayaquil (blue line) and Ibarra (green line). This graph was created using the Python script “plot_summary.py”. It provides a clear view of the total number of vehicles running simultaneously at specific time-steps during the simulation. Notice that the two graphs are the same as in figures 5.4 and 5.9, generated from SUMO GUI. This means we can obtain a quick and reliable comparison of graphs using Python scripts. Figure 5.10 shows that Guayaquil has 300 additional vehicles running simultaneously in comparison to Ibarra. Even though it is only a small sector, large cities such as Guayaquil tend to be overcrowded with vehicular use.

Figures 5.11 and 5.12 show the locations of all traffic lights in the specific area simulated for the cities of Guayaquil and Ibarra, respectively. These can be handy when trying to modify traffic light settings in specific sectors.

Figures 5.13 and 5.14 show the city of Guayaquil and Ibarra, respectively, with a color gradient that represents the different speed limits for each road. Red represents the highest speed limit and purple the lowest. Notice that the speed values go from 0 to 50. These values are defined in the SUMO website, and $50 = 180$ km/hours. The maximum speed limit within Ibarra is 50 km/hour = 13.88 (dark blue). The maximum speed limit within Guayaquil is 70 km/h = 19.44 (light blue). For this work, all roads simulated had the exact, real-world speed limit.

Figures 5.15 and 5.16 were generated from the simulation of Guayaquil and figures 5.17 and 5.18 from the simulation of Ibarra, using statistical analysis. First, all raw data was grouped in figures 5.15 and 5.17 to obtain the total and average vehicular GHG emitted during the one-hour simulation for Guayaquil and Ibarra. This data was later used to generate graphs and charts.

Once the data was grouped, we did a $\log(x+1)$ transformation. This logarithmic transformation can be seen in figures 5.16 and 5.18 for Guayaquil and Ibarra, respectively. This transformation generates smaller values that are easier to graph and analyze. Additionally, we present the number of GHG emissions calculated in (kg/Gal). All data generated can be used to compare with future data.

From figures 5.15 and 5.17 we generated pie charts to present the amount of CO, CO₂, HC, PM_x, and NO_x that both cities of Guayaquil and Ibarra generated during the one-hour simulation.

Figures 5.19 to 5.28 were generated using our collected GHG emissions. Notice Figure 5.19 shows the percentages of CO that were emitted by all vehicles in the Guayaquil simulation. Data from Figure 5.15 was used. Notice that cars are the main contributor of CO released into the atmosphere. Cars are responsible for 80.98% of all CO released. Motorcycles are the second-highest percentage of all CO emitted in the simulation with 8.69%. As Guayaquil has a higher number of personal-use cars and motorcycles transiting the city over other types of vehicles, this result is accurate and reflects reality. The same pie charts were generated for CO₂, HC, PM_x and NO_x for the cities of Guayaquil and Ibarra, respectively.

Comparing figures 5.19 and 5.24, we can see that personal-use cars in the city of Ibarra only contributed to 58.92% of all CO emissions. Taxis and motorcycles accounted for 25.38% and 11.13%, respectively. As stated previously, Guayaquil also counts with over 380,000 registered vehicles, while Ibarra counts with over 17,000 registered vehicles. Additionally, the residents of Ibarra frequently utilize buses and taxis to commute around the city in comparison to Guayaquil.

Figure 5.23 shows the percentages of NO_x emissions generated during the Guayaquil simulation. Here we can see that trucks, cars, and buses are the highest emitters of NO_x with a 63.01% and 16.88% and 16.18%, respectively.

Comparing with Figure 5.28, which presents the percentage of NO_x emitted by vehicles in the Ibarra simulation, we can see that trucks and buses account for the majority of emissions. Trucks account for 49.98% and buses for 38.84%, which accounts for a total of 88.82% of all NO_x emissions. In Ibarra, personal use cars only contributed 5.95% of all NO_x emitted. This is a third in comparison to the amount of NO_x that cars in Guayaquil produced.

Next, we have figures 5.29 and 5.30. These bar graphs were created using the $\log(x+1)$ transform data from figures 5.16 and 5.18. These bar graphs represent the total vehicular GHG emissions for all vehicles in the one-hour simulation for the cities of Guayaquil and Ibarra, respectively.

Notice in both cities, all vehicles release a high amount of CO_2 into the environment. Buses, trucks, and trailers, additionally, release higher quantities of PM_x and NO_x particles which are more damaging to the environment.

Lastly, Figure 5.31 is a bar graph comparing the emissions from both Guayaquil and Ibarra simulations side-by-side. This graph generated from figures 5.29 and 5.30.

More graphs and results can be found in Appendix 1.

Chapter 6

Conclusions

This work discussed and analyzed simulations for the cities of Guayaquil and Ibarra using SUMO and real-life traffic flows. Our work begins by explaining the history of car-following models. These include the first fundamental diagram introduced by Greenshields to the latest model which is the implementation of the Krauß car-following model in SUMO. Then we presented insight on smart cities and the danger of GHG emissions present in the environment as a result of vehicular combustion. Cities such as Ibarra and Guayaquil tend to face higher traffic congestion during peak hours, from 8 am - 12 pm and from 5 pm - 7 pm. For this reason, this work created a simulation using data obtained from one hour during peak traffic. The traffic flow was measured from 10 am to 11 am for both cities. The simulation for both cities was successful, showcasing the large traffic jams at peak hours. This long-lasting traffic congestion creates tons of GHG emissions that are detrimental to the atmosphere and the health of all inhabitants in the long run. As stated, this was one of the main concerns to take into consideration when trying to implement or create a new smart city, the need to measure and control vehicular GHG emission levels.

The use of new technological advances is crucial to help maintain the infrastructure of cities and avoid their collapse. The rapidly growing population means we need quick and environmentally friendly ways to accommodate for more housing, natural resources, clean air, and water. These are basic needs to maintain healthy living conditions for citizens. Works like this are of vast importance when living in third-world countries such as Ecuador where there is a tight budget for innovation and technology. The small investment that is obtained from the government must be optimally used to further enhance the quality of life in the country. One main focus of this work was to aid Ibarra and Guayaquil in generating data on vehicular GHG emissions using real-life simulations.

SUMO proved to be the ideal tool for achieving realistic simulations for Guayaquil and Ibarra as seen in Chapter 5. SUMO is so versatile, it can be used to implement vehicular GHG regulations and to offer intelligent solutions for cities suffering infrastructure problems. The results showed that we were able to recreate a real-world scenario for the cities of Guayaquil and Ibarra. Having recorded traffic flows from real-life traffic congestion data greatly benefited the simulation. Using real data returned output files with precise values on vehicular emissions. This generated data can be seen in Figure 5.16.

Collecting the traffic flow took time to accomplish as this occurred during times of Covid-19 and quarantine. For this reason, videos had to be recorded so that the vehicle

count could be done later as accurately as possible. It is important to keep in mind that the pandemic greatly reduced the number of vehicles transiting daily. During this period, vehicles with odd and even license plate numbers could only travel every other day of the week. This means that the results obtained in Chapter 5 are approximately half of all vehicular emissions generated hourly post-pandemic. This should be taken into consideration for future simulations.

In the end, we successfully achieved all the specific objectives. We obtained real-life data from traffic flows from Guayaquil and Ibarra. Using these traffic flows and SUMO, we were able to design and create a realistic simulation. Once the simulation was perfected, we were able to generate graphs on vehicular emissions from all running vehicles using SUMO and Python scripts. Finally, we successfully generated precise graphs on vehicular GHG emissions using output files from the simulation. From this, we achieved the general objective of this paper. Creating a realistic simulation of Ibarra and Guayaquil using real-life traffic flows and generating data on vehicular GHG emissions.

6.1 Recommendations

Recommendations to take into consideration

- Ask permission from the city council or the police stations (ECU911) for their videos from traffic cameras. If the camera can record the entire traffic flow, this could accelerate the process of vehicle count.
- Counting vehicles can be tedious, but it is a crucial step because this gives us the exact number of vehicles for the simulation. Without these values, we can not generate accurate results that approximate reality. It is useful to have the aid of people to help count more accurately and faster. This is handy when simulating an entire city with thousands of vehicle flows.
- SUMO and Python provides many scripts in their program folders that are useful but tricky to use. There are scripts to help organize the vehicle flows files by departure time. This is required or the simulation will not work correctly. Instead of organizing them one by one, the scripts save programmers precious time. Other scripts are used to obtain some of the graphs presented in Chapter 5. An example of how to use these scripts can be found on the SUMO website. As stated, some scripts require extra steps for them to work so do not get disappointed if they do not work on the first try.
- It was observed that at peak hours during the highest traffic congestion in Guayaquil, the simulation slowed down a bit. This was also seen when running the parameter network graphs. The performance of the simulation decreased drastically. This can be prevented by using a faster computer to help the simulations run smoother and allow the user to run several screens at the same time.

6.2 Future Works

SUMO is so versatile, having many functions that give the user full control of the simulation. This allows for infinitely many simulation scenarios to be created. All can generate useful results on vehicles, vehicle flows, and vehicular GHG emissions. The applications are limitless. Now, we detail some future ideas for those interested in further pursuing the topic of simulation or smart cities solutions.

- First, we want to implement the same simulation for the cities of Guayaquil and Ibarra but with traffic flow data gathered once Covid-19 ends. When life returns to normal, the results obtained on GHG emissions will vary greatly. Comparing the results from the ones obtained in this work will demonstrate the real levels of GHG emitted into the atmosphere.
- Before creating a new road, building, or bridge in a city, we can simulate new architecture within SUMO. Using real-world data to simulate vehicles and pedestrians we can see how this new construction affects the life of the citizens. We can see if it will generate higher traffic congestion, GHG emissions, or damage the living conditions of its citizens. With this simulation, if the results are negative we can save money and re-utilize it where it will best benefit the city.
- For this work, we focused on creating simulations for a small sector in the cities of Guayaquil and Ibarra. This was done with data generated from one hour of real-life traffic flow. It would be greatly beneficial to simulate an entire city, for 24 hours. The results generated on emissions would be precise and irrefutable. As stated, this is complex and time-consuming as the number of variables that must be modified is too vast for a small group of people.
- Lastly we recommend the implementation of smart parking around Ecuador. This is useful especially in big cities such as Guayaquil or Quito where the amount of traffic can be extremely high. Finding fast available parking saves citizens time and reduces the dangerous GHG emitted by running vehicles.

Bibliography

- [1] T. Alsop, “Smart city initiatives global spending 2018-2023,” Apr 2021. [Online]. Available: <https://www.statista.com/statistics/884092/worldwide-spending-smart-city-initiatives/>
- [2] [Online]. Available: <https://www.epa.gov/transportation-air-pollution-and-climate-change/carbon-pollution-transportation>
- [3] B. D. Greenshields, J. R. Bibbins, W. Channing, and H. H. Miller, “A study of traffic capacity,” 1935.
- [4] M. Authors, “Traffic and transportation simulation - looking back and looking ahead: Celebrating 50 years of traffic flow theory, a workshop,” *Transportation Research Circular*, 2015.
- [5] L. C. Edie, “Car-following and steady-state theory for noncongested traffic,” *Operations Research*, vol. 9, no. 1, p. 66–76, 1961.
- [6] J. Treiterer and J. A. Myers, “The hysteresis phenomenon in traffic flow,” 1974.
- [7] D. Krajzewicz, M. Hartinger, G. Hertkorn, P. Mieth, C. Rossel, J. Zimmer, and P. Wagner, “Using the road traffic simulation “sumo” for educational purposes,” *Traffic and Granular Flow '03*, p. 217–222.
- [8] [Online]. Available: <https://www.openstreetmap.org/>
- [9] R. Zalakeviciute, R. Vasquez, D. Bayas, A. Buenaño, D. Mejía, R. Zegarra, V. Díaz, and B. K. Lamb, “Drastic improvements in air quality in ecuador during the covid-19 outbreak,” *Aerosol and Air Quality Research*, vol. 20, pp. 1783–1792, 2020.
- [10] “Introducción.” [Online]. Available: <https://www.google.com/intl/es/earth/>
- [11] B. S. Kerner, “Introduction to modern traffic flow theory and control: The long road to three-phase traffic theory,” 2009.
- [12] S. Chanut and C. Buisson, “Macroscopic model and its numerical solution for two-flow mixed traffic with different speeds and lengths,” *Transportation Research Record*, vol. 1852, pp. 209 – 219, 2003.

- [13] C. Nunez, “Carbon dioxide in the atmosphere is at a record high. here’s what you need to know.” May 2021. [Online]. Available: <https://www.nationalgeographic.com/environment/article/greenhouse-gases#:~:text=Greenhousegaseshavefar-ranging,change caused by greenhouse gases.>
- [14] “Ozone.” [Online]. Available: <https://www.britannica.com/science/air-pollution/Ozone>
- [15] “Amazon.com. spend less. smile more.” [Online]. Available: <https://www.amazon.com/>
- [16] P. A. Lopez, M. Behrisch, L. Bieker-Walz, J. Erdmann, Y.-P. Flötteröd, R. Hilbrich, L. Lücken, J. Rummel, P. Wagner, and E. Wießner, “Microscopic traffic simulation using sumo,” in *The 21st IEEE International Conference on Intelligent Transportation Systems*. IEEE, 2018. [Online]. Available: <https://elib.dlr.de/124092/>
- [17] M. R. Miller, J. B. Raftis, J. P. Langrish, S. G. Mclean, P. Samutrtai, S. P. Connell, S. Wilson, A. T. Vesey, P. H. B. Fokkens, A. J. F. Boere, and et al., “Correction to “inhaled nanoparticles accumulate at sites of vascular disease”,” *ACS Nano*, vol. 11, no. 10, p. 10623–10624, 2017.
- [18] B. D. Greenshields, J. T. Thompson, H. C. Dickinson, and R. S. Swinton, “The photographic method of studying traffic behavior,” 1934.
- [19] J. Drake, J. L. Schofer, and A. D. May, “A statistical analysis of speed-density hypotheses,” 1965.
- [20] S. A. Smulders, “Control of freeway traffic flow by variable speed signs,” *Transportation Research Part B-methodological*, vol. 24, pp. 111–132, 1990.
- [21] C. F. Daganzo, “The cell transmission model: A dynamic representation of highway traffic consistent with the hydrodynamic theory,” *Transportation Research Part B-methodological*, vol. 28, pp. 269–287, 1994.
- [22] G. F. Newell, “Instability in dense highway traffic: A review.” 1965.
- [23] J. Olstam and A. Tapani, “Comparison of car-following models,” 2004.
- [24] S. Krauß, *Microscopic modeling of traffic flow: investigation of collision free vehicle dynamics*. DLR, 1998.
- [25] S. P. Hoogendoorn and P. H. L. Bovy, “State-of-the-art of vehicular traffic flow modelling,” *Proceedings of the Institution of Mechanical Engineers, Part I: Journal of Systems and Control Engineering*, vol. 215, pp. 283 – 303, 2001.
- [26] E. Kometani, “On the stability of traffic flow,” 1958.
- [27] R. Michaels, “Perceptual factors in car-following,” 1963.
- [28] P. G. Gipps, “A behavioural car-following model for computer simulation,” *Transportation Research Part B: Methodological*, vol. 15, no. 2, p. 105–111, 1981.

- [29] P. A. Seddon, “A program for simulating the dispersion of platoons of road traffic,” *Simulation*, vol. 18, no. 3, p. 81–90, 1972.
- [30] I. Spyropoulou, “Simulation using gipps car-following model—an in-depth analysis,” *Transportmetrica*, vol. 3, no. 3, p. 231–245, Jun 2007.
- [31] B. Stutzer, “Handbook emission factors for road transport.” [Online]. Available: <https://www.hbefa.net/e/index.html>
- [32] J. R. Gil-Garcia, T. A. Pardo, and T. Nam, “What makes a city smart? identifying core components and proposing an integrative and comprehensive conceptualization,” *Information Polity*, vol. 20, no. 1, p. 61–87, 2015.
- [33] C. Harrison, B. Eckman, R. Hamilton, P. Hartswick, J. Kalagnanam, J. Paraszczak, and P. Williams, “Foundations for smarter cities,” *IBM Journal of Research and Development*, vol. 54, no. 4, p. 1–16, 2010.
- [34] M. E. Kahn, “Sustainable and smart cities,” *Policy Research Working Papers*, Nov 2013.
- [35] H. Topacoglu, S. Katsakoglou, and A. Ipekci, “Effect of exhaust emissions on carbon monoxide levels in employees working at indoor car wash facilities,” Jan 2014.
- [36] “Automobiles and carbon monoxide,” *U.S Environmental Protection Agency Office of Mobile Sources*.
- [37] H. Ritchie, “Cars, planes, trains: where do co2 emissions from transport come from?” [Online]. Available: <https://ourworldindata.org/co2-emissions-from-transport>
- [38] “Carbon dioxide,” Jun 2021. [Online]. Available: <http://www.dhs.wisconsin.gov/chemical/carbondioxide.htm>
- [39] M. Srivastava, A. Srivastava, A. Yadav, and V. Rawat, “Source and control of hydrocarbon pollution,” Nov 2019. [Online]. Available: <https://www.intechopen.com/chapters/67349>
- [40] D. R. S. Engineer, D. Reichmuth, S. Engineer, J. H. D. o. Policy, J. Hamilton, D. o. Policy, K. C. C. Manager, K. Catalano, C. Manager, D. C. S. V. Analyst, and et al., “Air pollution from cars, trucks, and buses in the us: Everyone is exposed, but the burdens are not equally shared,” Jun 2021. [Online]. Available: <https://blog.ucsusa.org/dave-reichmuth/air-pollution-from-cars-trucks-and-buses-in-the-u-s-everyone-is-exposed-but-the-burdens-are-not-equally-shared/>
- [41] “Nitrogen oxides (nox), why and how they are controlled,” *Environmental Protection Agency*, 1999. [Online]. Available: <https://www3.epa.gov/ttn/catc/dir1/fnoxdoc.pdf>
- [42] L. Bieker-Walz, M. Behrisch, and M. Junghans, “Analysis of the traffic behavior of emergency vehicles in a microscopic traffic simulation,” *EPiC Series in Engineering*, vol. 2, p. 1–13, 2018.

- [43] J. Seung-Ju, “Design of traffic flow simulation system to minimize intersection waiting time,” *International Journal of Advanced Computer Science and Applications*, vol. 9, no. 5, 2018.
- [44] A. V. H. Heijmeijer and G. V. Alves, “Development of a middleware between sumo simulation tool and jacamo framework,” *ADCAIJ: Advances in Distributed Computing and Artificial Intelligence Journal*, vol. 7, no. 2, p. 5–15, 2018.
- [45] L. Codecá, J. Erdmann, and J. Harri, “A sumo-based parking management framework for large-scale smart cities simulations.”
- [46] U. Noyer, F. Rudolph, and M. Jung, “Simulating a multi-airport region on different abstraction levels by coupling several simulations,” *EPiC Series in Engineering*, vol. 2, p. 14–24, 2018.
- [47] X. Ma, X. Hu, T. Weber, and D. Schramm, “Evaluation of accuracy of traffic flow generation in sumo,” *Applied Sciences*, vol. 11, no. 6, p. 2584, 2021.
- [48] S. Akhter, M. N. Ahsan, S. J. S. Quaderi, M. A. A. Forhad, S. H. Sumit, and M. R. Rahman, “A sumo based simulation framework for intelligent traffic management system,” *Journal of Traffic and Logistics Engineering*, p. 1–5, 2020.
- [49] M. Authors, “Proposed mission: 100 climate-neutral cities by 2030 – by and for the citizens,” *European Union*, Sep 2020.
- [50] I. Lebrusán and J. Toutouh, “Using smart city tools to evaluate the effectiveness of a low emissions zone in spain: Madrid central,” *Smart Cities*, Jun 2020.
- [51] S. Ilarri, D. Sáez, and R. Trillo-Lado, “Traffic flow modelling for pollution awareness: The trafair experience in the city of zaragoza,” *Proceedings of the 16th International Conference on Web Information Systems and Technologies*, 2020.
- [52] A. S. M. Bakibillah, Y. F. Paw, M. A. S. Kamal, S. Susilawati, and C. P. Tan, “An incentive based dynamic ride-sharing system for smart cities,” *Smart Cities*, vol. 4, no. 2, p. 532–547, 2021.
- [53] N. Tubay, “Un carro por cada siete habitantes y otras cifras que retratan a guayaquil,” Nov 2020. [Online]. Available: <https://www.expreso.ec/guayaquil/carro-siete-personas-cifras-retratan-92839.html>
- [54] D. L. Hora, “Más de 17 mil vehículos transitan en ibarra - la hora.” [Online]. Available: <https://lahora.com.ec/noticia/653536/ms-de-17-mil-vehiculos-transitan-en-ibarra>

Appendices

Appendix 1

This chapter presents all additional figures, as well as the charts and graphs obtained from SUMO, Python, and using statistical analysis.

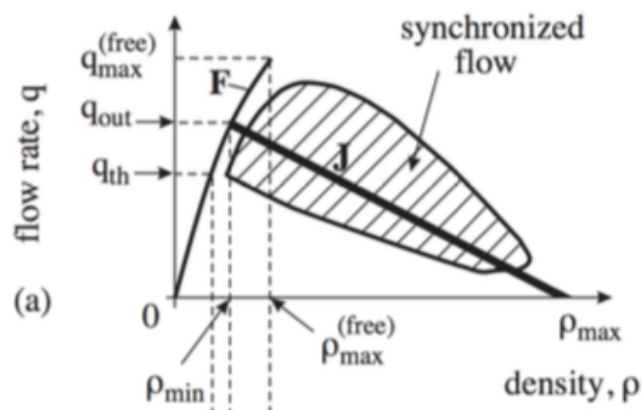


Figure 6.1: Fundamental diagram with infinitely admissible states in the congestion branch (shaded). Source: [11]

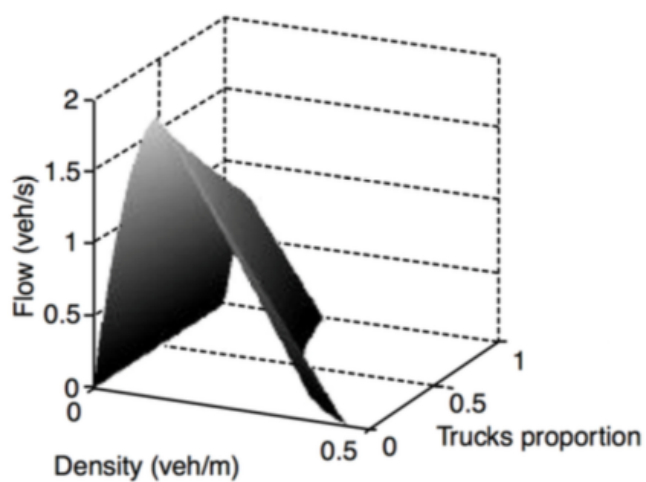


Figure 6.2: Three-Dimensional fundamental diagram, high proportion of trucks leads to lower flows and speeds. Source: [12]

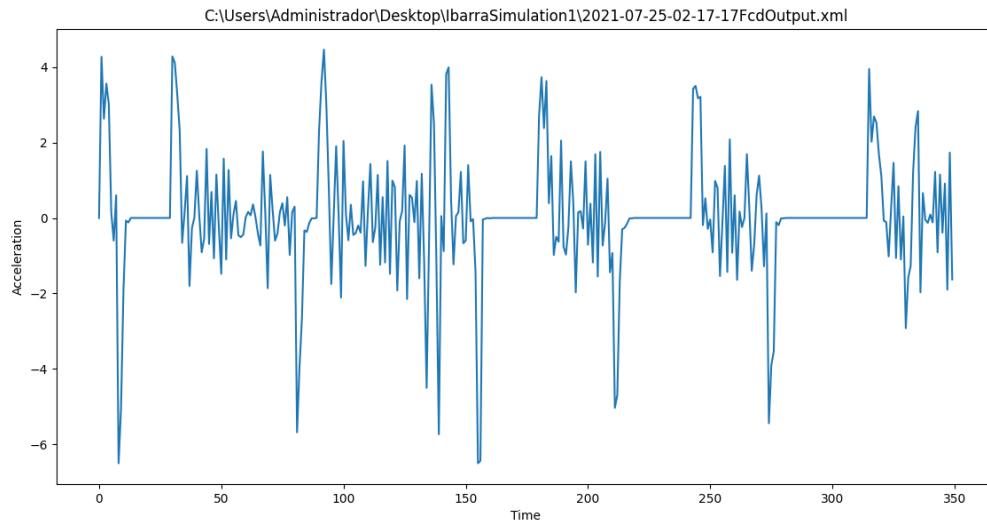


Figure 6.3: Time vs Acceleration graph for Ibarra simulation using only 1 vehicle

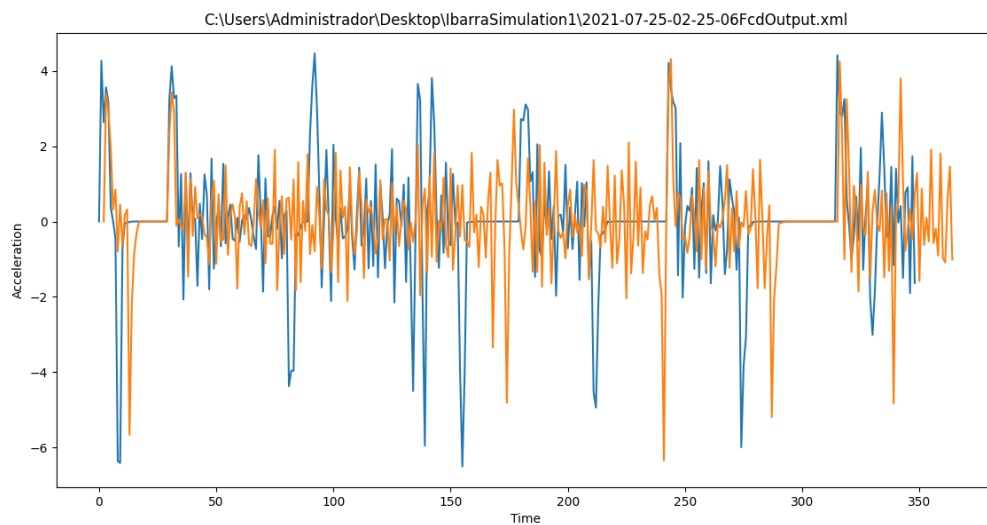


Figure 6.4: Time vs Acceleration graph for Ibarra simulation using only 2 vehicles

Figure 6.3 is a simulation of Ibarra running only 1 vehicle. This helps visualize the way vehicles accelerate and decelerate during the simulation. Figure 6.4 is the same simulation of Ibarra but instead running 2 vehicles at the same time. Each different-colored line represents a different vehicle. Notice that both vehicles behave similarly when accelerating and decelerating. This behavior is normal since vehicles can accelerate and decelerate very fast to avoid collisions.

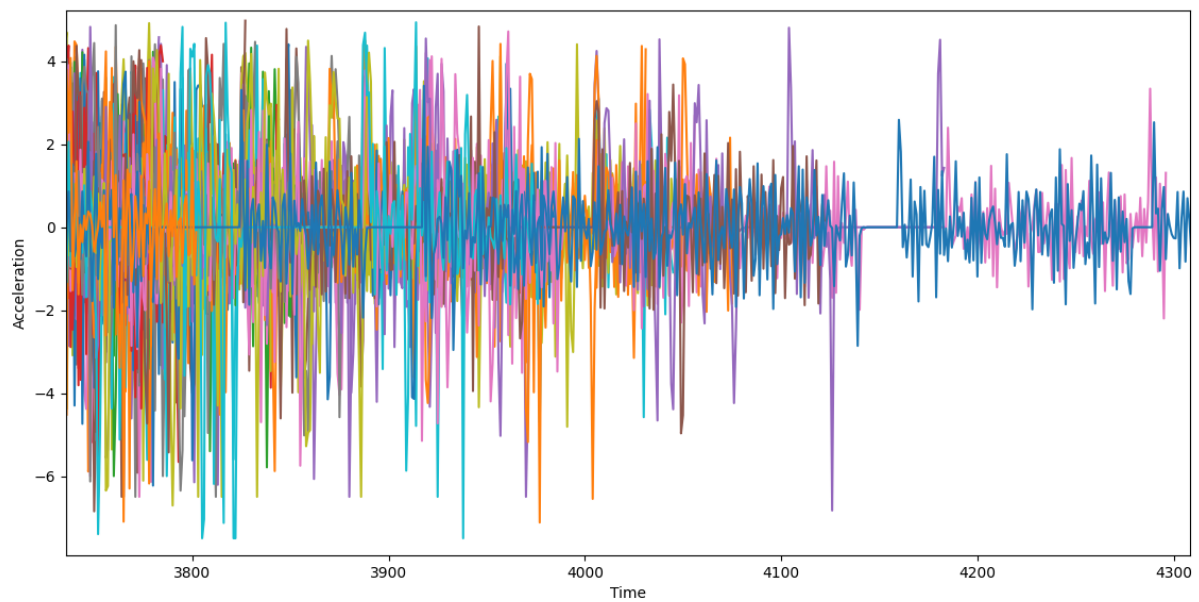


Figure 6.5: Time vs Acceleration graph for Ibarra simulation using vehicular flow

Figure 6.5 is the same time vs acceleration graph for Ibarra, but using the real-life vehicular flow. Here it is not easy to identify each vehicle independently, but using the Python scripts provided by SUMO, this is possible to do. Notice the figure is zoomed in. It presents the vehicular acceleration starting at the 3800 time-step (1 hour and 3 minutes) until all vehicles leave the simulation at the 4300 time-step (1 hour and 11 minutes). This and other graphs can be generated using Python scripts. The same graphs can be obtained for the Guayaquil simulation. Next, we present some maps that illustrate the location of traffic lights in the specified area for the cities of Guayaquil and Ibarra, respectively.

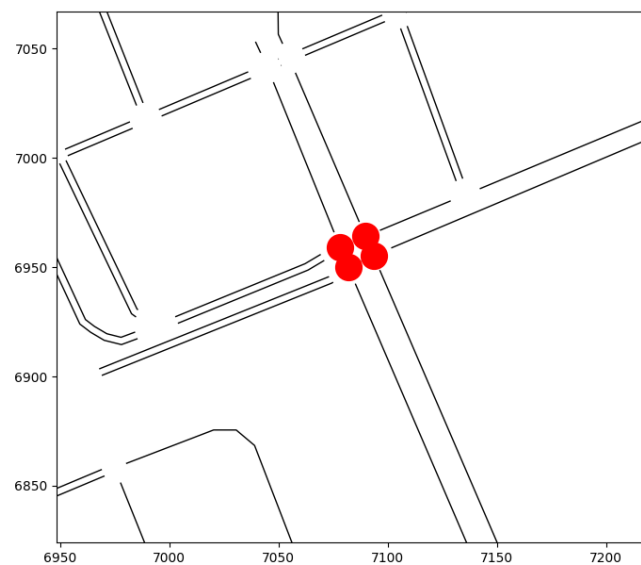


Figure 6.6: Traffic Lights 1x Zoom for Guayaquil at location (B)

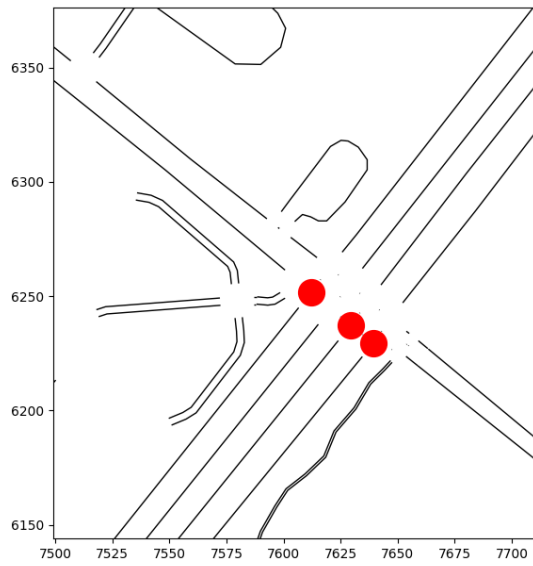


Figure 6.7: Traffic Lights 1x Zoom for Guayaquil at location (C)

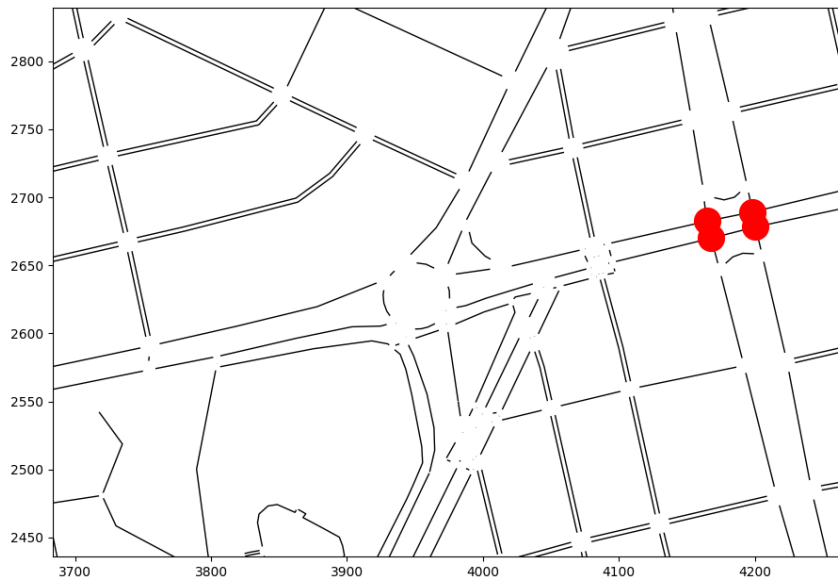


Figure 6.8: Traffic Lights 1x Zoom for Ibarra at location (A)

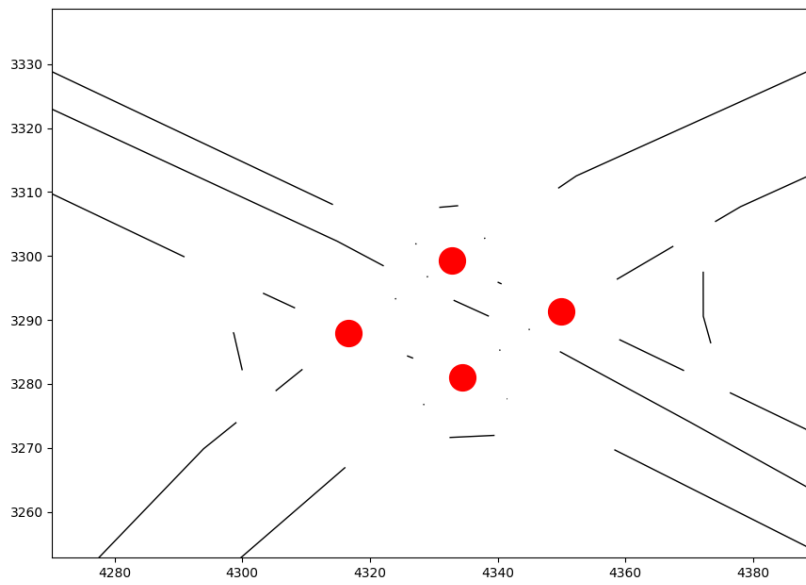


Figure 6.9: Traffic Lights 1x Zoom for Ibarra at location (B)

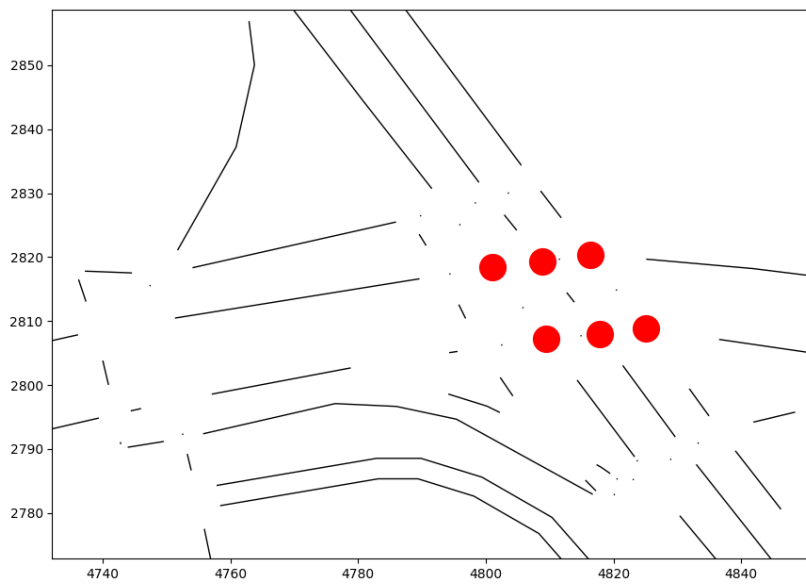


Figure 6.10: Traffic Lights 1x Zoom for Ibarra at location (C)

Now, we present some maps that illustrate the lane speed limit for the city of Guayaquil at specific locations.



Figure 6.11: Lane speed limit Zoom 1x for Guayaquil at location (C). (50km/h = 13.88 , 70km/h = 19.44)

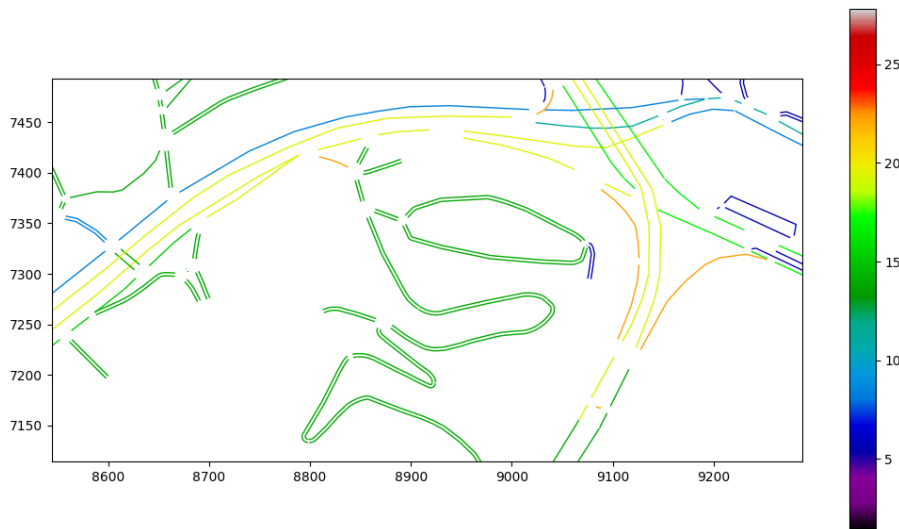


Figure 6.12: Lane speed limit Zoom 1x for Guayaquil at location (D). (50km/h = 13.88 , 70km/h = 19.44)